

**Retrofitting with Bioretention and a Swale
to Treat Bridge Deck Stormwater Runoff**

S.K. Luell¹, R. J. Winston², W. F. Hunt³

Department of Biological and Agricultural Engineering
North Carolina State University
Box 7625, Raleigh, NC 27695

NCDOT Research Project 2011-12
Final Report
North Carolina Department of Transportation
December 8, 2011



Table of Contents

Table of Contents	2
List of Tables	5
List of Figures	8
Preface	10
Executive Summary	10
Review of Literature	11
Bioretention.....	12
<i>Soil Media and Vegetation</i>	13
<i>Internal Storage Zones</i>	15
<i>Hydrology</i>	17
Swales	23
Research Goals.....	29
Methods	29
Study Site Background	29
Bioretention.....	31
<i>Bioretention Description and Characterization</i>	31
<i>Monitoring Equipment</i>	33
<i>Sampling Protocol</i>	37
Swale.....	37
<i>Swale Description and Characterization</i>	37
<i>Design Modification</i>	38
Sampling Methods and Analysis	41
Statistical Analysis.....	42
Results and Discussion	43
Bioretention.....	43
<i>Hydrology</i>	43
Peak Flow Rate	43
Drawdown Rate Effects and Overflow	43

Volume Reduction	46
Lag Time	49
<i>Nutrients and TSS</i>	49
Total Kjeldahl Nitrogen	49
Nitrate-Nitrite Nitrogen.....	51
Total Nitrogen	52
Ammonium Nitrogen	53
Total Phosphorous.....	55
Total Suspended Solids	56
<i>Nutrient and TSS Removal Summary</i>	57
<i>Heavy Metals</i>	61
<i>Pollutant Loads</i>	62
<i>Monitoring Challenges</i>	67
Swale.....	68
<i>Nutrients and TSS</i>	68
Pollutant Concentration Reductions.....	68
Nutrient and TSS Removal Summary.....	70
<i>Heavy Metals</i>	73
<i>Pollutant Loads</i>	74
<i>Particle Size Distribution Analysis</i>	76
<i>Monitoring Challenges</i>	82
Conclusions	84
Acknowledgements	86
References	87
Appendix A: Bioretention	94
Time of Concentration Calculation.....	94
Bioretention Hydrologic Data.....	95
Bioretention Inflow vs. Outflow Hydrographs	105
Bioretention Rain Depth Adjustment Multiplier	106
Antecedent Dry Period.....	109
Bioretention Water Quality Data	111

<i>Sampled Events</i>	111
<i>Raw Pollutant Data</i>	112
Initial Abstraction Runoff Volume Calculations	116
Load Data.....	117
Combined Water Quality/Hydrology Calculation	119
Fractionation of Load Reduction Attributed to Concentration and Volume Reduction	120
Appendix B: Swale	121
Swale Water Quality Sampled Events	121
Swale Pollutant Concentration Data	122
Swale Pollutant Load Data.....	125
Swale Initial Abstraction Runoff Volume Calculations	127
Swale Inflow Volume	128
Swale Concentration Calculations	130
Swale Soil Compaction.....	131
Swale Grass Length and Density Analysis	132
Swale Particle Size Distribution Analysis Results.....	134
Swale Flow Depth Calculations.....	137
<i>Swale Dimensions</i>	137
<i>Manning's Equation and Rational Method</i>	137
Appendix C: Bridge Deck Runoff Analyses	140
Bridge Deck First Flush Analysis	140

List of Tables

Table 1. Summary of nutrient and metal removals from bridge decks presented as site mean EMCs.	19
Table 2. Descriptions of previously studied bioretention cells.	19
Table 3. Summary of nutrient and metal removals from previously studied bioretention cells. .	21
Table 4. Descriptions of previously studied swales.	26
Table 5. Summary of nutrient and metal removals from previously studied swales.	27
Table 6. Seven day quarterly traffic data for NB and SB Mango Creek bridges.	29
Table 7. Design characteristics for bioretention cells at Mango Creek.	32
Table 8. As-built characteristics for bioretention cells at Mango Creek.	32
Table 9. Average grass density and length measurements ^[1]	38
Table 10. Nutrient, sediment, and metals analysis techniques.	42
Table 11. Large bioretention cell volume reduction based on storm size.	47
Table 12. Small bioretention cell volume reduction based on storm size.	47
Table 13. Median lag times associated with antecedent dry period in the large and small bioretention cells.	49
Table 14. Statistical analysis results for TKN.	50
Table 15. Statistical analysis results for NO _{2,3} -N.	51
Table 16. Statistical analysis results for TN.	53
Table 17. Statistical analysis results for NH ₄ -N.	54
Table 18. Statistical analysis results for TP.	55
Table 19. Statistical analysis results for TSS.	56
Table 20. Median concentrations by sampling location (mg/L)	59
Table 21. Mean nutrient and TSS concentrations by sampling location.	59
Table 22. Percent concentration reductions based upon means of pollutants at Mango Creek bioretention cells.	59
Table 23. Median total and dissolved heavy metal concentrations.	61
Table 24. Pollutant loads and reductions for the bioretention cells at Mango Creek as calculated using the summation of loads technique.	64
Table 25. Pollutant load reductions for the bioretention cells at Mango Creek as calculated using average mass reduction.	64
Table 26. Partitioning the cause of load reduction between concentration and volume reduction in the large cell.	65
Table 27. Partitioning the cause of load reduction between concentration and volume reduction in the small cell.	65
Table 28. Statistical comparison of pollutant loads for bioretention cells.	66
Table 29. Mean and median nutrient and TSS concentrations and mean EMC percent concentration reductions by sampling location (n=32 nutrients, 31 TSS).	68
Table 30. Statistical analysis results for nutrients and TSS.	69
Table 31. Median total and dissolved heavy metal concentrations for the Mango Creek swale. .	74
Table 32. Pollutant load reductions for the swale at Mango Creek, calculated using the summation of loads technique.	75
Table 33. Percent pollutant load reductions for the swale at Mango Creek as calculated using average mass reduction.	75

Table 34. Annual untreated and treated loads at the Mango Creek swale.....	76
Table 35. Hydrology and TSS data for storm events sampled for particle size distribution analysis.....	76
Table 36. Calculated inflow volumes and ISCO reported outflow volumes.....	96
Table 37. Edited flow data used in load reduction and flow volume calculations for large bioretention cell.....	98
Table 38. Edited flow data used in load reduction and flow volume calculations for small bioretention cell.....	99
Table 39. Peak inflow and outflow flowrates.....	101
Table 40. Large bioretention cell lag times per storm event.....	103
Table 41. Small bioretention cell lag times per storm event.....	104
Table 42. Mango Creek study site rain data and corrected rain depths.....	106
Table 43. Antecedent dry period.....	109
Table 44. Sampling date, rainfall depth, and samples taken at the bioretention cells for each sampled event.....	111
Table 45. Nutrient and TSS concentration data as reported by the NC State University Center for Applied Aquatic Ecology.....	112
Table 46. Metals concentration data reported by the North Carolina Division of Water Quality lab.....	115
Table 47. Initial abstractions and curve numbers for impervious surfaces under varying antecedent moisture conditions.....	116
Table 48. Large cell pollutant loads per storm event.....	117
Table 49. Small cell pollutant loads per storm event.....	118
Table 50. Sampling date, rainfall depth, and samples taken at the swale for each water quality sampled event.....	121
Table 51. Nutrient and TSS concentration data as reported by the NC State University Center for Applied Aquatic Ecology.....	122
Table 52. Metals concentration data as reported by the North Carolina Division of Water Quality lab.....	124
Table 53. Pollutant loads per storm event.....	125
Table 54. Initial abstractions and curve numbers for impervious surfaces under varying antecedent moisture conditions.....	127
Table 55. Calculated runoff volumes based on Initial Abstraction method (Pandit and Heck, 2009).....	128
Table 56. Spectrum SC900 Soil Compaction Meter readings for soil compaction along the swale measured in psi. The shallowest readings at or above 300 psi (2070 kP) are shaded red.....	131
Table 57. Grass length and count 2/21/10 raw data.....	133
Table 58. Grass density 2/21/10.....	133
Table 59. Grass length and count 9/10/10 raw data.....	133
Table 60. Grass density 9/10/10.....	134
Table 61. Particle size distribution analysis results reported by NC State University's Marine, Earth and Atmospheric Science Department.....	134
Table 62. Swale side slopes.....	137
Table 63. Thalweg slope.....	137

Table 64. Depths of flow and flowrate associated with peak rainfall intensities for select storms at the Mango Creek swale. 138

Table 65. TSS data associated with depth of flow and peak flowrates through Mango Creek swale. 139

Table 66. Northbound bridge deck mean nutrient and TSS runoff concentrations per rainfall depth range. 140

Table 67. Statistical results for difference in means of nutrient and TSS runoff concentrations per rainfall depth range for the northbound bridge deck. 140

Table 68. Southbound bridge deck mean nutrient and TSS runoff concentrations per rainfall depth range. 140

List of Figures

Figure 1. Bioretention cell cross-section illustration.	13
Figure 2. Illustration of a bioretention cell with ISZ.	16
Figure 3. Drainage pipe to bioretention cells.	30
Figure 4. Bridge deck runoff conveyance pipe (left) and view of the downspout (right).	30
Figure 5. Large bioretention cell (left) and small bioretention cell (right).	31
Figure 6. Bioretention flow distribution box (left) and sluice gates in bioretention.	31
distribution box (right).	31
Figure 7. Underdrains of large cell (left) and upturned elbow at the outlet structure (right).	33
Figure 8. Forebays of bioretention cells.	33
Figure 9. Manual rain gauge and ISCO 674 rain gauge.	34
Figure 10. Compound weir located at bioretention cell inlets.	34
Figure 11. Timed water collection into bucket (left) and measurement of volume collected (right).	35
Figure 12. Underdrain pipe outlet and drainage pipe fitted with a compound weir.	35
Figure 13. HOBO® water level logger (left) and installed wells at cell outlets (right).	36
Figure 14. Bioretention cell schematic identifying flow monitoring locations.	36
Figure 15. ISCO 6712™ portable sampler (left) and green housing boxes (right).	37
Figure 16. Bioretention cell schematic identifying sampling points.	37
Figure 17. Swale at Mango Creek.	38
Figure 18. Check dam looking downslope (left image) and outlet structure looking upslope (right image) of swale. Arrows point to check dam.	39
Figure 19. Compound weir located at swale inlet.	40
Figure 20. Baffled weir box at the outlet of the swale (top and front view).	40
Figure 21. Swale schematic identifying sampling points.	41
Figure 22. Fine soils on bioretention media surface (during construction) prior to removal (left image) and sediment build-up carried by runoff (right image).	44
Figure 23. Small bioretention cell overflow event for 7.26 cm (2.86 in) storm event.	45
Figure 24. Large bioretention cell inflow and outflow volumes and rainfall depth.	46
Figure 25. Small bioretention cell inflow and outflow volumes and rainfall depth.	46
Figure 26. Percent volume reductions and rainfall depths per storm event and season for the large bioretention cell.	48
Figure 27. Percent volume reductions and rainfall depths per storm event and season for the small bioretention cell.	48
Figure 28. Inlet and outlet TKN concentrations per sampled storm event.	51
Figure 29. Inlet and outlet NO _{2,3} -N concentrations per sampled storm event.	52
Figure 30. Inlet and outlet TN concentrations per sampled storm event.	53
Figure 31. Inlet and outlet NH ₄ -N concentrations per sampled storm event.	54
Figure 32. Inlet and outlet TP concentrations per sampled storm event.	56
Figure 33. Inlet and outlet TSS concentrations per sampled storm event.	57
Figure 34. Influent and effluent nutrient and TSS concentrations in Mango Creek bioretention cells. Horizontal lines represent target North Carolina water quality standards in the Piedmont region for TSS, TP, and TN.	58

Figure 35. Bioretention cumulative probability plot for TN.....	60
Figure 36. Bioretention Cumulative Probability Plot for TP.....	60
Figure 37. Bioretention Cumulative Probability Plot for TSS.....	61
Figure 38. Influent and effluent nutrient and TSS loads in Mango Creek bioretention cells.	67
Figure 39. Pressurized flow at large bioretention cell inlet during 3.05 cm (1.2 in) storm (June 2, 2010, left image) and near backwater conditions at small bioretention cell inlet during 0.76 cm (0.3 in) storm (July 27, 2010, right image).....	68
Figure 40. Inlet and outlet concentrations per sampled storm event.	70
Figure 41. Average influent and effluent nutrient concentrations in Mango Creek swale.	71
Figure 42. Average influent and effluent TSS concentrations in Mango Creek swale.....	72
Figure 43. Swale cumulative probability plot for TN.....	72
Figure 44. Swale cumulative probability plot for TP.	73
Figure 45. Swale cumulative probability plot for TSS.	73
Figure 46. Swale influent and effluent particle size distribution (October 14, 2010).	77
Figure 47. Swale influent and effluent particle size distribution (November 5, 2010).	79
Figure 48. Swale influent and effluent particle size distribution (December 12, 2010).....	80
Figure 49. Particle removals at the Mango Creek swale.	82
Figure 50. Swale inlet pipe (left) and outlet weir box (right) during 3.0 cm (1.2 in) storm (June 2, 2010).....	83
Figure 51. Sediment in swale inlet pipe directly behind weir.....	83
Figure 52. Swale inlet forebay prior to (left) and following (right) sand cleanout (July 13, 2010).	83
Figure 53. Soil compaction in Mango Creek swale during construction.....	84
Figure 54. Bioretention cell inlet and outlet weir schematic.	94
Figure 55. Example time of concentration calculation for northbound bridge deck drainage system.	94
Figure 56. Aerial view of northbound bridge deck and longest flow path for t_c calculations.	95
Figure 57. Large bioretention cell inflow and outflow hydrographs (1.07 cm storm).	105
Figure 58. Small bioretention cell inflow and outflow hydrographs (0.66 cm storm).	106
Figure 59. Time of concentration calculations for southbound bridge deck.	130
Figure 60. Aerial view of southbound bridge deck and longest flow path for t_c calculations. ..	131
Figure 61. Flag placement in swale (left) and grass counting template (right).	132

Preface

This final report has been written to satisfy NCDOT research contract 2011-12: “*Monitoring of Prospective Bridge Deck Runoff BMPs: Bioretention and Bioswale at Mango Creek/I-540.*” The research funding was spurred by the passage of Session Law 2008-107, The Current Operations and Capital Improvements Act of 2008, by the North Carolina General Assembly which required research into and installation of stormwater control measures for bridge decks. This study was designed to determine the hydrologic and water quality impacts of purposefully undersized bioretention, a standard bioretention basin, and a swale. The authors wish to thank NCDOT and URS Corporation for their aid throughout the project.

Executive Summary

In 2009, two bioretention cells and a swale were constructed in Knightdale, North Carolina, to treat bridge deck runoff from Interstate 540 as it passed over Mango Creek. One cell (“large”) was sized to capture runoff from a 25 mm (1 in) event. The second (“small”) cell was intentionally undersized and captured runoff from an 8 mm (0.3 in) event. Both had an internal water storage layer of 0.6 m (2 ft) for enhanced nitrate removal and exfiltration. The swale was 37 m (120 ft) long with a 2% longitudinal slope and was designed to pass the 10-year, 24-hour storm event. The bioretention cells were vegetated with centipede grass sod (*Eremochloa ophiuroides*) and the swale was vegetated with tall fescue (*Festuca arundinacea*). The bioretention cells and swale treated runoff from the northbound and southbound bridge decks, respectively.

Hydrologic data were analyzed at the site from October 2009 to December 2010 at the bioretention cells. Runoff volumes entering the SCMs were estimated per storm event using Pandit and Heck’s (2009) Initial Abstraction method. Peak discharges from the bridge deck were calculated using the Rational Method. For storms between 0.3 and 12.2 cm (0.1- 4.8 in), the large bioretention cell achieved an overall volume reduction of 30% (n=47) and a peak flowrate mitigation of 65% (n=48); the small bioretention cell had a 20% volume reduction (n=51) and 58% peak flowrate mitigation (n=61). This study revealed that while the large cell outperformed the small cell, both bioretention cells significantly reduced runoff volumes and attenuated peak flowrates.

Flow-weighted, composite water quality samples were collected at the inlets and outlets of the swale and the bioretention cells and were tested for TSS, TN, TKN, NH₄-N, NO₂₋₃-N, and TP, as well as Zn, Cu, and Pb in their total and dissolved states. TSS, TN, NH₄-N, and NO₂₋₃-N loads were significantly reduced (p<0.05) by both cells, while TP and TKN were not. In contrast, the swale was only able to significantly reduce TSS. Nutrient concentrations in the highway runoff were low prior to entering the SCMs which affected the ability of SCMs to provide further load removal. A PSD analysis performed for three storm events showed that the swale transported particles in the 0.4-40 micron range and most effectively captured particles in the range of 100-2000 microns.

Overall, both the bioretention cells and the swale were effective in treating bridge deck runoff to some degree. Small bioretention “punches more than its weight” in that, relative to a full sized bioretention cell, it provides more proportional benefit than its size. Currently, in the Piedmont of

North Carolina, bioretention cells with ISZs receive 85%, 40%, and 45% regulatory credit for TSS, TN, and TP, respectively (NCDENR, 2007). This study suggests that it may be reasonable for a bioretention cell undersized by one-half to be awarded at least 50% of the removal credits assigned to a fully sized system. Undersized bioretention cells are a viable retrofit option to achieve hydrologic and pollutant removal goals. Further, swales remove coarse sediment better than fine sediment. Since highway stormwater runoff is expected to contain relatively coarse sediment (Sansalone et al., 1998), swales are an appropriate means of TSS reduction from highway runoff. However, when a suite of hydrologic and water quality design goals are needed, swales may need to be used in combination with other practices.

Lastly, runoff leaving these bridge decks was not particularly dirty. While improvement in water quality is always welcome, investing limited resources to “clean” relatively clean water may not be ideal. This suggests some limited pre-design monitoring to discern pollutant concentrations for potential retrofit sites may be a wise investment.

Review of Literature

Nonpoint source pollution is recognized as a significant source of pollution to the nation’s waterways. Nonpoint source pollution is more difficult to prevent and treat than point source pollution because it is distributed. Obvious sources of nonpoint source pollution include activities on construction sites and agricultural land. Atmospheric deposition by dustfall and rainfall is also a major contributor to both nutrient loads and suspended solids (Wu et al., 1998). One common source is the contamination carried in runoff from the 257,495 km (160,000 mi) of highway (USDOT, 2011) stretching across the United States.

Despite the actions of the CWA to limit contamination, many states do not mandate the treatment of highway stormwater runoff (Sansalone et al., 2005). Due to the higher traffic volume of highways, highway runoff differs from the runoff originating from other trafficked impermeable surfaces, such as parking lots, and can have higher nitrogen concentrations due to the higher oxide nitrogen gas emissions (Passeport and Hunt, 2009). Vehicular component abrasion, vehicle body deterioration due to exposure to the elements, the burning of fuel, and road surface degradation from vehicle wear are just some of the many sources pollutants carried in highway runoff (Sansalone et al, 2005).

Barrett et al. (1998a) examined highway sites in Austin, Texas, that were located in both urban and rural settings. On the MoPac Expressway at 35th Street which was located in a commercial/residential area, the runoff was captured at a storm-drain inlet along the gutter of the highway’s southbound lanes, which carried an average traffic volume of approximately 58,000 vehicles per day. It was observed at this site that the median event mean concentrations (EMCs) for total suspended solids (TSS), nitrate-nitrogen (NO₃-N), total phosphorous (TP), iron (Fe), lead (Pb), and zinc (Zn) were 129 mg/L, 1.07 mg/L, 0.33 mg/L, 2.82 mg/L, 0.053 mg/L, and 0.222 mg/L, respectively. These concentrations varied significantly from concentrations observed on Convict Hill Road, located in a rural/residential area. The average daily traffic load on Convict Hill Road during the study was approximately 8,800 vehicles per day. Here, the median EMCs for total suspended solids, nitrate-nitrogen, total phosphorous, iron, lead, and zinc were 91 mg/L, 0.71 mg/L, 0.11 mg/L, 1.401 mg/L, 0.015 mg/L, and 0.044 mg/L respectively.

This study suggested that urban highways with higher traffic volumes typically produce higher concentrations of pollutants in their runoff than do rural highways with less traffic.

A similar comparison was made between urban and rural highway runoff in Guangzhou, China, in the Pearl River Delta (Gan et al., 2007). In this study, highway bridge deck runoff was monitored for the presence of several pollutant types, including nutrients, BOD₅, suspended solids, and heavy metals. Gan et al. (2007) attributed depth of rainfall and antecedent dry period as major rainfall-related factors in highway runoff quality, and attributed land use and traffic volume as the influential watershed-related factors. They concluded that highway runoff in rural areas is typically of better quality than urban runoff. The rural site had a higher traffic load (31,000 vehicles/day) than the urban site (22,170 vehicles/day), and also carried more diesel powered vehicles than the urban site, yet the rural pollutant EMCs were consistently lower, which was said to be a result of the surrounding land use. A relatively good correlation ($0.91 \geq r \geq 0.42$) was also made relating TP, Zn, Pb, COD, Cr, Ni, Cr, and Cu to suspended solids (SS), which supports the idea that heavy metals are often associated with particulate matter. The average concentrations of TN, TP, NO₃-N, and SS at the urban site were 7.32 mg/L, 0.39 mg/L, 3.49 mg/L, and 250.1 mg/L, respectively. These EMCs were comparable to the median EMCs observed by Barrett et al. (1998). Copper, zinc, and lead concentrations (0.14 mg/L, 1.76 mg/L, 118.2 μ/L, respectively), however, seemed quite high and were contributed to the erosion of galvanized establishments and noise barrier walls along the highway (Gan et al., 2007).

Yousef et al. (1984) investigated the presence of total and dissolved Pb, Zn, Cu, Cr, Fe, Ni, and Cd in highway bridge deck runoff from an Interstate 4 bridge that discharged its runoff directly into Lake Ivanhoe. The average daily traffic volume was 55,000 vehicles/day for each bridge deck. The total concentrations of Zn, Pb, Ni, and Fe in the runoff averaged between 4.7 to 20.8 times higher than in the lake. The heavy metals became immobilized within the lake sediments near the point of release. Table 1 summarizes the average heavy metal concentrations for all the studies summarized herein.

Wu et al. (1998) analyzed three highway sites in Charlotte, North Carolina to obtain highway runoff pollutant load data. They found that the TSS EMCs ranged from 30 mg/L in a light traffic area with mixed pervious/impervious land use to 283 mg/L coming directly from a highway bridge deck carrying an average traffic volume of 25,000 vehicles per day. Total nitrogen (TKN plus NO_{2,3}-N) loadings ranged from 11.3 to 35.0 kg/ha-year, and TP ranged from 3.5 to 9.1 kg/ha-year. Wu et al. (1998) concluded that pollutant loading rates from bridge deck surfaces are often higher than the loading rates observed for other impervious roadways because of the roadway management practices that are mandated on bridge decks, such as de-icing.

Bridges often pass over ecologically sensitive areas, such as streams and lakes (Sansalone et al., 2005). The placement of bridge decks often causes their discharge to fall directly into the waters below. It is important to consider the ways that stormwater discharge can be treated before it is introduced directly into receiving waters.

Bioretention

Bioretention cells are excavated basins that contain an underdrain system that is surrounded by a layer of gravel (Figure 1). The gravel layer is covered with fill soil which is then planted with

selected vegetation. The bioretention bowl is designed to pond a certain volume of water for storage above the media. The temporary ponding depth of a bioretention cell typically ranges from 10-35 cm (Davis et al., 2009; Davis et al., 2006; Davis, 2008; Li et al., 2009; Hunt et al. 2009; Passeport et al., 2009). Bioretention cells are designed according to their purpose and their contributing watershed size and composition.

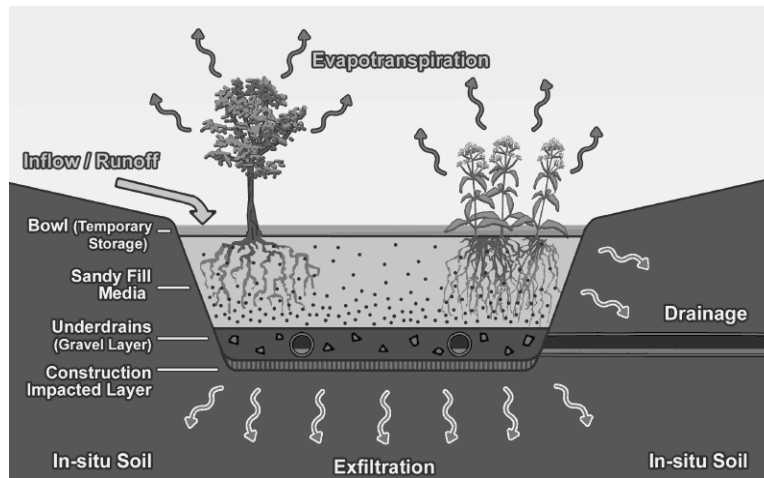


Figure 1. Bioretention cell cross-section illustration.

Table 2 gives the general descriptions of the cells, including their size, watershed composition, and whether or not they contained an internal storage zone. Table 3 shows removal efficiencies of several bioretention cell studies.

The combined surface storage of the cells studied by Dietz and Clausen (2005) were designed to capture the first 25 mm (1 in) of runoff. Both cells were lined underneath, though this is not typical practice in bioretention cell design. The cells provided adequate flow mitigation, as 98.8% of the flow that entered the cells left as subsurface flow, while only 0.8% of the inflow left as overflow and 0.4% left through evapotranspiration (Dietz and Clausen, 2005). Peak flows were also successfully mitigated in these cells. These results support the effectiveness of bioretention cells designed for the acceptance of the first 25 mm (1 in) of runoff.

Soil Media and Vegetation

Soil media in a bioretention cell is chosen based on parameters such as: 1) effect on hydrology and pollutant removal, 2) ability to support chosen vegetation, 3) ability to drain within a desirable amount of time, and 4) cost (Davis et al., 2009). Media depths range from approximately 0.5 to 1.2 m, and are typically a mixture of sand, organic matter, and clay with the dominant constituent typically being sand because of its rapid infiltration ability (Hunt et al., 2006; Hunt et al., 2008; Davis et al., 2001; Emerson and Traver, 2008; Dietz and Clausen, 2005; Dietz and Clausen, 2006; Brown and Hunt, 2010). Deeper media depths have been found to promote infiltration and evapotranspiration better than shallow media depths, consequently resulting in hydrology that is more closely approaching pre-development conditions (Li et al., 2009; Brown and Hunt, 2010). Brown and Hunt (2010) also observed that deeper media depths

promote larger fractions of exfiltration from the bioretention cell walls (37% loss through in the 0.9 m media depth versus 26% loss in the 0.6 m media depth).

Bratieres et al.'s (2008) column tests compared standard sandy loam media to that with added vermiculite/perlite as well as media with added organic matter (10% leaf compost and 10% mulch). All three types of soil were efficient at removing TSS (>95% concentration removal), while the standard sandy loam and the soil with added vermiculite/perlite performed better at removing TP (>88%) than soil with organic matter because of the production of phosphate that occurred within the latter soil type. Although the presence of organic matter in the soil is not preferred when TP removal is desired, its presence enhances the removal of certain metals, as observed by Davis et al. (2001). It has also been reported that organic nitrogen is captured well by organic material within media (Davis et al., 2009), though soils with high organic matter content have also been shown to increase nitrogen concentrations (Hunt et al., 2006).

Mulch cover on a bioretention cell can act as a sink for metals (Dietz and Clausen, 2006; Davis et al., 2001). Dietz and Clausen (2006) observed removal rates of 98% Cu, 36% Pb, and 16% Zn in the mulch layer. Uptake of total nitrogen and total phosphorous was also observed in the mulch, while the soil media acted as a source of these pollutants (Dietz and Clausen, 2006). TKN removal was observed in the bioretention facilities studied by Davis et al. (2006) in the first few centimeters of soil, suggesting that mulch plays a significant role in its removal as well. Davis et al. (2006) mentioned the effect of mulch on capturing organic nitrogen through adsorption and degrading organic nitrogen through high levels of microbial activity within the mulch. This microbial activity, however, converts organic nitrogen to ammonium and then to nitrate, thus the positive effect of the mulch can then become adverse because of the release of nitrate into solution (Davis et al., 2006). Similar observations were made by Brown and Hunt (2011) who saw $\text{NO}_{2,3}\text{-N}$ concentrations that were up to 20 times higher in the outflow than the inflow during five of nearly 12 months of monitoring. Brown and Hunt (2011) suggested the mulch, which was spread up to 20 cm thick in some areas, exported nitrate. Twenty centimeters is considered an unconventionally thick mulch depth for bioretention.

Bioretention cell vegetation is chosen for its ability to encourage biological activity, promote pollutant uptake, and promote evapotranspiration under stressful wet/dry growing conditions (Davis, 2008; Davis et al., 2006; Bratieres et al., 2008). Emerson and Traver (2008) mentioned the role that vegetation plays in improving hydraulic characteristics of soil media due to its tendency to create macropores with its root system, as well as its role in soil stability and structure. As shown in Table 2, typical plantings consist of an assortment of trees, shrubs, and flowers (Davis et al., 2001; Davis, 2008; Li et al., 2009; Hunt et al., 2006; Muthanna et al., 2008; Emerson and Traver, 2008; Dietz and Clausen, 2005). Davis et al. (2009) commented on the use of grass as the sole vegetation choice in bioretention cells, saying that this is a less expensive practice than other types of plantings like shrubs or trees; however, grass is not as effective in promoting media permeability or pollutant uptake. Passeport et al. (2009) conducted a study on two grassed bioretention cells in Graham, North Carolina. Both of the cells studied (North cell and South cell) contained an ISZ (Tables 2 and 3). This study showed that grassed bioretention cells have comparable removal efficiencies to vegetated cells for the constituents tested (Passeport et al., 2009). The North cell and South cell also mitigated flow, albeit slightly (18% peak flow reduction for North cell and 14% reduction for South cell), for nearly all of the storms

tested as a result of evapotranspiration, exfiltration beneath the cells, and containment within the soil media.

A column study performed by Bratieres et al. (2008) in Melbourne, Australia, found that vegetation is important in nitrogen uptake and removal, recommending the use of *Carex appressa* for its superior TN removal ability and its increased performance over time due to the dense, fine root structure that optimizes root surface area per soil volume. It is important to consider geography and climate when choosing vegetation for planting. Phosphorous removal can also be enhanced in bioretention cells due to plant uptake (Davis et al., 2006).

The pollutant removal rates reported by Davis et al. (2006) are summarized in Table 3 were based on a study done on two lab-scale prototype bioretention cells (Large box and Small box), which were described in an earlier paper by Davis et al. (2001) (Table 2).

Bioretention cells have been found to occasionally release pollutants in their outflow as compared to what enters the cell, causing an increase in concentration. Dietz and Clausen (2005) reported an extreme release of TP on a concentration basis for the combined bioretention systems (rain garden 1 and 2), as shown in Table 3. Initial soil disturbance at the beginning of the study period caused TP concentration in the effluent to decrease over time. The systems were most successful at retaining NH₃-N, which was most likely removed through conversion to NH₄-N and adsorption to soil particles.

An increase in pollutants was observed in the Greensboro cell G2 studied by Hunt et al. (2006), which exported higher concentrations of TSS, ammonia, TKN, and ortho-phosphate. The increase in total phosphorous was a result of TSS release as well as the leaching of phosphorous present on the soil media. The phosphorous index (P-index) of the soil media is an important factor when considering the amount of P that is able to be removed within a bioretention cell. The P-index indicates the soil's ability to adsorb phosphorous. A low P-index means that the soil has low levels of P adsorption, which means the soil can readily capture phosphorous present in the inflow. A high P-index indicates that the soil is already saturated with phosphorous and therefore has difficulty adsorbing any additional phosphorous (Hardy et al., 2003). In the study done by Hunt et al. (2006), cell G1 had medium P-index soil, while cell G2 had high P-index soil (Table 2). Of the 21 outflow samples collected from these two cells, 20 of the samples showed a lower TP concentration from cell G1. An increase in TKN may have been due to the presence of an organic carbon source within the soil media. Even though there was a significant increase in some pollutant concentrations, the overall nutrient mass was still decreased between the inflow and the outflow due to the successful reduction of flow volume (Hunt et al., 2006).

Internal Storage Zones

Traditional bioretention design calls for the inclusion of underdrains to allow for the release of infiltrated water in areas with *in situ* soils with low infiltration rates. Underdrains are often surrounded by gravel to allow for inflow into the pipes, and are covered with nonwoven geotextile material to discourage sediment from entering the perforations along the pipe to avoid clogging (Davis, 2008). In more recent designs, ISZs have been included to determine the effect they would have on the removal of nitrate from influent stormwater runoff (Hunt et al., 2006; Davis, 2008; Passeport et al., 2009; Dietz and Clausen, 2006). ISZs are created by fitting

underdrain systems with upturned elbows at their outlet end in order to create a saturated portion within the bottom of the cell, thus forming anaerobic conditions (Hunt et al., 2006) (Figure 2). This saturated layer is typically 0.45-0.75 m deep (Hunt et al., 2006; Passeport et al., 2009).

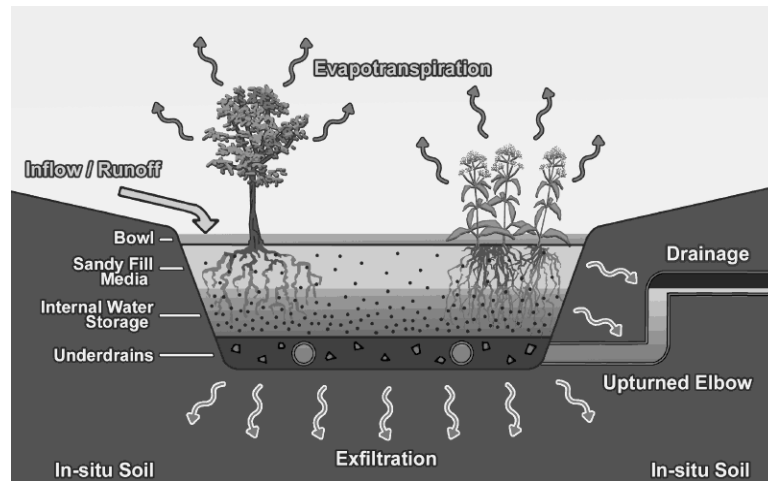


Figure 2. Illustration of a bioretention cell with ISZ.

The cooler, dryer climate conditions that accompany fall and winter months tend to slow the microbial activity necessary for denitrification to occur, thus nitrate removal may be higher in warmer months (Passeport et al., 2009). A study was performed by Dietz and Clausen (2006) which adapted the bioretention cells previously studied by Dietz and Clausen in 2005, to include an ISZ of 0.5 m. It was found during this study that $\text{NO}_3\text{-N}$ concentrations leaving the partly saturated system were significantly lower than those entering, possibly due to the transformation of $\text{NO}_3\text{-N}$ to other forms of nitrogen (Dietz and Clausen, 2006). Studies done by Hunt et al. (2006) showed that ISZs can have no impact on TN outflow concentrations. There is evidence that sediment-bound phosphorous can also be removed in the ISZ (Dietz and Clausen, 2006).

Significant nitrate removal is not expected in traditionally designed bioretention facilities (Hunt et al., 2008; Bratieres et al., 2008, Brown and Hunt, 2011). This is partly due to the fact that nitrate does not adsorb readily to soil particles (Davis et al., 2006). Nitrate is converted to nitrogen gas via denitrification (Richardson and Vepraskas, 2001). Slight denitrification may occur in a cell containing no ISZ if anoxic conditions happen to form in pockets of soil in the cell media (Davis et al., 2006; Hunt et al., 2006). Hunt et al. (2006) also attributed the high removal of $\text{NO}_3\text{-N}$ in cell G2 (75% removal) during the study to the high organic matter content in this cell, which may have been a sufficient carbon source to allow for microbial activity to convert some of the $\text{NO}_3\text{-N}$ to N_2 gas (Tables 2 and 3).

Kim et al. (2003) determined a most effective electron donor and carbon source suitable for the bacteria present in the anaerobic zone to perform denitrification. The column test used synthetic runoff to infiltrate through a sandy media. Of the electron-donating substrates tested (newspaper, leaf mulch compost, sawdust, wood chips, alfalfa, wheat straw, and sulfur), newspaper proved to be the most successful in promoting denitrification throughout the range of nitrate loadings and flowrates tested. This may have been partly due to newspaper's rapid decomposition rate as well as the ease by which bacteria could adhere to the material (Kim et al.,

2003). Davis et al. (2008) incorporated the findings from this study directly into the design of one cell (Cell A) constructed at the University of Maryland to treat asphalt parking lot runoff (Table 2). The ISZ of cell A consisted of a 17:1 mix of newspaper and sand, respectively (Davis, 2008).

Hydrology

Dietz (2007) attributed the macroporous nature of bioretention soil media for the ability of bioretention cells to have fairly consistent infiltration during ground freezing, claiming that rapid thawing occurs once stormwater runoff enters the system. Dietz and Clausen (2005), however, correlated overflow from their systems with a cold, snowy winter during which the systems experienced frequent frost. Muthanna et al. (2008) examined the effects of cold climate on bioretention cell hydrology. They recommended that bioretention cells installed in colder climates should contain underdrains that are installed below the frost line to prevent freezing within the pipes. It was also observed that bioretention systems do not achieve as high a hydraulic detention when ambient temperatures are below freezing. Lag times within the rain gardens also decreased from 69 minutes in the warm season to 59 minutes in the cold season, though this may have been partly a result of a higher maximum storm intensity in the cold season (Muthanna et al., 2008). Emerson and Traver (2008) reported a noticeable difference in hydraulic conductivity of the bioretention cell studied at Villanova University, Pennsylvania due to the variation in dynamic viscosity of water that occurred between winter and summer months.

Peak flow mitigation in a bioretention cell is directly associated with the size of the bioretention cell as well as the rate of infiltration and the potential for water storage within the soil pores (Davis et al., 2009; Hunt et al., 2008). Bioretention cells also promote evapotranspiration, as well as exfiltration into surrounding native soils, which encourages groundwater recharge (Davis et al., 2009; Jones et al., 2009; Li et al., 2009). Both infiltration and evapotranspiration necessarily decrease runoff. In the study performed by Davis (2008) (Table 3), Cell A and Cell B delayed peak flow by approximately two hours, and also reduced flow rates by 63 and 44% within Cell A and Cell B, respectively. Bioretention cells are often able to capture small storms in their entirety (Davis, 2008; Hunt et al., 2008; Li et al., 2009; Jones and Hunt, 2009), which supports their pollutant removal and hydrologic attenuation abilities. The antecedent moisture conditions within a bioretention system also have an effect on the hydrologic performance of the cell (Davis, 2008; Li et al., 2009). Hunt et al. (2006) analyzed seasonal effects on outflow reduction, reporting much higher ratios of outflow to runoff in the winter due to lower rates of evapotranspiration in winter as well as a higher water table level, also a result of lower evapotranspiration.

Li et al. (2009) found that bioretention improvements to hydrology are substantial for smaller rain events, but deteriorate for larger storms. Cells with larger volumes of soil media mitigate larger storm volumes better. Li et al. (2009) also found that an ISZ may not have a notable impact on outflow from larger events, but does serve to fully capture smaller events. Li et al. (2009) reported that cell G1 had 37% of its monitored storms produce outflow, while the nearly otherwise identical cell G2 (no ISZ) produced outflow from 65% of the storms (Table 3).

The literature suggests that bioretention is a highly effective means of pollutant reduction and peak flow dampening for stormwater runoff. It was noted that certain design aspects of

bioretention cells can actually increase concentrations of pollutants, such as the increase of phosphorous in soil media with a high P-index. It is also confirmed that including an ISZ in the bioretention cell can significantly improve the removal of nitrate from runoff.

The vast majority of studies analyzing the performance of bioretention cells focus their research on optimizing the function of appropriately-sized systems. This leaves a pressing need for research on undersized systems. Brown and Hunt (2011) examined undersized bioretention cells installed to treat parking lot runoff. The cells monitored by Brown and Hunt (2011) were undersized due to errors made during construction which resulted in ponding depths and surface storage volumes at 38% and 45% of the designed surface storage volumes for the 0.6 m and 0.9 m media depth cells, respectively (Table 2). Larger surface areas increased the likelihood that larger storms would be captured and treated due to decreased overflow. According to the design, only 18% of storms should have produced overflow, yet 62% and 57% of events generated overflow for the 0.6 m and 0.9 m deep cells, respectively. The deeper cells generated fewer overflows because of their capacity to infiltrate more water, supporting the benefits of deeper cell media.

Retrofitted bioretention cells are a popular SCM choice in urban settings, yet highly urbanized areas often have limited space suitable for the construction of a full-sized bioretention cell. There are also unique issues associated with the treatment of runoff from highway bridge decks, specifically due to their relatively inaccessible locations. SCMs commonly retrofitted to treat urban stormwater runoff are installed with difficulty near highways and bridge decks because of the lack of available space as well as the linearity of the highway systems and their surrounding land. Therefore, it is important to look further into the effectiveness of undersized bioretention cells in treating runoff from such urbanized locations, particularly if the undersized cell can be directly compared to a full-sized bioretention cell that is simultaneously treating runoff from the same watershed.

Table 1. Summary of nutrient and metal removals from bridge decks presented as site mean EMCs.

Author(s)	Location	Land Use	Traffic Load (veh/day)	Nutrients and Solids (mg/L)						Total Metal (µg/L)				Dissolved Metals (µg/L)			
				NO ₃ -N	NH ₃ -N	TKN	TN	TP	TSS	Cd	Cu	Pb	Zn	Cd	Cu	Pb	Zn
Gan et al. (2007)	Gangzhou, China	rural	31000	2.13	-	-	4.81	0.18	111.1	-	90	92.3	700	-	-	-	-
		urban	22170	3.49	-	-	7.32	0.39	250.1	-	140	118.2	1760	-	-	-	-
Yousef et al. (1984)	Orlando, FL	urban	55000	-	-	-	-	-	-	2	48	617	292	1	22	39	50

Table 2. Descriptions of previously studied bioretention cells.

Author(s)	Site Name	Location	Watershed Comp.	Watershed Size (ha)	S.A. to D.A. Ratio (%)	S.A. (m ²)	Fill Media Depth (m)	Fill Soil Type	Ponding Depth (m)	Veg/ Cover	Underdrain no. and size	ISZ	Description
Brown and Hunt (2011)	0.6 m media cells	Nashville, NC	asphalt parking lot	0.68	4.25	289	0.6	86-89% sand, 8-10% silt, 3-4% clay	0.13	shrubs, perenn, trees	4 @ 15.25 cm	no	storage capacity 38% of designed capacity
	0.9 m media cells	Nashville, NC	asphalt parking lot	0.43	4.79	206	0.9	86-89% sand, 8-10% silt, 3-4% clay	0.15	shrubs, perenn, trees	5 @ 15.25 cm	no	storage capacity 45% of designed capacity
Davis et al. (2001)	Small Box	MD	N/A	N/A	5	0.813	0.61	sandy loam	0.2	shrubs, mulch	3 @ 2.2 cm	no	Lab-scale prototype
	Large Box	MD	N/A	N/A	5	4.64	0.91	sandy loam	0.2	shrubs, mulch	6 @ 3.2 cm	no	Lab-scale prototype
Davis (2008)	Cell A	University of MD	asphalt parking lot	0.24	1.2	28	1.2	sand, topsoil, compost, clay	-	shrubs, mulch	1 @ 15.25 cm	yes	sand, newspaper; anoxic zone
	Cell B	University of MD	asphalt parking lot	0.24	1.2	28	0.9	sand, topsoil, compost, clay	-	shrubs, mulch	1 @ 15.25 cm	no	
Dietz and Clausen (2005)	Rain garden 1	Haddam, CT	rooftop	0.011	8.6	9.18	0.6	loamy sand	0.013	shrubs, mulch	1 @ 10.2 cm	no	EPDM liner (impermeable)
	Rain garden 2	Haddam, CT	rooftop	0.011	8.6	9.18	0.6	loamy sand	0.013	shrubs, mulch	2 @ 10.2 cm	no	EPDM liner (impermeable)
Emerson and Traver (2008)	Bioinfiltration Traffic Island	Villanova, PA	35% impervious	0.5	2.9	144	1.2	sandy loam	0.5	veg, mulch	-	no	

Hunt et al. (2006)	C1	Chapel Hill, NC	asphalt pavement	0.06	14.9	89.4	1.2	sand, low OM content	0.23	trees, shrubs, mulch	2 @ 15.25 cm	no	
	G1	Greensboro, NC	parking lot	0.5	5	250	1.2	loamy sand	0.23	trees, shrubs, mulch	2 @ 15.25 cm	yes	
	G2	Greensboro, NC	rooftop, parking lot	0.48	5	240	1.2	loamy sand	0.23	trees, shrubs, mulch	2 @ 15.25 cm	no	
Hunt et al. (2008)	HMBC	Charlotte, NC	municipal parking lot	0.37	6.2	229	1.2	loamy sand	0.18	trees, shrubs, grass, mulch	1 @ 15.25 cm	no	
Li et al. (2009)	Cell CP ^[1]	College Park, MD	parking lot, roadway	0.26	6	181	0.5-0.8	sandy loam	0.1-0.34	trees, shrubs, mulch	2 @ 15.25 cm	no	
	Cell SS ^[1]	Silver Spring, MD	parking lot, driveway	0.45	2	102	0.9	sandy clay loam	0.3	trees, shrubs, mulch	2 @ 15.25 cm	no	
	G1	Greensboro, NC	parking lot	0.5	5	250	1.2	loamy sand	0.23	trees, shrubs, mulch	2 @ 15.25 cm	yes	
	G2	Greensboro, NC	rooftop, parking lot	0.48	5	240	1.2	loamy sand	0.23	trees, shrubs, mulch	2 @ 15.25 cm	no	
	L1	Louisburg, NC	parking lot	0.36	4.5	162	0.5-0.6	sandy loam	0.15	trees, shrubs, mulch	2 @ 15.25 cm	no	
	L2	Louisburg, NC	parking lot, ball field	0.22	4.5	99	0.5-0.6	sandy loam	0.15	trees, shrubs, mulch	2 @ 15.25 cm	no	impermeable membrane
Muthanna et al. (2008)	Rain garden 1	Trondheim, Norway	impervious surface	0.002	5	0.96	0.5	top soil and sand	0.15	trees, flowers, shrubs, mulch	1 @ 0.2 cm	no	small-scale prototype

	Rain garden 2	Trondheim, Norway	impervious surface	0.002	5	0.96	0.5	top soil and sand	0.15	trees, flowers, shrubs, mulch	2 @ 0.2 cm	no	small-scale prototype
Passeport et al. (2009)	North Cell	Graham, NC	parking lot, residential	0.69	1.5	102	0.75	expanded slate fines, sand, OM	0.23	grass	2 @ 10 cm	yes	0.45 m ISZ
	South Cell	Graham, NC	parking lot, residential	0.69	1.5	102	1.05	expanded slate fines, sand, OM	0.23	grass	2 @ 10 cm	yes	0.75 m ISZ

[1] These cell descriptions are also the same for Li and Davis (2009).

Table 3. Summary of nutrient and metal removals from previously studied bioretention cells.

Author	Bioretention Cell Name	Description	Percent Removals												
			TSS	NO ₃ -N	NO ₂₋₃ -N	NH ₃ -N	TKN	TN	NH ₄ -N	O-PO ₄	TP	Cd	Cu	Pb	Zn
Brown and Hunt (2011) ^[1]	0.6 m media cells	Three cells, 0.6 m media depth	70	-	-86	-	36	8.2	77	-53	0.5	-	-	-	-
	0.9 m media cells	Two cells, 0.9 m media depth	84	-	-149	-	56	9.1	78	-18	41	-	-	-	-
Davis et al. (2001) ^[1]	Small Box	4.1 cm/hr flowrate, 6 hr	-	-	-	-	86	-	-	-	82	-	-	-	-
	Large Box		-	97	-	-	97	98	79	-	99	-	-	-	-
Davis et al. (2006) ^[1]	Small Box	3 hr duration	-	35	-	-	85	80	-	-	87	-	-	-	-
	Small Box	2 cm/hr flowrate	-	13	-	-	87	80	-	-	87	-	-	-	-
	Large Box	2 cm/hr flowrate	-	99	-	-	99	99	-	-	99	-	-	-	-
	Small Box	12 hr duration	-	8	-	-	74	49	-	-	78	-	-	-	-
	Small Box	8.1 cm/hr	-	15	-	-	32	30	-	-	52	-	-	-	-
	Large Box	8.1 cm/hr	-	70	-	-	73	72	-	-	73	-	-	-	-
	Small Box	Double Conc	-	31	-	-	83	79	-	-	91	-	-	-	-
Small Box	Half Conc	-	15	-	-	66	58	-	-	81	-	-	-	-	

	Large Box	Half Conc	-	96	-	-	94	94	-	-	92	-	-	-	-
Dietz and Clausen (2005) ^[2]	Rain garden 1 and 2	Combined removal	-	35.4	-	84.6	31.2	32	-	-	110.6	-	-	-	-
Hunt et al. (2006) ^[1]	C1		-	13	-	86	45	40	-	69	65	-	-	-	-
	G2		-170	75	-	-0.99	-4.9	40	-	-9.3	-240	-	99	81	98
Hunt et al. (2008) ^[2]	HMBC		59.5	-	-4.7	-	44.3	32.2	72.3	-	31.4	-	54	31.4	77
Li and Davis (2009) ^[3]	Cell CP ^[1]	trapezoid	96	-108	-	-	25	-3	-	-	-36	-	65	83	92
	Cell CP ^[2]		88	-170	-	-	-11	-53	-	-	-200	-	31	55	78
	Cell SS ^[1]	triangle	99	99	-	-	87	97	-	-	100	-	96	100	99
	Cell SS ^[2]		88	86	-	-	-30	-10	-	-	0	-	0	0	80
Passeport et al. (2009) ^[1]	North cell	0.45 m ISZ	-	-	43	78	48	56	-	52	53	-	-	-	-
	South Cell	0.75 m ISZ	-	-	1	88	68	47	-	77	68	-	-	-	-

[1] Mass reduction

[2] Concentration reduction

[3] Presented as median percentages

Swales

Swales are used most commonly as simple water conveyance structures located along streets and highways (Bäckström et al., 2006). They help direct flow and reduce velocities due to their mild slopes and vegetative cover (Yousef et al., 1987; US EPA, 1999; NC DENR, 2007; Barrett et al., 1998b). Swales are incorporated into stormwater drainage systems in place of curbs and gutters in areas where they can withstand flow velocities. Swales are a more cost effective means of flow routing than curb and gutter systems (Kercher et al., 1983). In the early 1980's, swales became recognized for their water quality improvement potential (Kercher et al., 1983; Yousef et al., 1985).

Lower removal efficiencies in swales are expected for pollutants that are dissolved, while the removal of heavy metals can be expected to approach 50%. Yu et al. (2001) discussed the importance of check dams in pollutant removal due to their role in slowing flow rates and enhancing sedimentation and retention time. Sedimentation is the primary means of runoff water quality enhancement in vegetated stormwater controls (Mazer, 2001). The data obtained from the experiments performed by Yu et al. (2001), presented in Tables 4 and 5, showed that check dams had an impact on pollutant removal because of their ability to increase retention time and temporarily decrease flow velocities. For instance, TP capture was 77% and 50% when the check dam was present and not present, respectively. However, no significant change in removal of TN was reported. Typical pollutant removal efficiencies expected in a vegetated swale according to the US EPA (1999) are shown in Table 5.

Yousef et al. (1985) found infiltration rate strongly correlated mass removal rates of phosphorous and nitrogen. Metal removal occurred with the removal of suspended solids because of the tendency for metals in the form of charged ions, such as iron (Fe) and zinc (Zn), to adsorb to soil particles (Table 5). When the particles settle out in the treatment system, attached metals are simultaneously removed. Metals that are complexed with inorganic species or those that have zero charge will not be easily removed, such as copper (Cu). Ionic species of nutrients, such as NH_4^+ , NO_2^- , NO_3^- , H_2PO_4^- , HPO_4^{2-} , and PO_4^{3-} are effectively retained within a swale by sorption, precipitation, and biological uptake (Yousef et al., 1985; Bäckström, 2003).

Swale length is also an important design consideration when removing total suspended solids (TSS) and nutrients. Larger particles with higher settling velocities tend to settle out of the influent flow within the first few meters of the channel length (Bäckström, 2002). Particle trapping efficiency decreases exponentially down the length of the channel to a certain point beyond which any remaining particles within the flow will remain suspended (Deletic, 1999). Yu et al. (2001) suggested that the removal efficiency of suspended particles and nutrients does not improve beyond a swale length 75 m, regardless of channel slope. The ability of particles of any size to settle is dependent to some degree on the velocity of the flow as well as the infiltration rate of the soil within the swale (Bäckström, 2003). Bäckström (2002) performed laboratory experiments on two five-meter long artificial swales as well as seven grassed swales in a field experiment during which runoff events were simulated with artificial stormwater which contained sediment from the streets of Lulea, Sweden. Table 4 shows some design specifications for these swales. This experiment showed that sedimentation accounted for a higher degree of trapping efficiency than did filtration, making the swale length an important design parameter due to an increased likelihood to trap smaller particles with an increase in length.

Barrett et al. (1998b) suggested that swale bottom length and slope are not as important as the slope and length of the sides of the swale in removing pollutants from highway runoff. The authors realized that the sides of the channel act as filter strips as the water travels toward the center of the channel in the form of sheet flow. Barrett et al. (1998b) recommended that swales be designed with a triangular cross-section to increase travel time over the side slopes. Nutrient and metal pollutant removal rates for this experiment are shown in Table 5, and the swale descriptions are shown in Table 4.

The role of vegetation in particle and nutrient removal has been debated among researchers. Bäckström (2002) observed that swales with short grass and thin vegetation had a TSS removal of 80%, while the swales with fully developed vegetation had TSS removals above 90% (Table 5). Sparsely vegetated swales are shown not only to trap less sediment, but also allow for erosion to occur within the channel. More densely vegetated channels, on the other hand, discourage re-suspension and erosion as well as slow flow velocities to encourage particle settlement (Bäckström, 2002). Deletic (1999) supported the idea of grass length being an influence on sediment removal through her tests on an artificial channel with varying grass lengths (2.56 cm and 3 cm). It was observed that sediment concentration decreases with an increase in grass length (Deletic, 1999).

The US EPA (1999) suggests that the depth of the water of the design storm passing through the swale should not exceed the height of the grass. This was bolstered by Bäckström (2003) who noted that higher velocities of flow occur above the grass. From this observation, however, it was concluded that a very dense turf may not be the most favorable design if the density of the grass encourages water to bypass the grass filtration and travel above the vegetation. Yousef et al. (1985) suggested that a grass cover of 20% or less may actually decrease contaminants more efficiently than grass cover of 80% or more because the thick grass cover actually decreases available soil sorption sites and increases organic litter, which contributes to suspended solid loads.

Mazer et al. (2001) found that frequent and prolonged inundation of a swale will negatively impact the ability for vegetation to establish, and that dry conditions in the summer benefit growth capabilities by allowing time for seed germination. Erosive flow did not prove to be an important factor in vegetation establishment in these studies; however, the amount of available sunlight was the limiting factor to a good standing of grass.

Bäckström (2003, 2006) suggested grassed swales do not consistently achieve high pollutant removal rates, but instead may be used to attenuate pollutant load extremes. This reinforces the idea of swales being used as a preliminary treatment device and not as the sole treatment device for impermeable surface runoff. In the Sodra Hamnleden swale, for instance, three of seven observed runoff events produced a reduction in suspended solids. It was observed that low concentrations of influent suspended solids had fewer suspended solids retained within the swale, and a removal efficiency of over 50% was only achieved when influent suspended solids concentrations were over 100 mg/L (Bäckström, 2003). Bäckström observed that swales act as a pollutant source rather than a pollutant sink if the influent pollutant concentration is below a certain point, therefore making swales unreliable at reducing pollutant concentrations because of their dependence upon the condition of the influent runoff. These results also suggest that certain pollutants are not permanently held in the swale and may become re-suspended within the flow.

Similar observations were made by Bäckström (2003) about the variable heavy metal removal, reporting that the observed swales acted as a source for Cu, Pb, and Zn during flows containing low influent concentrations. The highest removal efficiencies were found for Zn, while the EMCs of dissolved Cu were two to four times higher in swale outflow than in road runoff (Bäckström, 2003). Bäckström et al.'s (2006) study suggested that copper was released rather than trapped due to its affinity for organic complexes and colloids which were transported from the swale in the water phase. They also observed no significant difference in lead between the swale inflow and outflow; the EMCs of zinc decreased through the swale in all but one of the four storm events observed for metals removal (Table 5).

Soil infiltration can play an important role in pollutant removal in a swale. It is recommended that swales be built on highly permeable, dry soil with high infiltration rates. Swales built on sites that are consistently wet do not remove contaminants as effectively (Yousef et al., 1987); one exception may be the removal of nitrate. Table 5 shows the range of infiltration rates observed in the field swales studied by Bäckström (2002), and descriptions of these swales are shown in Table 4. Four of the seven field swales infiltrated 33% of inflow volume (F1, F3, F5, F7), while the swales F2 and F6, despite their steeper centerline slope, infiltrated 66% of the inflow volume, as these swales were constructed on more permeable soil. Bäckström also observed that swales F2 and F6 captured the largest fraction of particles without experiencing re-suspension. Swale F6, for example, captured 80% of the influent particles at a settling velocity of 0.1 m/h (Bäckström, 2002). The efficiency of swales F2 and F6 may also be partly attributed to their well-established vegetative cover (Bäckström, 2002).

Limited data are available for the potential flow mitigation of swales. Yousef et al. (1987) performed a hydrologic analysis in the grassed swales previously studied by Yousef et al. (1985) in Orlando, Florida (Maitland and Epcot swales) (Tables 4 and 5). The hydraulic and hydrologic data analyses showed that in the Maitland swale, average inflow rates ranged from 0.036 to 0.154 m³/m²-hr, while average outflow rates ranged from 0.0 to 0.068 m³/m²-hr. For the Epcot swale, average inflow rates ranged from 0.053 to 0.105 m³/m²-hr, while average outflow rates fell between 0.039 and 0.071 m³/m²-hr. Also from the Epcot site, it was determined that 90% of the inflow left the swale as outflow when the swale soil was saturated (Yousef et al., 1987).

The literature suggests that swales have a modest to moderate effect on the treatment of stormwater runoff, but should not be used as the only means of water treatment. Swales should be used in conjunction with other SCMs to achieve sufficient treatment levels (US EPA, 1999; Yousef et al., 1987; Bäckström, 2003). Influent concentrations and influent flow volumes had an effect on the treatment capabilities of the swale, impacting whether the swale would either trap or export nutrients (Bäckström, 2003).

Swales are a widely used stormwater conveyance design commonly incorporated into the linear environments surrounding roadways and highways. Their widespread use supports the need for research to determine their effectiveness as natural highway runoff treatment facilities.

Table 4. Descriptions of previously studied swales.

Author(s)	Site Name	Location	Drainage Area (m ²)	Watershed Composition	Grass Height (mm)	Grass Spacing (mm)	Swale Length (m)	Cross-Sectional Shape	Side Slope (%)	Centerline Slope (%)	Description
Bäckström (2002)	L1	Lulea, Sweden	simulated events	-	25	2.5	5	triangular	20	0.5	laboratory swales
	L2	Lulea, Sweden	simulated events	-	45	7	5	triangular	20	0.5	laboratory swales
	F1	Lulea, Sweden	simulated events	-	50	20	5	triangular	15	1	field swales
	F2	Lulea, Sweden	simulated events	-	50	15	5	triangular	27	7.3	field swales
	F3	Lulea, Sweden	simulated events	-	100	37	5	triangular	33	3.2	field swales
	F4	Lulea, Sweden	simulated events	-	60	15	5	triangular	15	4.9	field swales
	F5	Lulea, Sweden	simulated events	-	50	20	10	triangular	15	1	field swales
	F6	Lulea, Sweden	simulated events	-	50	15	10	triangular	27	7.3	field swales
	F7	Lulea, Sweden	simulated events	-	100	37	10	triangular	33	3.2	field swales
Bäckström (2003)	N/A	N. Sweden, Lulea	simulated events	-	50-100	15-37	10	triangular	15-27	1-7.3	
	N/A	Sodra Hamnleden, Lulea	-	road	-	-	110	triangular, round bottom	-	1	7,400 veh/day traffic
	N/A	Central Lulea	-	highway	-	-	-	triangular	-	-	20,000 veh/day traffic, during snowmelt
Barrett et al. (1998)	Walnut Creek	Austin, TX	104,600	highway	-	-	1055	triangular, round bottom	9.4	1.7	47,000 veh/day traffic
	US 183	Austin, TX	13,000	highway	-	-	356	triangular, round bottom	12.1	0.73	111,000 veh/day traffic

Yousef et al. (1987)	Maitland	Orlando, FL	simulated events	highway	50-100	-	53	-	>17	0.6	Maitland/I-4 Interchange, older constructed
	Epcot	Orlando, FL	simulated events	highway	-	-	170	-	>17	0.1	EPCOT/I-4 Interchange, newly constructed
Yu et al. (2001)	N/A	Natl. Taiwan Univ., Taiwan	simulated events	-	-	-	30	parabolic	-	1	-
	GC	Northern Virginia	-	highway	-	-	274.5	-	-	3	39,000 veh/day traffic

Table 5. Summary of nutrient and metal removals from previously studied swales.

Author	Swale Name	Description	Swale Length (m)	Infilt (%)	TSS	Percent Removals										
						NO ₃ -N	NO ₂₋₃ -N	TKN	TN	NH ₄ -N	O-PO ₄	TP	Cd	Cu	Pb	Zn
Bäckström (2002) ^[2]	L1, L2	Laboratory swales	5	0	80-90+	-	-	-	-	-	-	-	-	-	-	-
	F1-F7	Field Swales	5 to 10	33-66	80-98	-	-	-	-	-	-	-	-	-	-	-
Bäckström (2003)		Northern Sweden, Lulea ^[2]	10	33-66	70-98	-	-	-	-	-	-	-	-	-	-	-
		Sodra Hamnleden, Lulea ^[3]	110	54	70	-	-	-	-	-	-	-	-	34	-	66
		Central Lulea during snowmelt ^[2]	-	-	96-99	-	-	-	-	-	-	-	-	93-96	96-99	78-94
Barrett et al. (1998b) ^[3]	Walnut Creek		1055	-	87	36	-	54	-	-	-	45	-	-	31	79
	US 183		356	-	89	59	-	46	-	-	-	55	-	-	52	93
US EPA ^[1]			-	-	81	38	-	-	-	-	-	9	42	51	67	71
Yousef et al. (1985) ^[2]	Maitland	Maitland/I-4 Interchange	53	-	-	-	13	-	11	31	24	25			0	86
	Epcot	Epcot/I-4 Interchange	170	-	-	-	-11	-	-7	-2	9	3	43	8	57	62
Yu et al. (2001) ^[3]	TA	4.2x10 ⁻³ m ³ /s inflow, check dam	30	-	69.7	-	-	-	20.9	-	-	76.9	-	-	-	-

	TB	0.86x10 ⁻³ m ³ /s inflow, check dam	30	-	86.3	-	-	-	23.1	-	-	58.1	-	-	-	-
	TC	4.0x10 ⁻³ m ³ /s inflow, no check dam	30	-	47.7	-	-	-	20	-	-	50.3	-	-	-	-
	TD	0.9x10 ⁻³ m ³ /s inflow, no check dam	30	-	67.2	-	-	-	13.8	-	-	28.8	-	-	-	-

[1] Median percent removal [2] Concentration reduction [3] Mass reduction

Research Goals

The goals of this research were threefold: (1) Examine the quality and quantity of runoff from a raised bridge deck located on I-540 in Knightdale, North Carolina; (2) Examine the impact that a full-sized bioretention cell and a undersized bioretention cell has on bridge deck runoff; and (3) examine the impact of a swale on bridge deck runoff.

Methods

Study Site Background

The study site was located in Knightdale, Wake County, North Carolina, in an easement of two I-540 bridge decks which passed over Mango Creek (35°47'3.4"N, 78°30'48.4"W). In 2010, the average annual daily traffic load for the bridge decks (combined northbound and southbound) was estimated to be 34,000 vehicles per day (all lanes, both directions) (NCDOT, 2010). Table 6 was adapted from 7-day quarterly traffic data for the bridge decks over Mango Creek and provides traffic count breakdowns by lane for the northbound (NB) and southbound (SB) bridge decks (NCDOT, 2010). The northbound bridge deck was treated by the bioretention cells. The swale treated runoff from the southbound bridge deck.

Table 6. Seven day quarterly traffic data for NB and SB Mango Creek bridges.

Quarter	Lane 4	Lane 5	Lane 6	Quarterly Avg. Daily Traffic
Q2 NB ^[1]	9889	44489	68989	17624
Q3 NB	10079	45801	70313	18028
Q4 NB	8514	41718	66428	16666
Q2 SB ^[1]	72519	39010	5345	16696
Q3 SB	73528	40412	5364	17043
Q4 SB	68371	37160	4455	15712

[1] No data available for first quarter.

Prior to bioretention cell construction, the runoff from the northbound bridge deck drained through the roadside scuppers directly to a wetland and creek below. Prior to construction of the swale, the runoff from the southbound bridge deck drained through roadside scuppers (circular drainage openings) directly to a wetland below. This wetland was located approximately 18 m (60 ft) from the outlet of the retrofitted swale.

The drainage area for the bioretention cells was 0.4 ha (0.98 ac) of 100% impervious concrete (CN 98; NRCS, 2004 a, b). The bridge deck had a 2% cross slope and 0.5% longitudinal slope. Runoff from the bridge deck drained into the scuppers located along the bridge deck's outer edge (Figure 3). Thirty-two scuppers spaced 3.35 m (11 ft) apart (centerline to centerline) were retrofitted to a 30.5 cm (12 in) diameter PVC pipe which was installed in October 2009. The pipe rerouted runoff to a splitter box. The highway leading up to the bridge deck was hydraulically isolated from the bridge as it was drained separately by drop structures upslope of the bridge. The inside shoulder of the bridge deck (4 m (12 ft) width) also did not contribute runoff. The time of concentration for the entire catchment area, including the pipes leading to

the bioretention cells, was 12 minutes, as determined by modeling the catchment in PCSWMM (CHI 2009; US EPA 2009b) and by direct observation.



Figure 3. Drainage pipe to bioretention cells.

The drainage area contributing to the swale was 0.46 ha (1.13 acres) of 100% impervious concrete (CN 98; USDA NRCS, 2004 a, b). The bridge deck had a 2% cross slope and 0.5% longitudinal slope. Runoff from the bridge deck drained into the scuppers located along the bridge deck's outer edge (Figure 4). A portion of these scuppers were retrofitted to a 30 cm (12 in) diameter PVC pipe in October 2009. Forty-three scuppers spaced 3.4 m (11 ft) apart, centerline to centerline, were connected to the pipe which routed stormwater to the inlet of the swale. The highway leading up to the bridge deck contributed negligible amounts of runoff to the bridge as it was drained separately by drop structures situated upslope of the bridge. The inside shoulder of the bridge deck was not part of the catchment, as its slope broke toward the inside barrier wall. The time of concentration for the entire catchment area, including the pipes leading to the swale, was 13 minutes, as determined by PCSWMM (CHI 2009; US EPA 2009b).



Figure 4. Bridge deck runoff conveyance pipe (left) and view of the downspout (right).

Bioretention

Bioretention Description and Characterization

Figure 5 shows both bioretention cells installed adjacent to the I-540 bridge deck. One of the bioretention cells was designed to be undersized while the other was designed to meet current North Carolina standards (NCDENR, 2007). The cells were designed by URS Corporation.



Figure 5. Large bioretention cell (left) and small bioretention cell (right).

The inlet flow from the northbound lanes was split relatively evenly to the inlets of two bioretention cells by a distribution box structure (Figure 6). The flow from the bridge deck entered the distribution box through a 38 cm (15 in) high-density polyethylene (HDPE) pipe where it then flowed to the large cell and small cell HDPE inlet pipes, both 30 cm (12 in) in diameter. Sluice gates were installed at the entrance of the three outlet ports in the distribution box to control outflow to the SCMs (Figure 6). The sluice gates to the large and small bioretention cells were kept open while the third sluice gate was kept closed throughout the duration of the study to prevent the flow to travel to a third LID practice which was not part of the study. Cinder blocks were placed in the center of the distribution box to help still the flow and prevent the water from “short circuiting” the large cell by traveling from the bridge deck pipe straight to the small cell inlet pipe.



Figure 6. Bioretention flow distribution box (left) and sluice gates in bioretention distribution box (right).

Both cells were designed with a 0.6 m (2 ft) deep internal water storage zone. The engineered soil media supplied by Wade Moore Equipment Company (Louisburg, NC) was 2.9% gravel, 86.8% sand, 7.8% silt, and 2.5% clay (NCDOT, 2011) with 3-5% of the total soil mix consisting of pine mulch organic matter. The media was in accordance with NC DENR's (2007) specification. *Design* characteristics for both cells are shown in Table 7.

Table 7. Design characteristics for bioretention cells at Mango Creek.

Characteristic	Large Bioretention Cell	Small Bioretention Cell
Length (m)	31	22
Width (m)	6	4
Surface Area (m ²)	186	93
Ponding Volume (m ³)	43	21
Soil Media Depth (cm)	51	51
Ponding Depth (m)	0.23	0.23

A survey of the cells was performed using a total station on October 29, 2010, to determine the *as-built* characteristics (Table 8). Soil media depth and ponding depth shown in the table are mean values.

Table 8. As-built characteristics for bioretention cells at Mango Creek.

Characteristic	Large Bioretention Cell	Small Bioretention Cell
Length (m)	31	22
Avg. Width (m)	6	4
Surface Area (m ²)	187.5	101
Ponding Volume (m ³) ^[1]	50.84	14.03
Avg. Soil Media Depth (cm)	61	74
Avg. Ponding Depth (m)	0.19	0.12
Range of Ponding Depth (m)	0.09 to 0.34	0 to 0.26

[1] Includes storage in the forebay.

Based on these values, the surface storage of the large bioretention cell was sized appropriately while the small cell was even further undersized than intended. The large cell and small cell surface areas were approximately 10% and 5% of their respective catchment areas, or 10% and 5% of one-half the bridge deck area. However, the large and small cell bowl volumes were 118% and 67% of their designed volumes, respectively. As a result, the large bioretention cell was able to capture the first 2.5 cm (1 in) of rainfall from the contributing drainage area as specified by the NCDENR Stormwater Best Management Practices Manual (2007) while the small cell was only able to capture runoff from 0.76 cm (0.3 in) of rain, which is less than the intended 1.27 cm (0.5 in) design storm.

Two 15cm (6 in) diameter perforated HDPE underdrains ran along the bottom of each bioretention cell to drain the infiltrated water within the cells into concrete outlet structures. The underdrains were wrapped with nonwoven geotextile material to prevent clogging. The bottoms of the cells were filled 30 cm (12 in) deep with washed No. 57 stone (Muench, 2003) which enveloped the underdrains.

Polypropylene woven monofilament geotextile fabric was placed between the soil media and the stone in order to prevent settling of soil into the stone layer. To create the 0.6 m (2 ft) ISZ, the underdrains had an upturned elbow (Figure 7). Both bioretention cells were lined with permeable geotextile filter fabric below the No. 57 stone, vegetated with Centipede grass sod (*Eremochloa ophiuroides*), and designed with Class A riprap-lined forebays (also lined with geotextile fabric) at each of their inlets to still the runoff (Figure 8).



Figure 7. Underdrains of large cell (left) and upturned elbow at the outlet structure (right).

Overflow exited each bioretention cell by weir-flow over the cell's outlet structure. Once the underdrain flow and overflow entered the outlet structures of both cells, it was then conveyed offsite through a 30 cm (12 in) diameter HDPE pipe into a preformed scour hole.



Figure 8. Forebays of bioretention cells.

Monitoring Equipment

Monitoring equipment was installed to collect rainfall data and flow data. Rainfall intensity and depth were measured by an ISCO 674TM automatic tipping-bucket rain gauge and rain depth was also measured with a manual rain gauge (Figure 9). The automatic rain gauge was wired to an ISCO 6712TM portable sampler located at the inlet of the large bioretention cell. This portable sampler stored the rainfall data. The manual rain gauge was used to correct the rain data gathered by the automatic rain gauge. The tipping bucket did not tip fast enough (0.25 cm (0.01 in) interval) for some of the more intense storms to be accurately represented, thus the automatic

rain gauge occasionally underpredicted some storm intensities, thus underpredicting total rainfall depths. The rain gauges were mounted on a wooden post located between the two bioretention cells. This area was clear of trees and other obstructions.



Figure 9. Manual rain gauge and ISCO 674 rain gauge.

To monitor hydrologic data, the inlet pipes of the bioretention cells were fitted with a compound weir that consisted of a 120° v-notch lower portion and a rectangular upper portion (Figure 10, details in Appendix A).



Figure 10. Compound weir located at bioretention cell inlets.

ISCO 730™ bubbler flow modules, which were attached to the ISCO 6712™ portable samplers, were used to measure the height of the water over the invert of the weir. A stepwise stage/discharge relationship was developed for the weirs to relate water level to flowrate (ISCO, 1978). This relationship was field-verified by performing a bucket test at the inlets of both

bioretention cells which allowed for the inflow to be controlled and the discharge volume to be measured at different heights above the weir invert (Figure 11).



Figure 11. Timed water collection into bucket (left) and measurement of volume collected (right).

The drop inlet boxes which served as the outlet structures of the bioretention cells were fitted with 30 cm (12 in) outlet weirs, identical to those in the bioretention inlet pipes (Figure 12). Outflow from the cells was measured as a combination of underdrain flow and overflow.



Figure 12. Underdrain pipe outlet and drainage pipe fitted with a compound weir.

Water levels were measured in the bowl and media by HOBOTM water level loggers from August 2010 to October 2010. The water level loggers were installed in PVC wells located near the bioretention cell outlet structures (Figure 13). The wells were perforated every few centimeters to allow for water to enter. A mesh sock covered the wells to keep fines from entering.



Figure 13. HOBO® water level logger (left) and installed wells at cell outlets (right).

The ISCO 730™ bubbler-recorded water level readings were used to calculate flow rate, based on the measured stage/discharge relationship. Flow data were obtained from the locations shown in Figure 14. ISCO 6712™ samplers took flow-proportional, composite water quality samples. The samplers pulled a 200 mL aliquot per a specific volume of flow. Flow pacing was intermittently adjusted based on storm size and intensity (Appendix C). The portable samplers' pacing was set to pull samples for storm events between 0.5 and 5 cm (0.2 and 2 in). The sampler was programmed to pull a minimum of 5 aliquots and a maximum of 50. Bioretention inflow samples were obtained within the inlet pipe, 10 cm (4 in) behind weir. Bioretention outflow samples were pulled from the outlet structures. Sampling locations were in areas of well-mixed flow. Figure 15 shows an ISCO 6712™ portable sampler and some of the monitoring assembly.

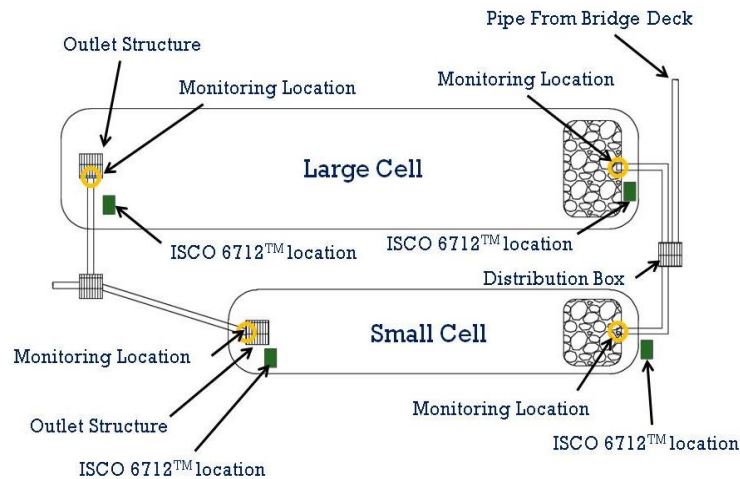


Figure 14. Bioretention cell schematic identifying flow monitoring locations.



Figure 15. ISCO 6712™ portable sampler (left) and green housing boxes (right).

Sampling Protocol

Samples were obtained from the locations shown in Figure 16. Inlet water quality samples were only taken at the entrance to the large cell. Since inflow was divided at the splitter box, it was assumed that the quality of water entering the small cell was similar to that entering the large cell.

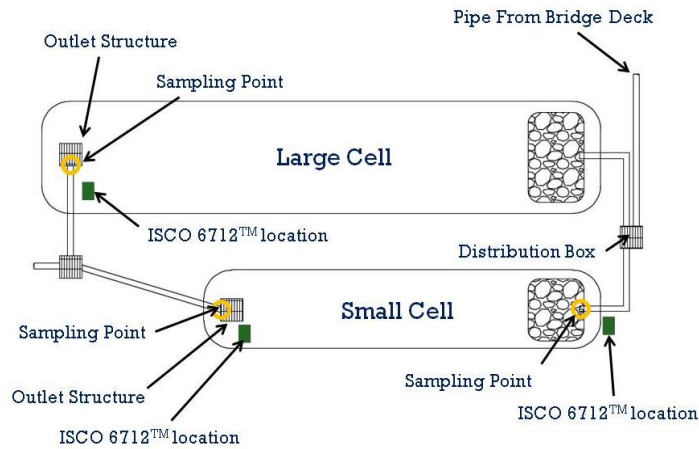


Figure 16. Bioretention cell schematic identifying sampling points.

Swale

Swale Description and Characterization

The swale, partially located underneath the southbound bridge deck, was designed by URS Corporation to convey the 10-year, 24 hour storm event. A Class A riprap-lined forebay and straw wattles were used to still flow as it entered the swale (Figure 17). The swale had a v-shaped cross-section (approximately 8:1 side slopes, average 6.4 m (21 ft) top width) with a 1.1 sinuosity, 2% longitudinal slope, and 37 m (120 ft) centerline length (Figure 17). The swale was vegetated with tall fescue sod (*Festuca arundinacea*). Average grass density and length measurements taken on 21 February, 2010, and 10 September, 2010, are shown in Table 9.

Table 9. Average grass density and length measurements^[1].

Date	Avg side slope grass density (blade/m ²)	Avg centerline grass density (blade/m ²)	Avg side slope grass height (m)	Avg centerline grass height (m)
2/22/2010	20667	9484	0.24	0.19
9/10/2010	15796	7183	0.25	0.26

[1] Grass sod laid on 15 September 2009.



Figure 17. Swale at Mango Creek.

Design Modification

Initially, the swale was designed and constructed with a centerline length of 46 m (150 ft). Shortly after construction (late October 2009), however, the soil around the outlet structure of the swale was observed to be sinking due to insufficient soil compaction around the box. The resulting damage from the settling of the box and soil was repaired, and a new swale exit point was constructed (Figure 18). The centerline length from the beginning of the swale (immediately after the rock-lined forebay) to the new high-density polyethylene (HDPE) outlet pipe of the swale was approximately 37 m (120 ft), or 80% of the original length.



Figure 18. Check dam looking downslope (left image) and outlet structure looking upslope (right image) of swale. Arrows point to check dam.

To monitor hydrologic data, the inlet pipe of the swale was fitted with a compound weir that consisted of a 120° v-notch lower portion and a rectangular upper portion (Figure 19, dimensions in Appendix H. See more information at related discussion in Chapter 2).



Figure 19. Compound weir located at swale inlet.

ISCO 730™ bubbler flow modules, which were attached to the ISCO 6712™ portable samplers, measured the height of the water over the invert of the weir. A stepwise stage/discharge relationship was developed for the weirs (Appendix H) to relate water level to flowrate (ISCO, 1978).

The weir located at the swale outlet was modified due to high velocity flow exiting the swale. The outlet pipe had a 16% slope, creating a substantial amount of elevation head on the outflow. The end of the swale outlet pipe was fitted with a baffled weir box on 21December, 2009, to still the outflow prior to traveling over the bubbler module and the compound weir (Figure 20).



Figure 20. Baffled weir box at the outlet of the swale (top and front view).

The ISCO 730™ bubbler module-recorded water level readings were used to calculate flow rate derived from the stage/discharge relationship. ISCO 6712™ samplers took flow-proportional, composite water quality samples (Figure 15). The samplers pulled a 200 mL aliquot per a specific volume of flow. Samples were obtained from the locations shown in Figure 21.

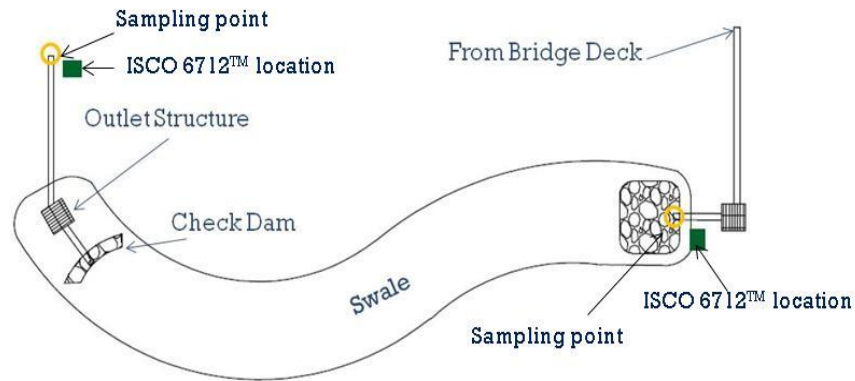


Figure 21. Swale schematic identifying sampling points.

Particle size distribution samples were collected between October 15, 2010 and December 13, 2010. Any remaining sample volume in the 10L jars was used in determining particle size distributions at the swale inlet and outlet. These samples were taken to The North Carolina State University Marine, Earth and Atmospheric Science Department's Sedimentology Laboratory for analysis in a Beckman-Coulter Laser Particle Size analyzer LS13-320®, capable of measuring particle sizes ranging from 0.04 to 2000 microns (Beckman Coulter, 2011).

Sampling Methods and Analysis

Sampling began by removing the 10L composite collection jar from within the ISCO 6712™ portable sampler, placing a cap on the jar, swirling the water to re-suspend particles and pollutants, and then pouring the contents of the collection jar into a plastic, 1000 mL TSS collection bottle. From the TSS bottle, approximately 125 mL were then poured into a plastic, pre-acidified nutrient sample bottle and about 150 mL were poured into a 500 mL container for total metals. With the remaining water in the TSS collection bottle, about 100 mL were syringed out and then collected into a dissolved metals bottle through a syringe-driven 0.45 µm filter unit (33 mm diameter), swirling the TSS bottle periodically to keep particles suspended and evenly distributed. Dissolved and total metals were collected independently into 500 mL plastic containers which were not pre-acidified. Nitric acid ampoules were added to the 500 mL containers in the field immediately after sample collection. Metals samples were collected between August 10, 2010 and December 13, 2010. Nutrient and TSS samples were collected from November 2009 to July 2011.

Sample collection took place within 24 hours of the end of a rain event. Rain events were defined by an antecedent dry period of at least six hours. Sampling was undergone in order of least-polluted sampling point to most-polluted sampling point in an attempt to eliminate the introduction of external contamination. Several pairs of latex gloves were worn and discarded throughout the sampling process. Once the samples were collected, they were immediately put on ice for preservation during transport. The sample tubing through which the aliquots passed en route to the composite sample jar was purged with deionized water after approximately every third sampling event during the period of metals sampling.

Nutrient and TSS samples were taken to the North Carolina State University Center for Applied Aquatic Ecology. Metals samples were taken to the North Carolina Department of Environment and Natural Resources environmental chemistry lab. Both labs were located in Raleigh, NC. The laboratory techniques used to analyze nutrients, sediment, and metals are shown in Table 10. Laboratory analysis was performed for total suspended solids (TSS), total Kjeldahl nitrogen (TKN), ammonium-nitrogen (NH₄-N), nitrate- and nitrite-nitrogen (NO_{2,3}-N), total phosphorous (TP), and total and dissolved Pb, Zn, and Cu. Total nitrogen (TN) was determined later by summing the concentrations of TKN and NO_{2,3}-N for each sampled storm event.

Table 10. Nutrient, sediment, and metals analysis techniques.

Constituent	Laboratory Testing Methods	Detection Limits/ Reporting Limits
Pb	EPA Method 200.8 (US EPA, 1993)	DL = 10 µg/L
Zn	EPA Method 200.8 (US EPA, 1993)	DL = 10 µg/L
Cu	EPA Method 200.8 (US EPA, 1993)	DL = 2 µg/L
NH ₄ -N	Std Method 4500 NH ₃ H (APHA, 1998)	RL = 0.007 mg/L
TKN	EPA Method 351.1 (US EPA, 1993)	RL = 0.140 mg/L
NO _{2,3} -N	Std Method 4500 NO ₃ F (APHA, 1998)	RL = 0.0056 mg/L
TP	Std Method 4500 P F (APHA, 1998)	RL = 0.010 mg/L
TSS	Std Method 2540 D (APHA, 1998)	RL = 1 mg/L

Statistical Analysis

The statistical software SAS[®] 9.2 (SAS, 2008) was used to compare bioretention cell volume reduction and peak flow attenuation to statistically compare inflow to outflow hydrology. PROC UNIVARIATE code was used in SAS for this analysis. The data were paired; inflow to outflow. All statistical tests used a significance level of $\alpha=0.05$. The difference between paired inflow and outflow data was checked for normality using the Kolmogorov-Smirnov, Carmer-von Mises, and Anderson-Darling goodness-of-fit tests. If the results of the goodness-of-fit tests were not significant (if $p>0.05$) then the data were considered normally distributed and a Student's t test was used to determine if the two data sets were significantly different. Significant goodness-of-fit tests ($p<0.05$) meant the data were not normally distributed and the raw data were then log transformed to correct for the lack of normality. If the log transformation resulted in a normally distributed data set, a Student's t test determined if the data sets were significantly different (Ott and Longnecker, 2001). Data that remained non-normally distributed were checked for outliers by examining their box plots. If only one outlier existed in the data set, the Wilcoxon signed rank test was used. Two or more outliers resulted in the use of the sign test as an alternative to the Student's t test and the Wilcoxon signed rank test. Both the Wilcoxon signed rank test and the sign test are non-parametric tests and do not assume the data are normally distributed (Ott and Longnecker, 2001).

Results and Discussion

Bioretention

Hydrology

Peak Flow Rate

Peak discharges from the bridge deck were calculated using the Rational Method (equation 1) (Haan et al., 1994):

$$Q_p = ciA \quad (1)$$

Where,

Q_p = Peak discharge (cfs)
 c = Runoff coefficient
 i = Peak rainfall intensity (in/hr)
 A = total drainage area (ac)

The typical range of runoff coefficients for concrete or asphalt is 0.7-0.95; 0.95 was used in the calculations (Haan et al., 1994). Peak rainfall intensities per twelve minute time interval were determined from the ISCO reported rainfall data. The twelve minute time interval was chosen based on the time of concentration of the northbound bridge deck as calculated using PCSWMM (CHI 2009; US EPA 2009b). Using calculated inflow peaks and ISCO 6712TM-reported outflow peaks, it was determined that the large cell (n=48) achieved a peak flowrate mitigation of 65% while the small cell (n=61) reduced peak flowrates by 58%. These fared better than the 42% average peak flow reduction observed by Muthanna et al. (2007) in their small-scale rain gardens (n=44). The Hal Marshall bioretention cell in Charlotte, North Carolina, which treated a municipal parking lot, reduced outflow peaks by 96.5% (n=16) for storms between 2.0 to 39.9 mm (0.08 and 1.6 in) (Hunt et al., 2008). This high reduction percentage may have been a result of the small storm sizes and the ability of the bioretention cell to nearly or entirely capture the events, as was the case in the Mango Creek bioretention cells. Of the storms monitored for peak flowrate at Mango Creek, approximately 80% of the events were less than 2.5 cm (1 in).

Both bioretention cells were successful at mitigating peak flows because of their surface storage capabilities and slow drawdown rates. Several smaller storms were 100% captured, directly impacting peak flow attenuation. Changes in flowrate between each cell's inlet and outlet were significant per the Sign rank test (n=48 large cell, n=61 small cell). Outflow peaks were significantly different between the cells (n=37) per the Student's t test and were lower for the large cell.

Drawdown Rate Effects and Overflow

DWQ policy requires that underdrains be installed if *in situ* soil drainage is less than 5 cm/hr (2 in/hr) or if there is *in situ* loamy soil or tighter. Also, it is required that ponded water completely drains into the bioretention media within 12 hours and to a level 0.6 m (2 ft) below the cell surface within 48 hours of a rain event (NCDENR, 2007).

Average drawdown rates from the ponded water into the soil media for the large and small cell during the monitored period were 0.59 cm/hr (0.23 in/hr) and 0.82 cm/hr (0.32 in/hr). Based on these measurements, the 12 hour drawdown time (as required by NCDWQ regulations) was not met in either cell (NCDENR, 2007). On several occasions, ponded water was still present in the bowls at the outlet ends of the bioretention cells at least 24 hours after the end of a rain event. Extended periods of ponding near the outlet structures may have been due to 1) the underdrain configuration—the underdrains entered the front of the outlet structures and did not extend past the outlets to the end of the cells, causing slower drawdown beyond the outlets, 2) media compaction around the outlet structures which may have occurred during construction, 3) a build-up of *in situ* soil fines that washed onto the cells during construction (Figure 22, left), and/or 4) sediment accumulation on the cell surfaces carried by bridge deck runoff (Figure 2.12, right). Though the top layer of *in situ* sediment was removed from the media before any further cell construction took place, it is possible that it had a lasting clogging effect. All of this considered, the drawdown rates recorded by the HOBO[®] loggers, located adjacent to the outlets in both cells, may have been slightly lower than the drawdown rates further away from the outlet structures.



Figure 22. Fine soils on bioretention media surface (during construction) prior to removal (left image) and sediment build-up carried by runoff (right image).

Maximum drainage rates from the cells' underdrains were determined by analyzing ISCO 730[™] flow data for storms greater than 7.6 cm (3 in). It was assumed that the bioretention cells were entirely saturated and fully ponded for these storms. Observed periods of drainage excluded times of overflow. Maximum drainage rates for both cells were within 12-20 cm/day (5-8 in/day), or 0.5-0.8 cm/hr (0.2- 0.3 in/hr) per bioretention surface area. The average soil media depth was 0.74 m (2.43 ft) in the small cell and 0.61 m (2.00 ft) in the large cell—part of this depth being within the internal storage zone. The cells were not meeting the required drainage rate of 0.6 m (2 ft) below the cell surface within 48 hours (NCDENR, 2007). The underdrains' proximities to the bioretention cells' surfaces and subsequent shallow ponding within the cells relative to the surface also decreased the hydraulic gradient from the bioretention surface to the ISZ due to a decrease in hydraulic head, also affecting drainage rates.

The saturated hydraulic conductivity of the bioretention media was 3.05 cm/hr (1.2 in/hr), or 0.73 m/day (2.4 ft/day), based on the constant head permeability test (Klute, 1986). Therefore, the underdrain drainage rate was the limiting factor for water exiting the system.

Average exfiltration rates from the bioretention cells' internal storage zones into the *in situ* soils were 0.16 cm/hr (0.06 in/hr) and 0.40 cm/hr (0.16 in/hr) in the large and small cell, respectively. These low exfiltration rates caused the ISZs to retain water within the cells for extended periods, which affected the cells' ability to receive water from subsequent storm events due to a decrease in available storage volume.

As a result of undersized bowl storage and slow drainage/exfiltration rates, there was an increased likelihood of overflow. Overflow occurred during 16 of 51 events (31%) in the small cell and often occurred more than once during an event. The frequent occurrence of overflow inversely affected pollutant load reductions and volume reductions. Overflow occurred during 14 of 47 storm events (30%) in the large cell, sometimes more than once during an event.

Figure 23 shows an example of an overflow hydrograph associated with a 5.6 cm (2.2 in) storm in the small bioretention cell. Overflow volumes are shown as the areas above the dashed red lines on the hydrograph. The volume below the red dashed line represents underdrain flow. The abrupt spikes in the hydrograph indicate a sudden surge of flow which is indicative of the occurrence of overflow into the outlet structure. The rainfall depth per two minute time step is also shown. Figure 23 shows that the initial spikes in rain intensity do not correspond with overflow because rainfall was captured and flows were mitigated due to surface storage capacity and cell infiltration. The latter spikes in rainfall intensity, however, correlate directly with overflow occurrences. This supports the theory that once the bioretention cell surface storage was filled, the bioretention cell acted as a flow-through system with minimal impact on lag time, volume reduction, or peak flow reduction.

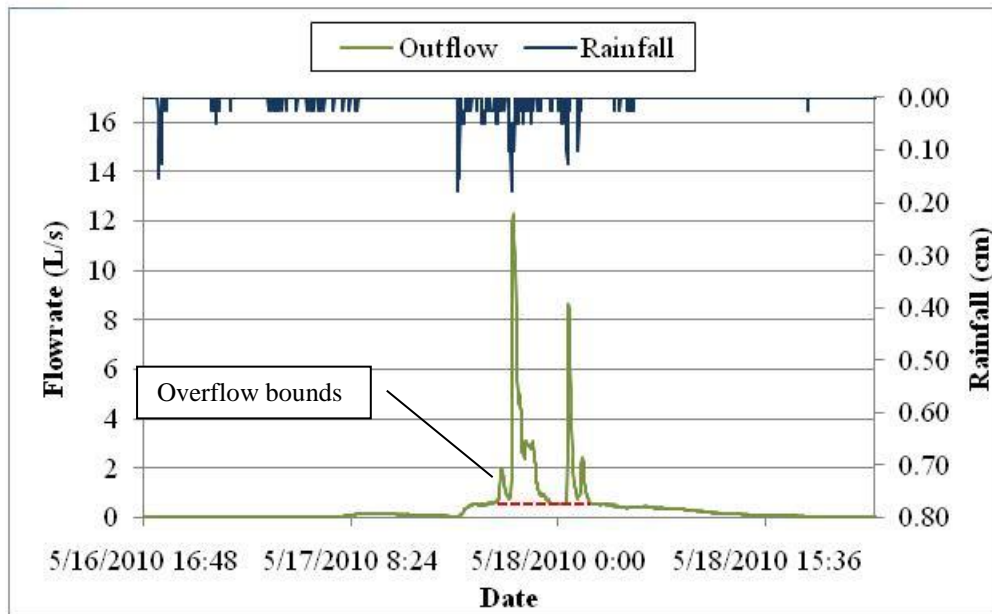


Figure 23. Small bioretention cell overflow event for 7.26 cm (2.86 in) storm event.

Volume Reduction

Rainfall, inflow, and outflow volumes are shown in Figures 24 and 25. Some events were combined due to continuous, non-distinguishable outflow from the bioretention cells.

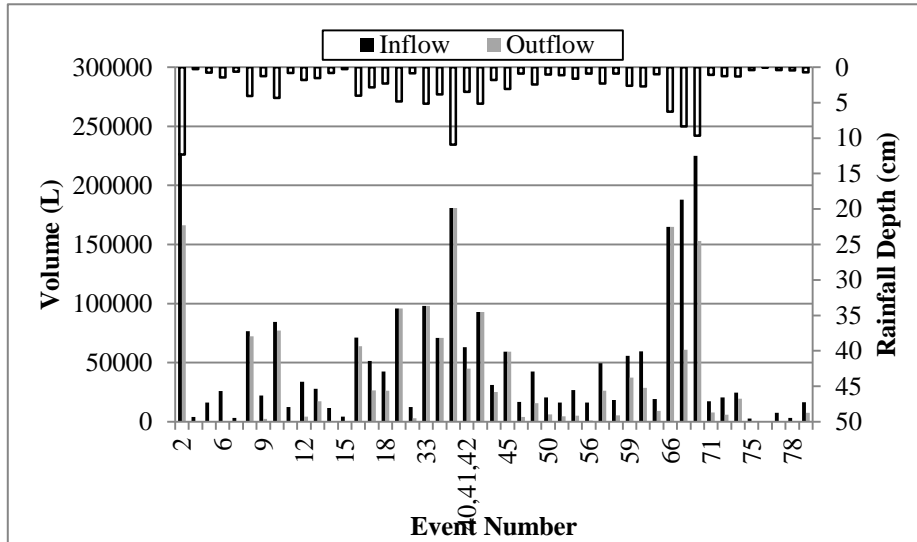


Figure 24. Large bioretention cell inflow and outflow volumes and rainfall depth.

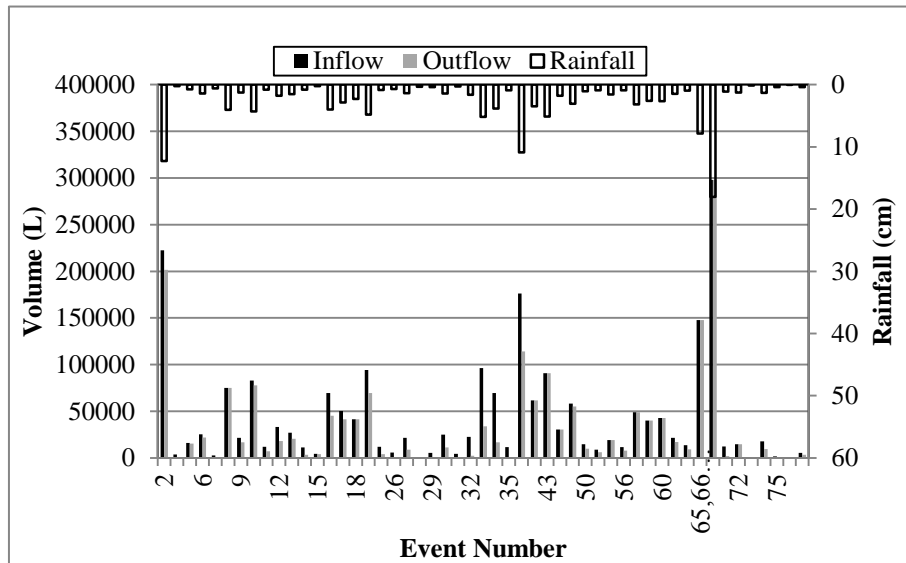


Figure 25. Small bioretention cell inflow and outflow volumes and rainfall depth.

An artificial cutoff of 0.25 cm (0.1 in) of rainfall was used for analyzing the hydrology data since storms much smaller than this would most likely produce flow readings too low to be accurate due to instrument precision (Teledyne ISCO, 1995). This only removed one storm from the analysis for the large cell and two storms from the small cell. For the length of the monitoring period, the large cell (n=47) achieved a cumulative volume reduction of 30%. The small cell (n=51) achieved a 20% volume reduction. The values were based on inflows calculated by the Initial Abstraction method (Pandit and Heck, 2009) and outflows measured by the ISCO 6712™

bubbler flow modules. For events with overflow, a conservative approach was taken and outflow volume was set equal to the inflow volume. The bubblers at the outlets did not take accurate readings during overflow periods due to water turbulence in the outlet structures. Overall volume reductions were likely greater than what was calculated using this conservative approach. Paired inflow and outflow volumes were non-normal and were tested for significance using the sign test. Both the large cell and small cell volume reductions were significant. Differences in paired outflow volumes between the cells were log transformed and found to be not significant (n=27) by the Student's t test.

Two grassed bioretention cells studied by Passeport et al. (2009) were installed in Graham, North Carolina to treat parking lot runoff. The cells had ISZ layers and underdrain systems. Outflow volumes from the Graham cells were not significantly less than the sum of inflow and direct rainfall into the cells. There were also instances of higher outflow volumes or rates, likely due to underestimation of inflow volumes (Passeport et al., 2009). Two bioretention cells (L1 and L2) in Louisburg, North Carolina, reduced outflow by 27% and 19%, respectively. Volume loss was attributed to evapotranspiration and exfiltration; the latter of which, however, did not contribute to loss in L2 because the cell was lined with an impermeable layer (Li et al., 2009).

Tables 11 and 12 show volume reductions achieved by the bioretention cells based on storm size. When partitioned this way, the cells displayed a much better performance for smaller storm events (Hunt et al., 2008; Davis, 2008; Li et al., 2009; Brown and Hunt, 2011) because of their ability to be better captured and stored in the bowl and media with less likelihood of overflow. The volume reduction for storms greater than 2.5 cm (1 in) was much less than for events less than 2.5 cm (1 in). Overflow occurred in the large cell for 80% of the storms between 2.5-5.1 cm (1-2 in), and 67% of the storms greater than 5.1cm (2 in), which may explain why the volume reduction was less for mid-sized storms than large storms because outflow volume was set equal to the inflow volume for storms with overflow (Table 11).

Table 11. Large bioretention cell volume reduction based on storm size.

Rainfall Depth (cm)	< 2.5	2.5 - 5.1	> 5.1
n	29	10	6
Mean Inflow (L)	19501.9	68810.3	180659.6
Mean Outflow (L)	6787.6	57647.7	137354.4
Vol Reduction	65.2%	16.2%	24.0%

Table 12. Small bioretention cell volume reduction based on storm size.

Rainfall Depth (cm)	< 2.5	2.5 - 5.1	> 5.1
n	32	11	6
Mean Inflow (L)	15002.3	63064.8	171949.3
Mean Outflow (L)	9576.8	52250.5	147721.3
Vol Reduction	36.2%	17.1%	14.1%

Figures 26 and 27 show seasonal volume reductions and rainfall events. An inverse relationship between storm size and percent volume reduction was apparent in most cases and the lowest percent volume reductions occurred in the warmer months for both bioretention cells. The “flashy” nature of spring and summer storms in the southeastern United States is characterized by high intensity periods. These periods increased the likelihood of overwhelming the bowl and causing overflow, which may have counteracted the tendency for the bioretention media to more easily infiltration water in warmer weather due to warmer soil temperatures and lower water viscosity (Constantz and Murphy, 1990; Emerson and Traver, 2008). Some small/medium sized storms show no percent reduction in Figures 26 and 27 (eg. events 40-44, 57-60) because outflow was set equal to inflow.

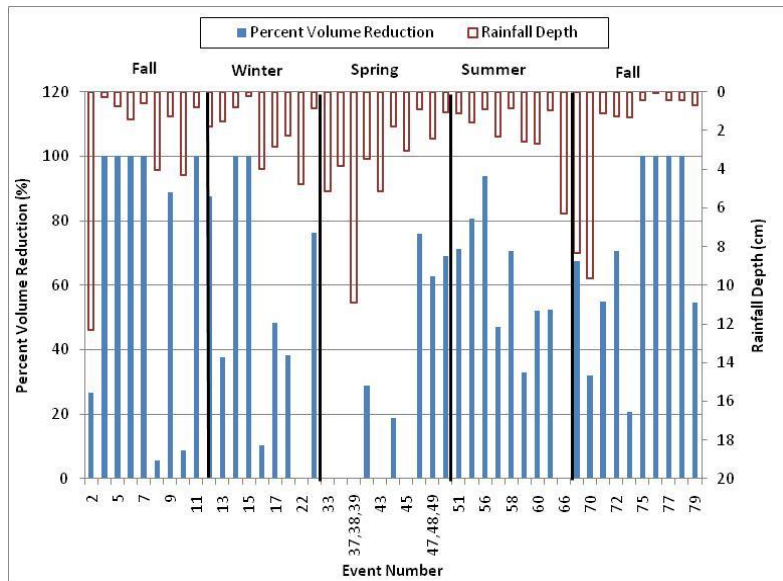


Figure 26. Percent volume reductions and rainfall depths per storm event and season for the large bioretention cell.

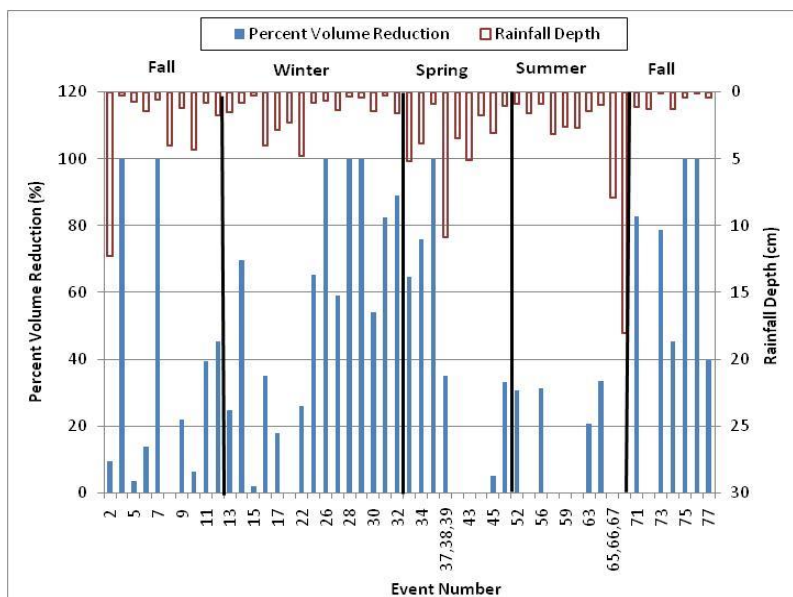


Figure 27. Percent volume reductions and rainfall depths per storm event and season for the small bioretention cell.

Lag Time

Lag time between peak inflow and peak outflow is associated with flow volume attenuation and indicates temporary volume storage. Peak inflow rates were calculated using the Rational Method (Haan et al., 1994). Outflow peak flowrates were found using the flow monitoring program Flowlink 5.1TM (2005). Mean and median lag times for the large cell (n=36) were 3.91 hours and 3.42 hours, respectively. Mean and median lag times for the small cell (n=38) were 2.56 hours and 0.45 hours, respectively. These times were typically greater than the 1.5 hour average lag time observed by Muthanna et al. (2007) in their small-scale bioretention systems which treated 20 m² (215 ft²) of impervious surface. Muthanna et al. (2007) argued that lag time is most dependent on antecedent dry period. Table 13 supports this idea, showing that in the Mango Creek bioretention cells, the median lag times of peak discharge associated with antecedent dry periods less than 24 hours are *less* than the lag times associated with dry weather periods greater than 24 hours.

Table 13. Median lag times associated with antecedent dry period in the large and small bioretention cells.

Antecedent Dry Period	Median Lag Time (hr)	
	Large Cell	Small Cell
<24 hr	1.60	0.10
>24 hr	4.43	0.47

Nutrients and TSS

Total Kjeldahl Nitrogen

Total Kjeldahl nitrogen EMC removal rates were 22% for the small cell (n=30 inlet, n=29 outlet) and 41% for the large cell (n=30 inlet, n=24 outlet). The number of sampled storms at the cell inlets and outlets differ because some storms did not produce sufficient outflow, if any. Efficiency ratios (expressed as percent removal) were based on average pollutant concentrations and calculated using Equation 3.1.

$$\% \text{ concentration reduction} = \frac{(C_{in} - C_{out})}{C_{in}} * 100 \quad (3.1)$$

Where,

C_{in} = EMC of pollutant at the SCM inlet (mg/L)

C_{out} = EMC of the pollutant at the SCM outlet (mg/L)

A significant difference in the mean TKN concentration between the highway runoff and the large cell outflow was found, but not between the highway runoff and the small cell outflow (Table 14). For storm events that produced outflow from both bioretention cells (n=23), the

effluent EMCs were statistically different between the two cells. Average TKN effluent concentrations were 0.423 mg/L and 0.319 mg/L for the small and large cell, respectively.

Table 14. Statistical analysis results for TKN.

Location	n	Distribution	Test of Significance	p-value	Significant difference?
Inlet to Large Cell Outlet	24	Log-normal	Student's t	0.0044	Yes
Inlet to Small Cell Outlet	29	Log-normal	Student's t	0.1014	No
Large and Small Cell Outlets	23	Normal	Student's t	0.0004	Yes

Figure 28 and Appendix E show the concentrations for each storm event with outflow from both cells. TKN concentrations were higher in the bioretention outflow than in the highway runoff on thirteen occasions for the small cell (n=29) and seven occasions for large cell (n=24). The average TKN influent concentrations associated with higher effluent concentrations were 0.37 and 0.32 mg/L in the small and large cell, respectively. It has been suggested that the removal of organic N via sorption to organic surface layers (commonly a mulch layer) is a likely driver for TKN reduction (Davis et al., 2006) since TKN consists of organic N and ammonium nitrogen. Not having this type of layer present in the Mango Creek bioretention cells may have had an effect on their ability to remove TKN. TKN removal may have also been hindered by low TKN influent concentration, which may have entered the cells at a near irreducible level. The average concentration of TKN from the bridge deck runoff was 0.543 mg/L which was less than one-half that observed in Wu et al.'s (1998) bridge deck study. Two bioretention cells (Cell CP and Cell SS) studied by Li and Davis (2009) had median influent EMC TKN concentrations of 1.2 mg/L and 0.5 mg/L, respectively, which were also considered low compared to other published roadway data. Cell CP and Cell SS *increased* TKN median EMCs by 11% and 30%, respectively, further supporting the notion of irreducible pollutant concentrations.

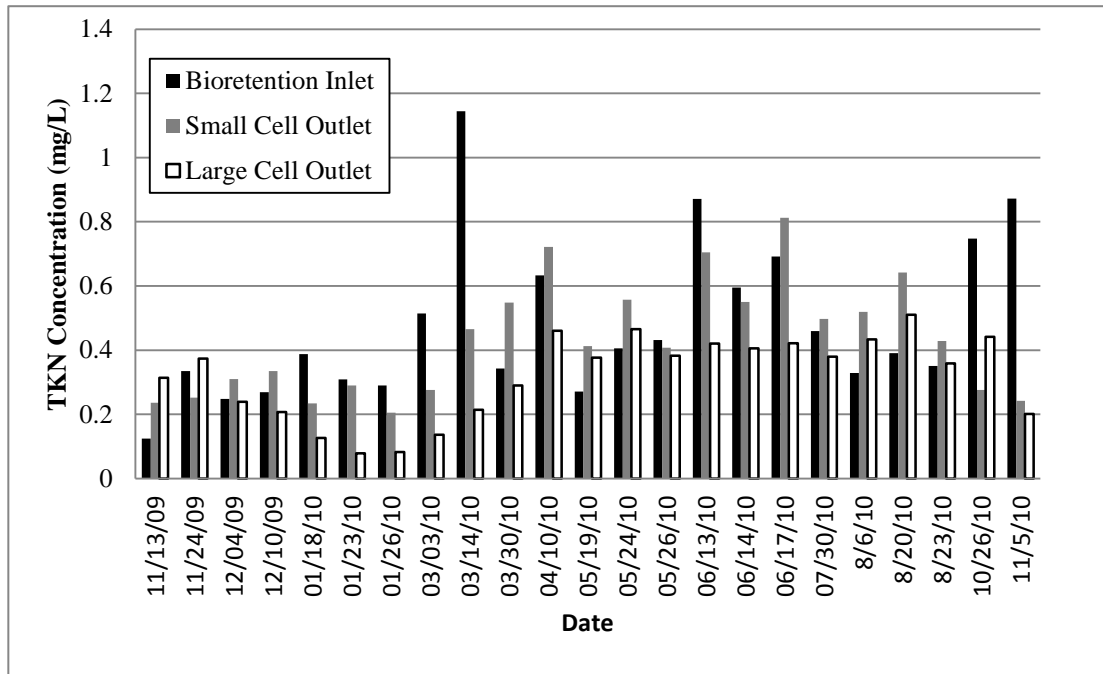


Figure 28. Inlet and outlet TKN concentrations per sampled storm event.

Nitrate-Nitrite Nitrogen

Nitrate-nitrite nitrogen EMC removal rates were 76% and 58% for the large cell (n=30 inlet, n=24 outlet) and the small cell (n=30 inlet, n=29 outlet), respectively. The results showed a significant difference in the mean concentration of NO_{2,3}-N between the highway runoff and both cell outflows (Table 15). For sampled storm events that produced outflow from both bioretention cells (n=23), the effluent EMCs were statistically different between the two cells. The average concentration of NO_{2,3}-N from the bridge deck runoff was 0.335 mg/L, which was low compared to the nitrate-nitrogen runoff concentrations of 2.13 mg/L and 3.49 mg/L in the runoff from the rural and urban highways, respectively, studied by Gan et al. (2007). Average NO_{2,3}-N outflow concentrations were 0.141 mg/L and 0.080 mg/L for the small and large cell, respectively, at Mango Creek.

Table 15. Statistical analysis results for NO_{2,3}-N.

Location	n	Distribution	Test of Significance	p-value	Significant difference?
Inlet to Large Cell Outlet	24	Log-normal	Student's t	<0.0001	Yes
Inlet to Small Cell Outlet	29	Not normal	Signed rank	<0.0001	Yes
Large and Small Cell Outlets	23	Normal	Student's t	0.0027	Yes

Figure 29 and Appendix E show the NO_{2,3}-N concentrations for each storm event having outflow from both cells. NO_{2,3}-N concentrations were higher in the bioretention outflow than in the

highway runoff on three occasions for the small cell (n=29) and zero occasions for large cell (n=24). These nitrate-nitrite nitrogen removal rates were better than conventionally designed bioretention cells with no ISZ. Nitrate-nitrogen is weakly held by soils and readily leaches through sandy soils particularly; therefore, bioretention cells are expected to provide little, if any, nitrate removal if they do not include an internal storage zone (Davis et al., 2006; Brown and Hunt, 2011; Hunt et al., 2008; Sparks, 2003). The $\text{NO}_{2,3}\text{-N}$ removal achieved in the Mango Creek cells was attributed to denitrification which likely occurred in the ISZ layers of the cells. During denitrification, decomposable organic matter is used as an electron donor and $\text{NO}_3\text{-N}$ is the electron acceptor in the absence of oxygen (Richardson and Vepraskas, 2001). In this case, the source of organic matter was the pine mulch material mixed in with the bioretention soil media. The largest influx of $\text{NO}_{2,3}\text{-N}$ concentration seemed to occur in the months of May through August 2010; because these were among the warmer and wetter months (consistently wet antecedent moisture conditions), saturation appeared to have developed, promoting high rates of denitrification.

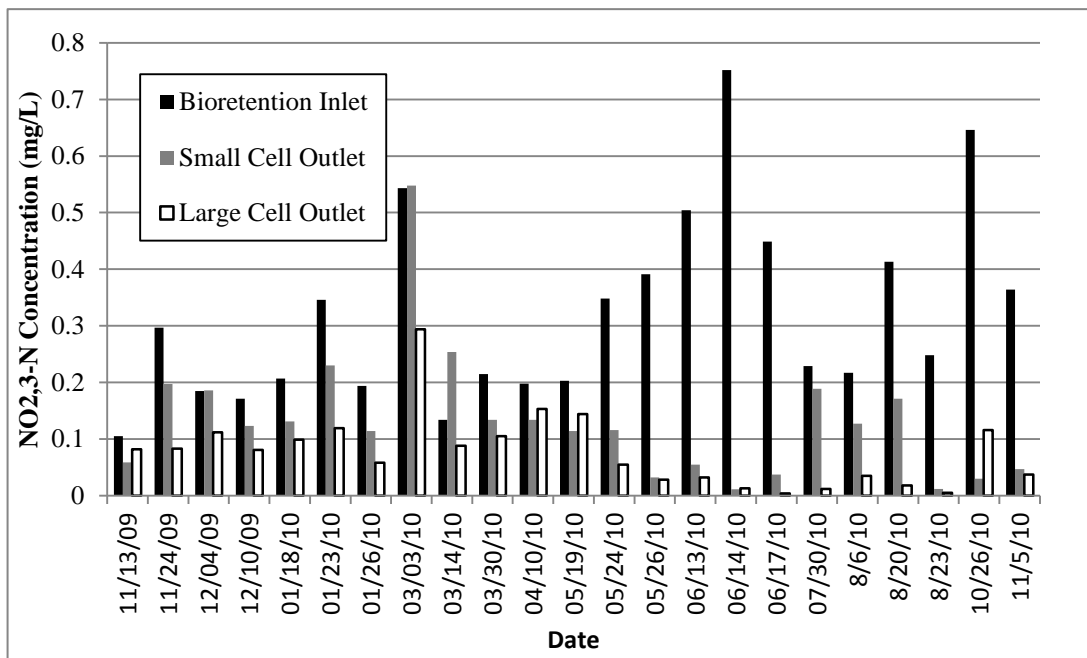


Figure 29. Inlet and outlet $\text{NO}_{2,3}\text{-N}$ concentrations per sampled storm event.

Total Nitrogen

Total nitrogen was calculated as the sum of TKN and $\text{NO}_{2,3}\text{-N}$ concentrations, with TKN being the largest contributor. Statistical results (Table 16) showed that TN effluent concentrations were significantly different between the highway runoff and the effluent from the cells. The large cell had an EMC reduction of 53% (n=30 inlet, n=24 outlet), and the small cell achieved an EMC reduction of 37% (n=30 inlet, n=29 outlet). These removals were comparable to those of Passeport et al. (2009) who saw 56% and 47% concentration reductions through two grassed bioretention cells which also contained internal storage zones in Piedmont North Carolina. The

average TN inflow concentration was 0.857 mg/L from the bridge deck. Average TN outflow concentrations were 0.399 mg/L and 0.539 mg/L and from the large and small cells, respectively.

Table 16. Statistical analysis results for TN.

Location	n	Distribution	Test of Significance	p-value	Significant difference?
Inlet to Large Cell Outlet	24	Normal	Student's t	<0.0001	Yes
Inlet to Small Cell Outlet	29	Log-normal	Student's t	<0.0001	Yes
Large and Small Cell Outlets	23	Normal	Student's t	0.0056	Yes

Figure 30 shows the TN concentration for each storm event having outflow from both cells. TN concentrations were higher in the bioretention outflow than in the highway runoff on three occasions for large cell (n=24) and seven occasions for the small cell (n=29). The average TN influent concentrations associated with higher effluent concentrations were 0.50 and 0.30 mg/L in the small and large cell, respectively.

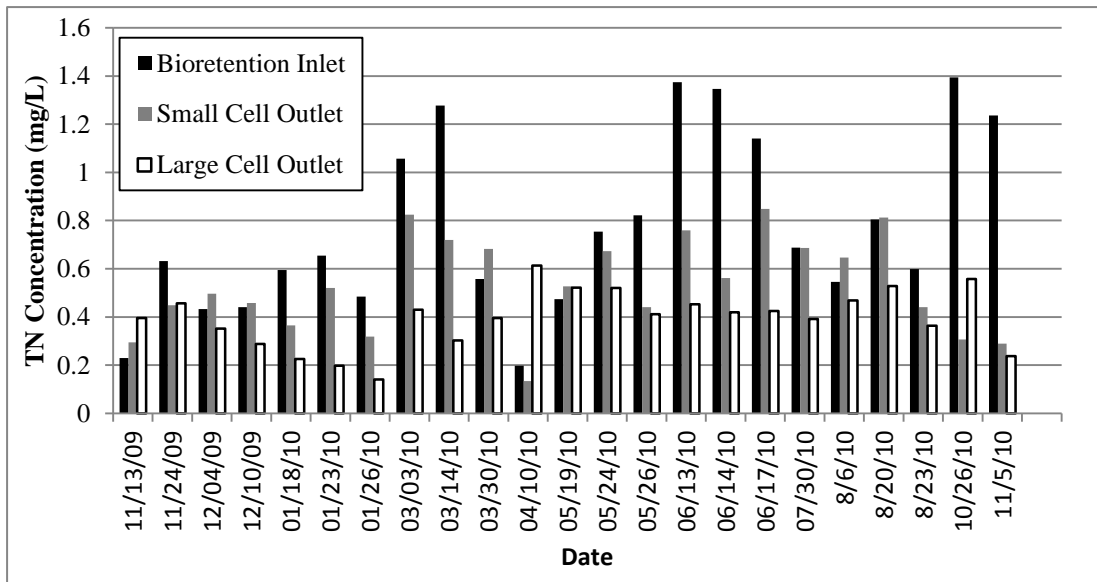


Figure 30. Inlet and outlet TN concentrations per sampled storm event.

Ammonium Nitrogen

The highway runoff EMC for ammonium nitrogen was 0.084 mg/L, while the EMCs at the large cell and small cell outlets were 0.037 mg/L and 0.043 mg/L, respectively. The results of the Student's t test (Table 17) showed significant changes in ammonium nitrogen concentrations through both cells, with a 56% reduction in the large cell (n=30 inlet, n=24 outlet) and a 49% reduction in the small cell (n=30 inlet, n=29 outlet). NH₄-N removal was likely a result of nitrification, the production of nitrate from ammonium in aerobic soils (Richardson and

Vepraskas, 2001). Since nitrification is limited by the amount of oxygen present in the soil, the process most likely occurred toward the surface of the bioretention cell media.

Table 17. Statistical analysis results for NH₄-N.

Location	n	Distribution	Test of Significance	p-value	Significant difference?
Inlet to Large Cell Outlet	24	Log-normal	Student's t	0.0081	Yes
Inlet to Small Cell Outlet	29	Log-normal	Student's t	0.0092	Yes
Large and Small Cell Outlets	23	Log-normal	Student's t	0.8680	No

In six of the 29 sampled events that produced outflow from the small cell, the effluent NH₄-N concentration was higher than the concentration present in the inflow. This was the case for five of the 24 sampled events producing outflow from the large cell. These cases were infrequent because there was not a substantial source of organic matter, such as a mulch layer, available to support microbial activity that would degrade and convert organic N to ammonium within the cells. Figure 31 shows NH₄-N concentrations from all sampled storm events that produced outflow from both cells. Ammonium nitrogen inflow concentrations appeared to be generally higher in the winter months than in other months. Unusually high amounts of ammonium nitrogen concentration were present in the highway runoff periodically throughout the monitoring period, as well (3 March, 2010; 13 June, 2010; 5 November, 2010) (Figure 31). The reason for this is unknown. Although the influent concentrations were high relative to what was typically seen at the Mango Creek site, the concentrations were low compared to other highway studies. A study performed by Crabtree et al. (2006) on six non-urban highways (n=60) revealed a mean NH₄-N runoff concentration of 0.25 mg/L. An urban highway bridge deck study showed a mean EMC NH₃-N concentration of 0.83 mg/L (Wu et al., 1998).

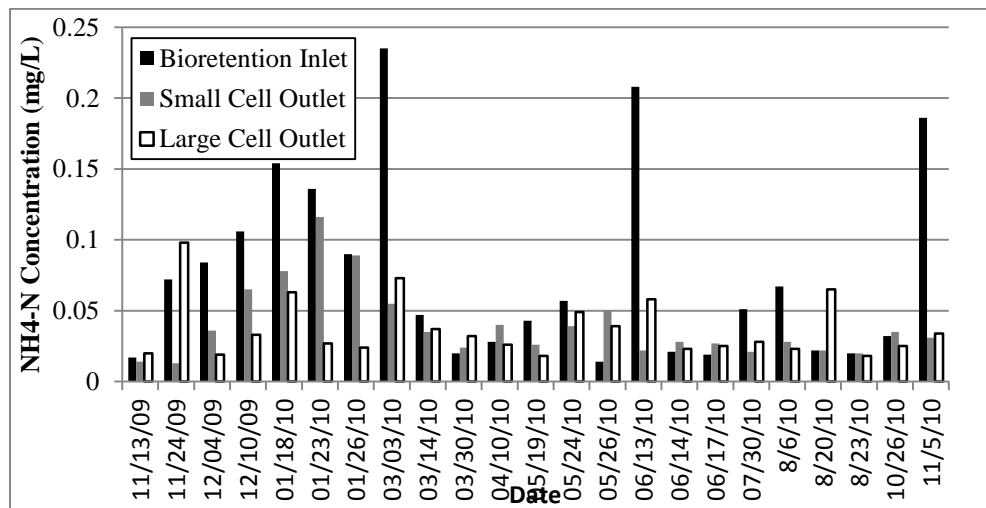


Figure 31. Inlet and outlet NH₄-N concentrations per sampled storm event.

Total Phosphorous

Neither the large nor small cell effluent EMCs for total phosphorous were significantly different from that of the bridge deck runoff (Table 18). Also, the large and small cell effluent TP concentrations were significantly, but not substantially, different from one another. The mean influent TP concentration was 0.114 mg/L while the large cell and small cell effluent concentrations were 0.106 mg/L and 0.126 mg/L, respectively. These results suggest the TP from the bridge deck was already at an irreducible or baseline concentration before entering the bioretention cells (Strecker et al., 2001). When compared to TP concentrations from other bridge deck studies, the average I-540 TP concentration of 0.114 mg/L was quite low (Gan et al., 2007; Yousef et al., 1984; Wu et al., 1998).

TP reduction is often related to the phosphorous sorbtive potential, as characterized by the P-Index of the bioretention fill media (Hunt et al., 2006). A soil test report from the North Carolina Department of Agricultural and Consumer Services (NCDA&CS), completed in June 2010, reported a P-Index of 4 for the Mango Creek cell media which falls in low-to-medium P-Index range (Hardy et al., 2003). This bioretention media had low levels of adsorbed phosphorous and therefore had a high affinity for capturing and binding phosphorous. The fact that the bioretention cells had minimal effect on TP percent concentration reductions, despite the media's low P-Index value, supports the idea of irreducible concentrations. On two occasions of relatively high TP inflow concentrations (14 March, 2010 and 13 June, 2010), the cells reduced concentration by 66% in the large cell and 54% in the small cell and discharged TP concentrations at a level comparable to the cells' average effluent concentrations observed during the study. This indicates that the bioretention cells were capable of greater levels of removal had TP inflow concentration been higher. The shallow-rooted grass within the cells may have done little for biological uptake of phosphorous (Davis et al., 2009); any decomposing grass may have acted as a TP source.

Table 18. Statistical analysis results for TP.

Location	n	Distribution	Test of Significance	p-value	Significant difference?
Inlet to Large Cell Outlet	24	Log-normal	Student's t	0.6657	No
Inlet to Small Cell Outlet	29	Log-normal	Student's t	0.10111	No
Large and Small Cell Outlets	23	Normal	Student's t	0.0281	Yes

Figure 32 shows TP concentrations for events that produced outflow from both cells. Spikes in TP inflow concentration occurred on 14 March, 2010, and 13 June, 2010. While these two TP concentrations were high for what was typical at the study site, they were near the average TP EMC levels seen in other highway bridge deck studies (Gan et al., 2007; Wu et al., 1998). For all storm events that produced outflow from either the large or small cell (Appendix E), TP concentrations were higher in the bioretention outflow than in the highway runoff on 13 occasions for large cell (n=24) and 20 occasions for the small cell (n=29).

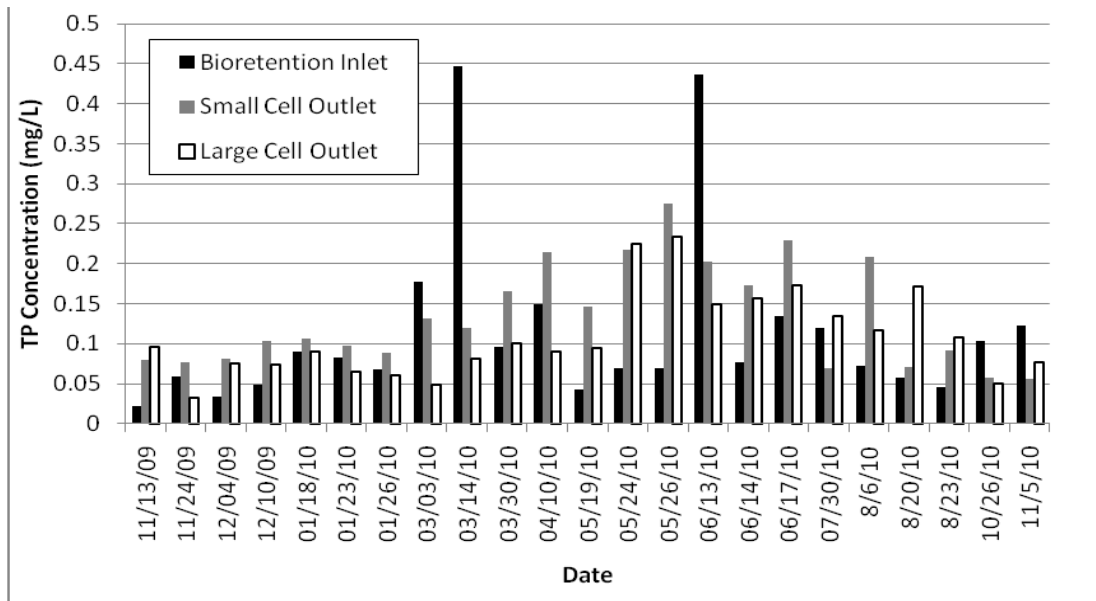


Figure 32. Inlet and outlet TP concentrations per sampled storm event.

Total Suspended Solids

Both the large and small bioretention cells discharged outflow TSS concentrations that were significantly different from the highway runoff EMC (Table 19). The large cell (n=30 inlet, n=24 outlet) and small cell (n=30 inlet, n=29 outlet) reduced TSS concentrations by 58% and 47% on average, respectively. The bridge deck runoff EMC was 49 mg/L while the large and small cell had effluent concentrations of 20 mg/L and 26 mg/L, respectively. The two cells' effluent concentrations were not significantly different from one another.

Table 19. Statistical analysis results for TSS.

Location	n	Distribution	Test of Significance	p-value	Significant difference?
Inlet to Large Cell Outlet	24	Log-normal	Student's t	0.0037	Yes
Inlet to Small Cell Outlet	29	Log-normal	Student's t	0.0235	Yes
Large and Small Cell Outlets	23	Normal	Student's t	0.2018	No

Figure 33 shows spikes in TSS similar to what was seen in the TP concentration data. On 14 March, 2010, it was noted in the field that excessive debris (straw, trash, sand, etc.) was found in the inlet pipe to the large bioretention cell. Excessive debris (trash, sand, etc.) was also present in the inlet pipe on 13 June, 2010 and 17 June, 2010 which may have been related to the elevated TSS levels on these days. Rainfall amounts were less than 1.3 cm (0.5 in) for each of these storms. Due to the high TSS concentrations on these days, the fraction of sediment removed was very high. For example, on 14 March 2010, TSS concentrations were reduced by 95% in the small cell and 93% in the large cell. TSS removal was a result of filtration and sedimentation. On six occasions, TSS increased from the inlet to the outlet of the large cell. On seven

occasions, TSS increased from the inlet to the outlet of the small cell. The median influent TSS concentration for these events was 14 mg/L for both cells. This suggests that during these storm events, TSS may have been entering the cell near irreducible concentrations.

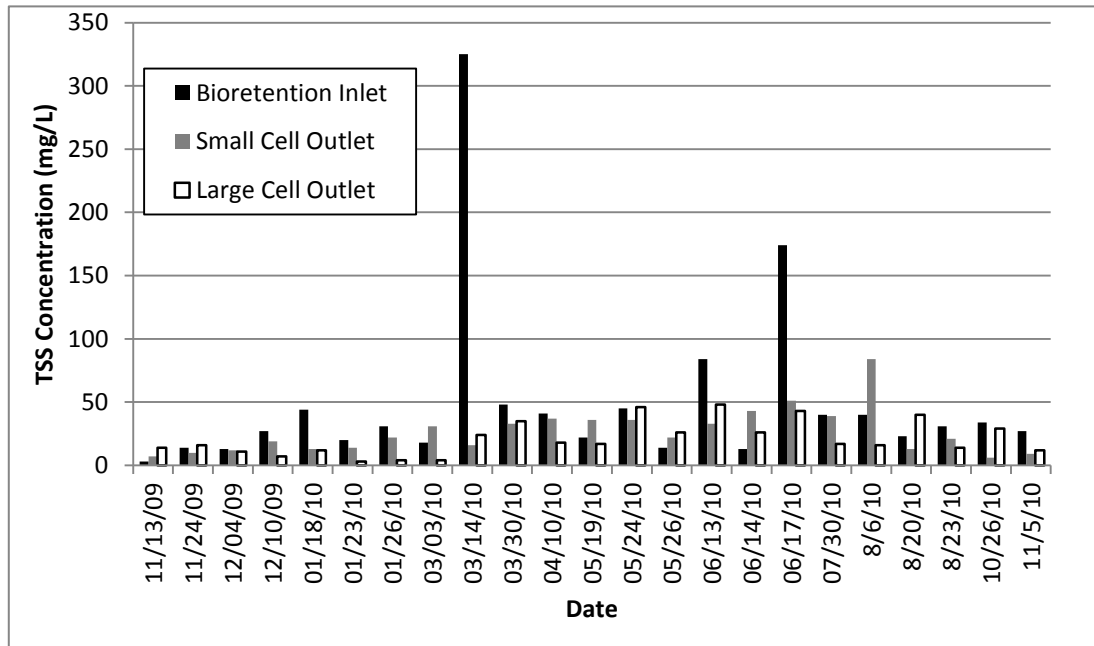


Figure 33. Inlet and outlet TSS concentrations per sampled storm event.

Nutrient and TSS Removal Summary

Effluent concentrations can be used to assess stormwater SCM performance and are thought to be a more effective means of characterizing SCM efficiency than analyzing fractional removals (Strecker et al., 2001; Li and Davis, 2009). McNett et al. (2010) characterized water quality levels by correlating various in-stream pollutant concentrations to benthic macroinvertebrate health. In the Piedmont of North Carolina, “good” water quality concentrations for TN and TP were 0.99 mg/L and 0.11 mg/L, respectively. “Good” water quality supported intolerant benthic macroinvertebrates, such as *Ephemeroptera* (mayflies) and *Trichoptera* (caddisflies). Target concentrations for TSS were 25 mg/L (Barrett et al., 2004). These target values are shown in Figure 34 for TN, TP, and TSS as horizontal lines. Figure 34 shows the distribution of the paired influent and effluent concentration data (n= 24 for the inlet to large cell outlet, n=29 for the inlet to small cell outlet, and n=23 for the large cell outlet to small cell outlet). The box plots were created in R[®] statistical software (R, 2010). Standard deviations of the influent and effluent concentrations are also shown.

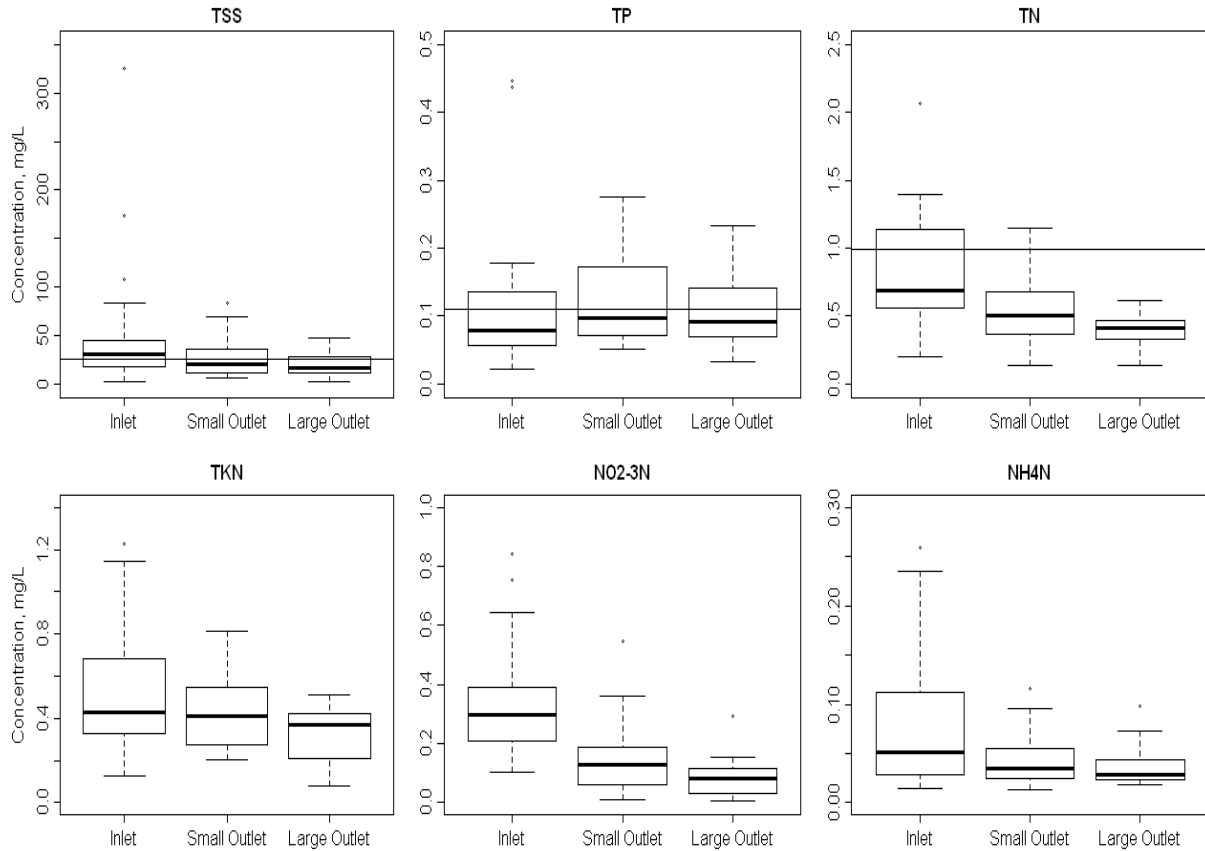


Figure 34. Influent and effluent nutrient and TSS concentrations in Mango Creek bioretention cells. Horizontal lines represent target North Carolina water quality standards in the Piedmont region for TSS, TP, and TN.

It is clear from Figure 34 that the runoff coming from the bridge deck had low nutrient concentrations when compared to target nutrient concentrations. The median TN and TP concentrations of the bridge deck runoff were less than their targets before runoff entered the bioretention cells. When analyzing the pollutant concentrations based on this metric, the bioretention cells' inability to significantly reduce the TP concentrations in the runoff was not necessarily a sign of inadequately functioning bioretention cells. The median effluent concentrations from the bioretention cells were at "good" to "excellent" water quality levels (McNett et al., 2010) for TN and TP. The median TSS concentration was reduced beyond the target concentration in both cells. Further, the median NH₄-N concentration entered the cells between the "good" and "good/fair" levels (0.04 and 0.06 mg/L, respectively) and was reduced below the "good" target concentration (Table 20). Median and mean nutrient and TSS concentrations are shown in Tables 20 and 21. Percent concentration reductions of the pollutants are shown in Table 22.

Table 20. Median concentrations by sampling location (mg/L)

	Bioretention Inlet (mg/L)	Small Cell Outlet (mg/L)	Large Cell Outlet (mg/L)
No. of storms sampled	30	29	24
TKN	0.44	0.41	0.37
NO_{2,3}-N	0.30	0.13	0.08
TN	0.72	0.50	0.42
NH₄-N	0.05	0.04	0.03
TP	0.08	0.10	0.09
TSS	30	21	17

Table 21. Mean nutrient and TSS concentrations by sampling location.

	Bioretention Inlet (mg/L)	Small Cell Outlet (mg/L)	Large Cell Outlet (mg/L)
No. of storms sampled	30	29	24
TKN	0.54	0.42	0.32
NO_{2,3}-N	0.34	0.14	0.08
TN	0.86	0.54	0.40
NH₄-N	0.08	0.04	0.04
TP	0.11	0.13	0.11
TSS	49	26	20

Table 22. Percent concentration reductions based upon means of pollutants at Mango Creek bioretention cells.

	Large Cell (%)	Small Cell (%)
# of storms sampled	n=30 inlet, n=24 outlet	n= 30 inlet, n= 29 outlet
TKN	41	22
NO_{2,3}-N	76	58
TN	53	37
NH₄-N	56	49
TP	7	-10
TSS	58	47

Cumulative probability plots (Figures 35-37) were created by ranking influent and effluent concentrations to illustrate the relative probability that a concentration would exceed the “good” water quality benchmark. Storm events with no outflow were represented as a 0.001 mg/L concentration. For TN, effluent concentrations for both the large and small cells were always less than the target water quality level except for one instance at the small cell outlet. For TP, 73% and 60% of the outflow concentrations from the large cell and small cell, respectively, were less than the 0.11 mg/L benchmark. For TSS, 73% and 63% of the outflow concentrations from the large and small cell, respectively, were below the 25 mg/L benchmark. Influent stormwater pollutant concentrations were low for TN, TP, and TSS, with nearly half the data points less than the “good” water quality concentrations for each pollutant.

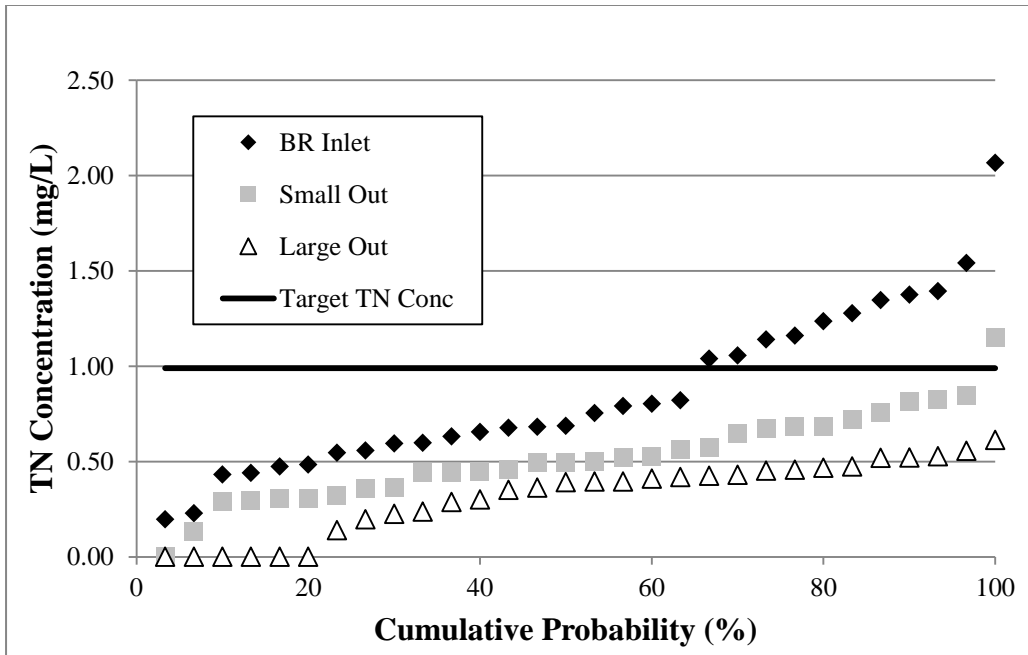


Figure 35. Bioretention cumulative probability plot for TN.

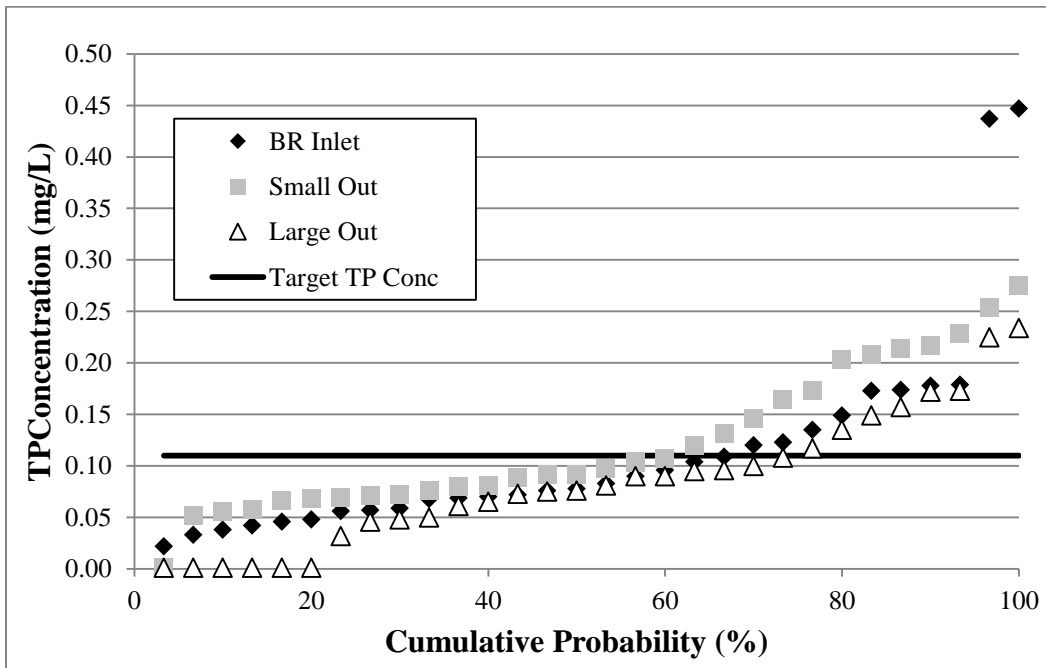


Figure 36. Bioretention Cumulative Probability Plot for TP.

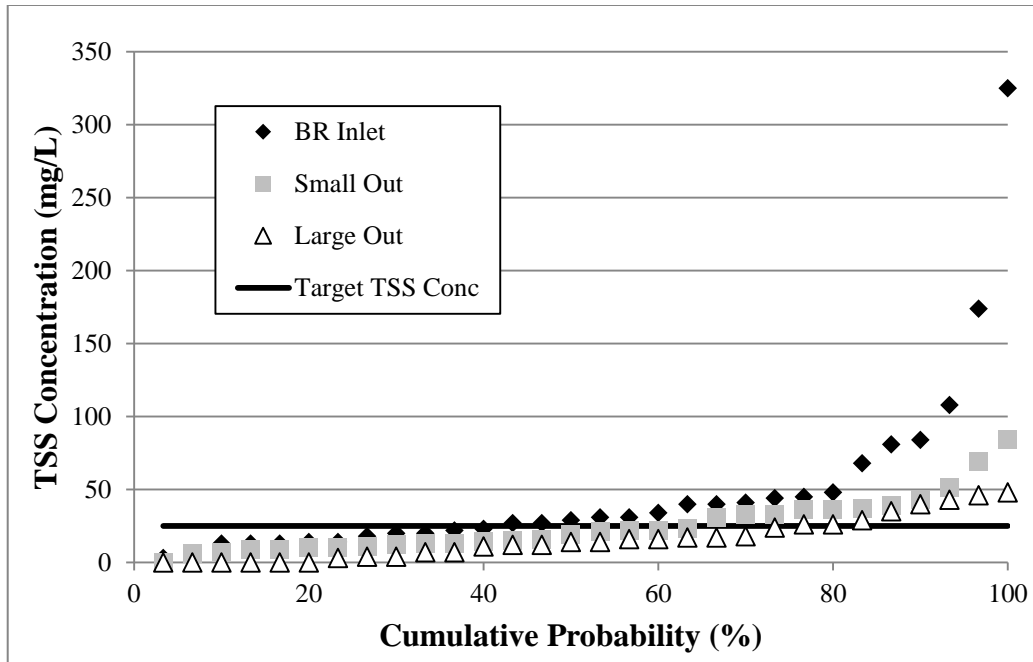


Figure 37. Bioretention Cumulative Probability Plot for TSS.

Heavy Metals

Heavy metals are toxins found in materials associated with highway construction and usage. Copper, for instance, is associated with brake emissions, while zinc is sourced to tire wear (Davis et al., 2001). Lead is related to both of these sources as well. Median heavy metal concentrations for ten storm events at the Mango Creek bioretention cells are shown in Table 23.

Table 23. Median total and dissolved heavy metal concentrations.

Sampling Location	Median Concentrations					
	Total Metals ($\mu\text{g/L}$) ^[1]			Dissolved Metals ($\mu\text{g/L}$)		
	Cu	Zn	Pb	Cu	Zn	Pb
Bioretention Inlet	13.0	52.5	4.2	4.2	10.5	BDL
Small Cell Outlet	10.0*	10.0*	2.6	4.3	BDL ^[2]	BDL
Large Cell Outlet	9.2	11.0*	2.9	5.9	BDL	BDL

[1] Detection limit (DL) for Cu and Pb was 2 $\mu\text{g/L}$ and 10 $\mu\text{g/L}$ for Zn.

[2] BDL = Below the Detection Limit

* Statistically significant reduction in metal concentration when compared to inlet concentration

A total of ten paired samples were collected for heavy metal analysis from the small and large bioretention cell, respectively. Statistically significant reductions in total copper and zinc were observed for the small cell, while total zinc was the only metal that was significantly reduced by the large cell. While the large cell reduced total copper concentrations substantially, one outlier event prevented statistical significance, as copper concentrations increased by nearly 100% in that event.

Based on median values, it appeared that total copper and zinc concentrations were reduced through both bioretention cells. Dissolved copper concentrations appeared to increase through

both bioretention cells, while the opposite was true for dissolved zinc. No definitive conclusions could be drawn about the lead removal efficiencies of the cells, as the inlet concentrations were below the detection limit. I-540 bridge deck metals runoff concentrations were compared to those of other bridge deck studies. The 13 µg/L influent copper concentration was comparable to the 15 µg/L median concentration for another bridge deck located in North Carolina (Wu et al., 1998) with similar surrounding land use and traffic loading. However, a bridge deck study conducted in central Florida, also with a similar average daily traffic volume, found average concentrations to be 292 µg/L, 617 µg/L, and 48 µg/L for total Zn, Pb, and Cu, respectively (Yousef et al., 1984). Dissolved concentrations of Zn, Pb, and Cu at the central Florida site were 50 µg/L, 39 µg/L, and 22 µg/L, respectively. A study performed on highway bridge deck runoff in Guangzhou, China, (Gan et al., 2007) reported copper, zinc, and lead concentrations (140 mg/L, 1760 mg/L, 118.2 µg/L, respectively) that seemed quite high and were contributed to the erosion of galvanized structures and noise barrier walls along the highway (Gan et al., 2007).

Since metals tend to bind to particulate matter at the near-neutral pH levels often observed in stormwater runoff, sediment-bound Zn and Cu associated with TSS may have been removed by sedimentation and filtration (Sparks, 2003; Opher and Friedler, 2010). Mango Creek bioretention cells significantly reduced suspended solids, which partly explains the (in some cases modest) removal of copper and zinc. Another means of removal may have been the binding of metals to the clay and organics fraction of the fill media within the cells (Sparks, 2003). Clays constituted 2.5% of the non-organic soil media and organic material made up 3-5% of the entire soil mix. Heavy metal sequestration tends to concentrate within the upper few centimeters of the soil column (Yousef et al., 1984; Davis et al., 2003; Hatt et al., 2008). As a result, bioretention cell size and depth may have minimal effect on metals capture.

Pollutant Loads

Pollutant load reductions are often considered more telling than concentration reductions because they account for the amount of volume reduced by the SCM. Pollutant loads were calculated for TSS and nutrients at Mango Creek using Equation 2.

$$C_{\text{pollutant}} * Q = \Theta \quad (2)$$

Where,

- Θ = Pollutant load (mg)
- $C_{\text{pollutant}}$ = EMC of the pollutant (mg/L)
- Q = Flow volume (L)

Some storm events had overlapping outflow hydrology and, as a result, the beginning and end of the outflow hydrographs were unable to be accurately separated into unique storm event outflows. In these cases, regardless of whether the storms had an antecedent dry period of six hours, their inflow and outflow hydrology data were combined. Also, the monitoring equipment was often incapable of taking accurate level readings in the outlet structures during overflow because of turbulence. In these situations, a conservative approach was taken— outflow volumes were set equal to inflow volumes. In three instances, concentration data were weighted among multiple storm events with overlapping hydrology. Weighting of concentrations was

based on inflow volumes. The first instance was for storms occurring between 16 May, 2010 and 19 May, 2010 (Appendix F). The storm that began on 16 May, 2010 was sampled as an individual water quality event and the storms that began on 17 May, 2010 and 19 May, 2010 were sampled as a combined water quality event. However, all three storms had overlapping outflow hydrology and it was therefore necessary to proportionally combine concentration data to produce single inflow and outflow load values. A similar approach was used for the three storms that occurred between 22 May, 2010, and 24 May, 2010, as well as the storms between 12 June, 2010 and 13 June, 2010 (Appendix F).

Average pollutant load reductions, based on calculated inflow (including direct rainfall) and monitored outflow volumes, are presented in Table 24. These load reductions accounted for runoff from 62.5 cm (24.6 in) and 67.8 cm (26.7 in) of total rainfall at the large cell and small cell, respectively. The results in Table 24 were calculated using Equation 3.

$$\% \text{ load removed} = \frac{(\Sigma \Theta_{\text{in}} - \Sigma \Theta_{\text{out}})}{(\Sigma \Theta_{\text{in}})} * 100 \quad (3)$$

Where,

- $\Sigma \Theta_{\text{in}}$ = sum of per-storm-event pollutant loads at SCM inlet for a given constituent (mg)
- $\Sigma \Theta_{\text{out}}$ = sum of per-storm-event pollutant loads at SCM outlet for a given constituent (mg)

A second load reduction method was also used (Equation 3.4) which calculated the load reductions per storm event and then averaged these reductions over the total number of sampled storms. This method equally weighted each storm.

$$\% \text{ load removed} = \frac{\left(\sum_{i=1}^n \frac{(\Theta_{\text{in}} - \Theta_{\text{out}})}{\Theta_{\text{in}}} \right)}{n} * 100 \quad (4)$$

Where,

- Θ_{in} = pollutant load at SCM inlet for a given constituent during a given storm (mg)
- Θ_{out} = pollutant load at the SCM outlet for a given constituent during a given storm (mg)
- n = total number of storm events

The summation of loads technique allowed the largest events, and their associated loads, to proportionally influence the result. For all nitrogen constituents and TSS, the percent load reductions were greater than the percent concentration reductions in the small cell, illustrating the importance of considering flow volumes when determining the effectiveness of a bioretention cell. Conversely, the concentration reductions remained higher than load reductions in the large cell for all constituents except $\text{NH}_4\text{-N}$. This may have been a result of the conservative approach taken for events with overlapping outflow hydrology and overflow events. The large bioretention cell had a higher pollutant load reduction than the small cell for all pollutants because it reduced both flow volumes and pollutant concentrations better.

Table 24. Pollutant loads and reductions for the bioretention cells at Mango Creek as calculated using the summation of loads technique.

Constituent	Sum of Influent Pollutant Loads (kg)	Sum of Effluent Pollutant Loads (kg)	Summation of Loads (%)
Small Cell (n=25)			
TKN	0.46	0.34	25.9
NO _{2,3} -N	0.30	0.12	58.0
TN	0.71	0.45	37.3
NH ₄ -N	0.08	0.04	54.1
TP	0.10	0.11	-13.3
TSS	42.84	21.80	49.1
Large Cell (n=21)			
TKN	0.44	0.29	35.0
NO _{2,3} -N	0.29	0.09	68.4
TN	0.69	0.38	44.9
NH ₄ -N	0.08	0.03	68.0
TP	0.10	0.09	4.4
TSS	38.34	16.74	56.3

Mean load reduction results are summarized in Table 25. This method of load reduction yielded a more positive performance because large storm events had no proportional influence. For instance, the flow volume associated with the 10.8 cm (4.2 in) storm on 13 November, 2009 constituted 16.7% of the total flow data used to calculate the summation of loads (Equation 3), but only 3.4% of the total flow data used to calculate mean load reduction (Equation 4).

Table 25. Pollutant load reductions for the bioretention cells at Mango Creek as calculated using average mass reduction.

Mean Load Reduction (%)		
	Small Cell	Large Cell
No. storms sampled	n= 25	n=21
TKN	30.7	51.9
NO_{2,3}-N	64.3	77.6
TN	46.5	51.5
NH₄-N	47.5	64.8
TP	-11.5	12.0
TSS	41.9	56.7

When compared to pollutant concentration reductions, the load reductions presented in Tables 26 and 27 are only marginally higher. The results suggest that concentration reductions, and not volume reductions, were the major driver for pollutant removal in these two bioretention cells. This was mostly a result of larger storms' load reductions, which had lesser volume mitigation and greater dilution of pollutant concentrations.

Each load reduction was partitioned into the fraction associated with reduced volume and the fraction associated with reduced concentration (Table 26 and 27). The results show that in the large and small cells, volume reduction was the main reason why TN loads were reduced. The loads of NO_{2,3}-N and NH₄-N were nearly equally reduced by concentration reduction and volume reduction. Since TP concentrations were not significantly reduced in either cell, and TKN concentrations were not significantly reduced in the small cell, it was assumed that their load reductions were entirely a result of volume reduction and were therefore not shown in Tables 26 and 27.

Table 26. Partitioning the cause of load reduction between concentration and volume reduction in the large cell.

Pollutant	Load Removal Attributed to:	
	Concentration (%)	Volume (%)
TKN	3.0	97.0
NO _{2,3} -N	52.6	47.4
TN	22.6	77.4
NH ₄ -N	53.7	46.3
TSS	45.1	54.9

Table 27. Partitioning the cause of load reduction between concentration and volume reduction in the small cell.

Pollutant	Load Removal Attributed to:	
	Concentration (%)	Volume (%)
NO _{2,3} -N	53.7	46.3
TN	24.4	75.6
NH ₄ -N	51.4	48.6
TSS	22.0	78.0

Student's t tests were performed on paired load data to determine if there was a significant difference between the loads of bioretention cell inlets and outlets and also between the cells' outlets (Table 28). Statistics were run on events that had complete inflow and outflow load data for both cells. All of the pollutant loads were significantly different between the inlet and the outlet for both bioretention cells; exceptions were TP loads in the large and small cells and TKN loads in the small cell. When comparing effluent loads, no significant difference was found between the large and small cell. However, the median effluent loads from the small cell were higher than those from the large cell in every case (Figure 38).

Table 28. Statistical comparison of pollutant loads for bioretention cells.

Location	n	Constituent	Distribution	Test of Significance	p value	Significantly Different?
Inlet to Large Cell Outlet	19	TKN	Log normal	Student's t	0.0015	Yes
		NO _{2,3} -N	normal	Student's t	<0.0001	Yes
		TN	Log normal	Student's t	0.0012	Yes
		NH ₄ -N	normal	Student's t	0.0006	Yes
		TP	Log normal	Student's t	0.4781	No
		TSS	normal	Student's t	0.0013	Yes
Inlet to Small Cell Outlet	19	TKN	normal	Student's t	0.095	No
		NO _{2,3} -N	Log normal	Student's t	<0.0001	Yes
		TN	Log normal	Student's t	0.0002	Yes
		NH ₄ -N	normal	Student's t	0.0023	Yes
		TP	Log normal	Student's t	0.8217	No
		TSS	Log normal	Student's t	0.0056	Yes
Large and Small Cell Outlets	19	TKN	Normal	Student's t	0.7167	No
		NO _{2,3} -N	Not Normal	Signed Rank	0.5678	No
		TN	Normal	Student's t	0.7806	No
		NH ₄ -N	Normal	Student's t	0.1338	No
		TP	Normal	Student's t	0.5842	No
		TSS	Normal	Student's t	0.2607	No

The box plots in Figure 38 illustrate the paired data for which statistics were run. The plots show the distribution of data collected at each sampling point (n=19).

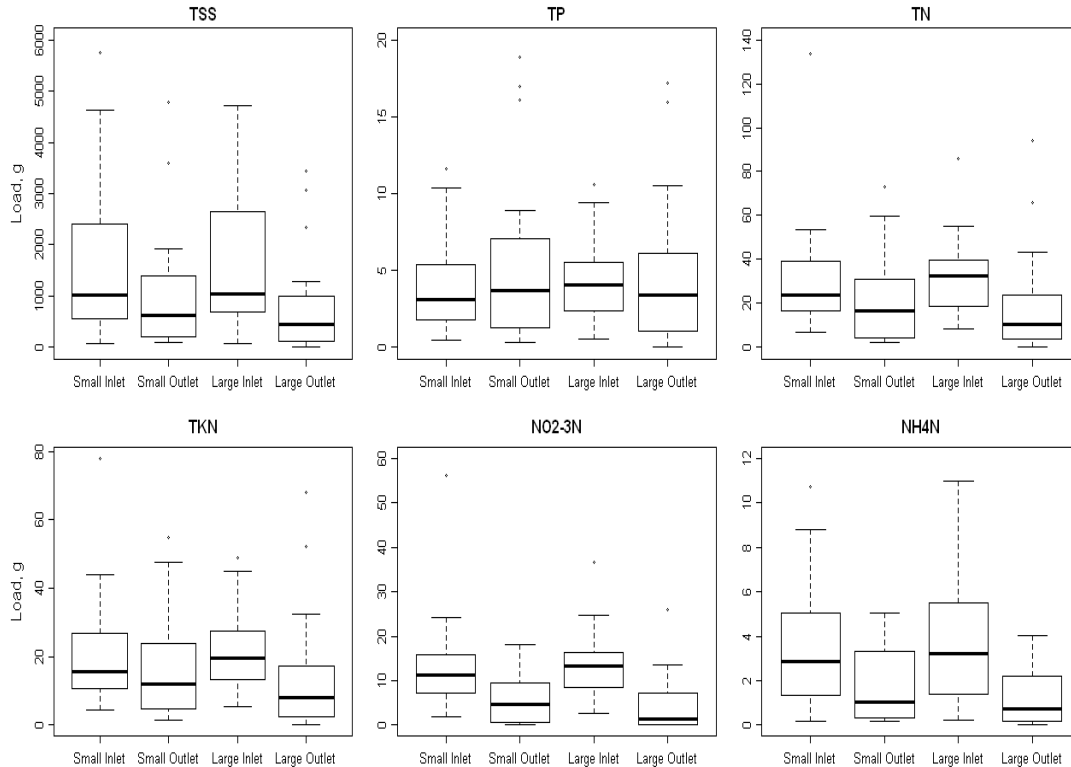


Figure 38. Influent and effluent nutrient and TSS loads in Mango Creek bioretention cells.

In general, the large cell achieved greater load reductions than the small cell as a combination of better volume and pollutant concentration reduction. The results show that on a per-event basis, the removals of pollutants with low influent concentrations were more heavily dependent on volume reduction than concentration reduction, due to the impact of small storm capture.

Monitoring Challenges

During the monitoring period (19 October, 2009 to 12 December, 2010), 79 storms were monitored for hydrology. However, not all of these storms were used in the hydrologic analysis. Several accuracy-related issues were encountered during the study. Anecdotal observations confirmed that when water levels exceeded the v-notch portion of the weir, flow became turbulent, leading to inaccurate water level readings. On 2 June, 2010, a storm event was observed supporting the assumption that the inflow data were sometimes inaccurate and underpredicted (Figure 39). During that storm, pressurized flow was observed from the large bioretention cell inlet pipe and the water level also rose above the top of the compound weir, making the flow data reported by the ISCO 6712™ invalid. Although backwater was not directly observed, it is possible that the high water level would not allow for freefall conditions over the weir during a larger storm. Due to the number of difficulties in measurement, all inflow data were instead calculated for each storm event using the Initial Abstraction method (Pandit and Heck, 2009) (Appendix A).



Figure 39. Pressurized flow at large bioretention cell inlet during 3.05 cm (1.2 in) storm (June 2, 2010, left image) and near backwater conditions at small bioretention cell inlet during 0.76 cm (0.3 in) storm (July 27, 2010, right image).

Several storms produced flow data that were indistinguishable when observed in Flowlink 5.1™ (2005). This was due to clogged bubbler tubing or unexplained monitoring equipment error. On several occasions, the flow volumes reported by Flowlink 5.1™ at the bioretention outlets were *higher* than the inlet volumes. This could not occur unless the antecedent dry period was extremely short and a previous storm event was still draining.

Swale

Nutrients and TSS

Pollutant Concentration Reductions

Mean and median TSS and nutrient EMCs are presented in Table 29 for the Mango Creek swale. Percent concentration reductions of mean pollutant EMCs are shown in Table 4.5

Table 29. Mean and median nutrient and TSS concentrations and mean EMC percent concentration reductions by sampling location (n=32 nutrients, 31 TSS).

Constituent	Mean Values		Median Values		Percent Mean Conc. Reduction (%)
	Swale Inlet (mg/L)	Swale Outlet (mg/L)	Swale Inlet (mg/L)	Swale Outlet (mg/L)	
TKN	0.67	0.62	0.60	0.54	7.9
NO _{2,3} -N	0.38	0.37	0.28	0.24	0.2
TN	1.05	0.99	0.89	0.83	5.1
NH ₄ -N	0.08	0.07	0.05	0.05	16.2
TP	0.17	0.16	0.11	0.13	6.3
TSS	72	39	55	30	45.4

Results from the statistical analysis performed on paired nutrient data showed there was no significant difference in influent and effluent nutrient concentrations. However, there was a statistical difference in the mean influent and effluent TSS concentrations (Table 30).

Table 30. Statistical analysis results for nutrients and TSS.

Constituent	n	Distribution	Test of Significance	p-value	Significant difference?
TKN	32	Log-normal	Student's t	0.6422	no
NO _{2,3} -N	32	Normal	Student's t	0.9797	no
TN	32	Log-normal	Student's t	0.6702	no
NH ₄ -N	32	Log-normal	Student's t	0.0599	no
TP	32	Not normal	Signed Rank	0.6526	no
TSS	31	Log-normal	Student's t	<0.0001	yes

Figure 40 shows inflow and outflow concentrations of each sampled storm event. In several cases, outflow concentrations were equal to or greater than inflow concentrations. It has been argued that swales do not permanently bind pollutants within their vegetation and soil but instead attenuate loads on a storm-by-storm basis. The release of nutrients and sediment from swales is typical and is particularly common when the swale receives low influent pollutant concentrations (Bäckström et al., 2006), which was the case for the I-540 bridge deck. In the Sodra Hamnleden swale studied by Bäckström et al. (2003), a decrease in influent suspended solids caused a decrease in the suspended solids retained within the swale (Bäckström, 2003). Bäckström (2006) observed that swales act as a pollutant source rather than a pollutant sink if the influent pollutant concentration is below a certain point, therefore making swales unreliable at reducing pollutant concentrations because of their dependence upon the condition of the influent runoff.

Influent nutrient concentrations that were considered high relative to the average trend of concentrations from the I-540 bridge deck were still at or below average concentrations at other study sites (Wu et al., 1998; Gan et al., 2007). The spikes in TSS concentration on 14 March, 2010 and 15 October, 2010, however, reached levels that were higher than average when compared to other studies (Wu et al., 1998; Gan et al., 2007).

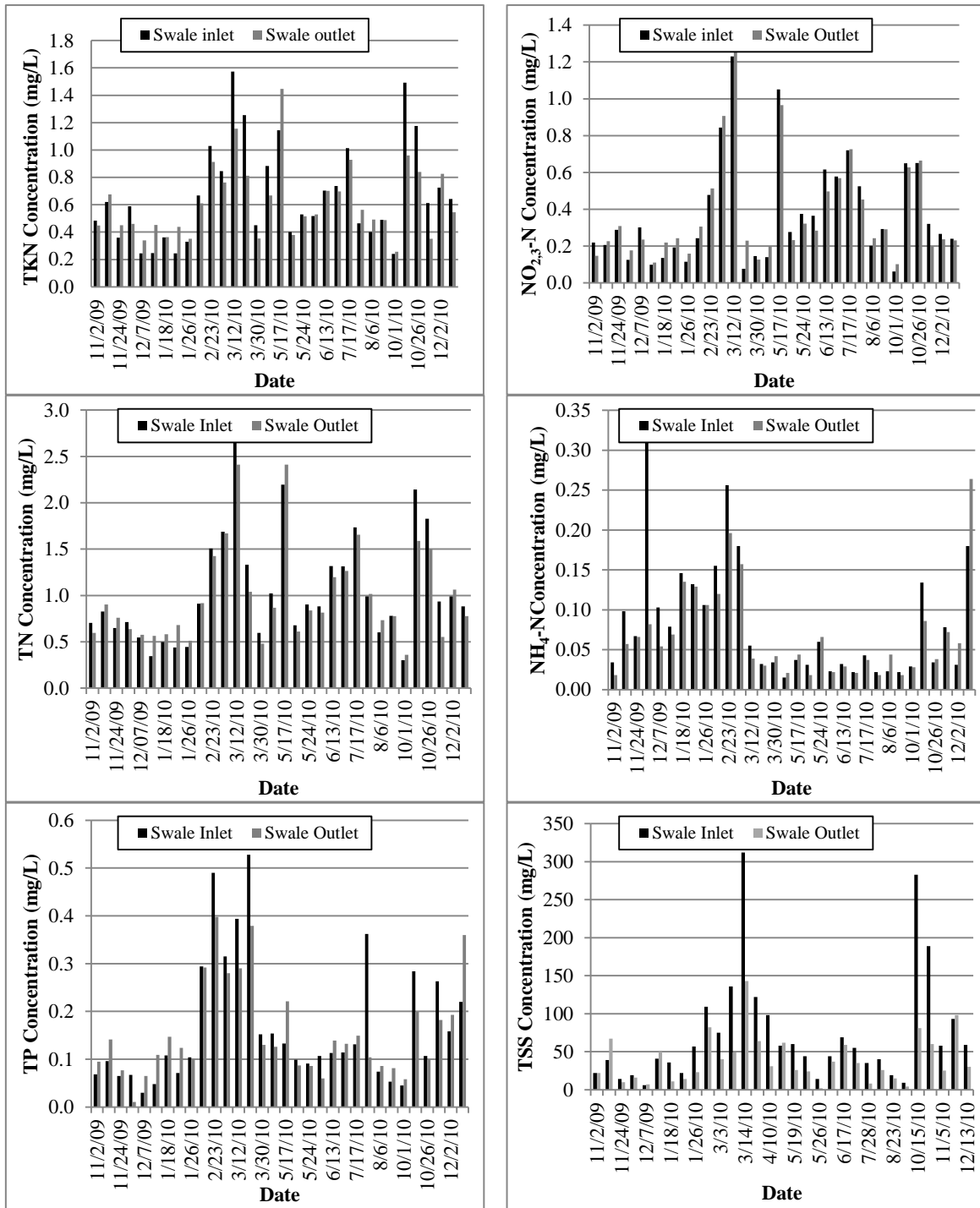


Figure 40. Inlet and outlet concentrations per sampled storm event.

Nutrient and TSS Removal Summary

Target effluent concentrations are a metric to assess stormwater SCM performance. McNett et al. (2010) characterized water quality levels by correlating various in-stream pollutant

concentrations to benthic macroinvertebrate health. In the Piedmont of North Carolina, “good” water quality concentrations for TN and TP were 0.99 mg/L and 0.11 mg/L, respectively (Figure 41). “Good” water quality supported intolerant benthic macroinvertebrates, such as *Ephemeroptera* (mayflies) and *Trichoptera* (caddisflies). The target concentration for TSS was 25 mg/L (Barrett et al., 2004) (Figure 42).

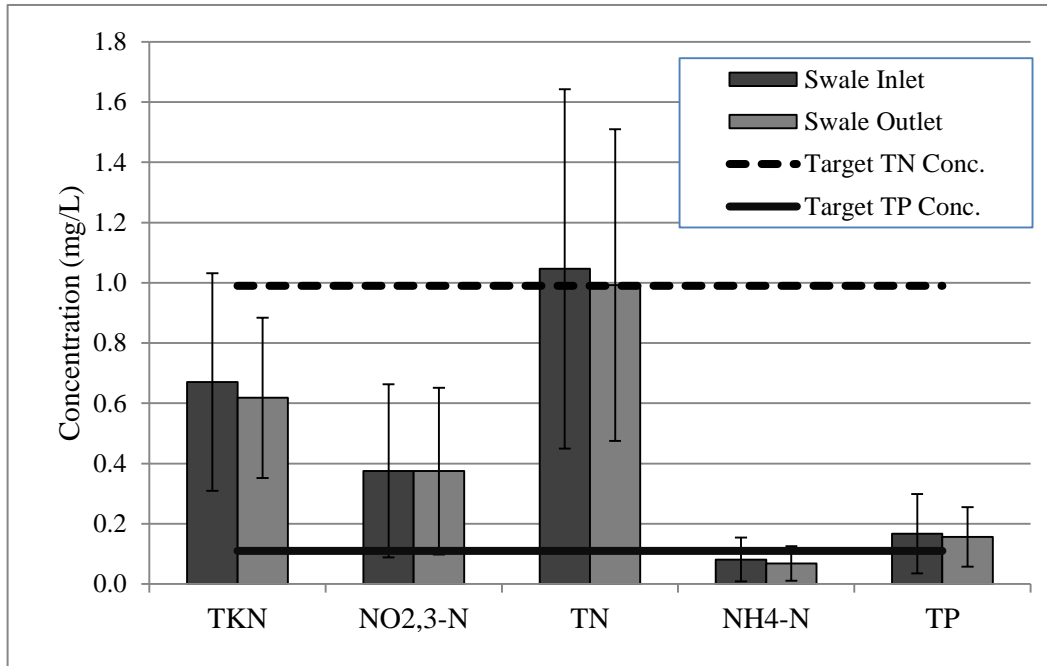


Figure 41. Average influent and effluent nutrient concentrations in Mango Creek swale.

The I-540 bridge deck runoff contained low pollutant concentrations when compared to target nutrient concentrations. Both TN and TP were slightly above the “good” water quality target concentration prior to entering the swale. When analyzing the pollutant concentrations based on this metric, the swale’s inability to significantly reduce the TP concentrations in the runoff may have been partly a result of irreducible concentrations (Strecker et al., 2001; Lenhart and Hunt, 2011). The outflow from the swale reached a “good” water quality level for TN but the TP outflow concentration (0.16 mg/L) reached a water quality rating that was between the “fair” and “good/fair” median pollutant concentrations of 0.22 mg/L and 0.13 mg/L, respectively (McNett et al., 2010). Further, the median NH₄-N concentration entered the swale between the “good” and “good/fair” levels (0.04 and 0.06 mg/L, respectively) and was not reduced to the “good” target concentration (Figure 41). Total suspended solids (Figure 42) were not reduced to the target level.

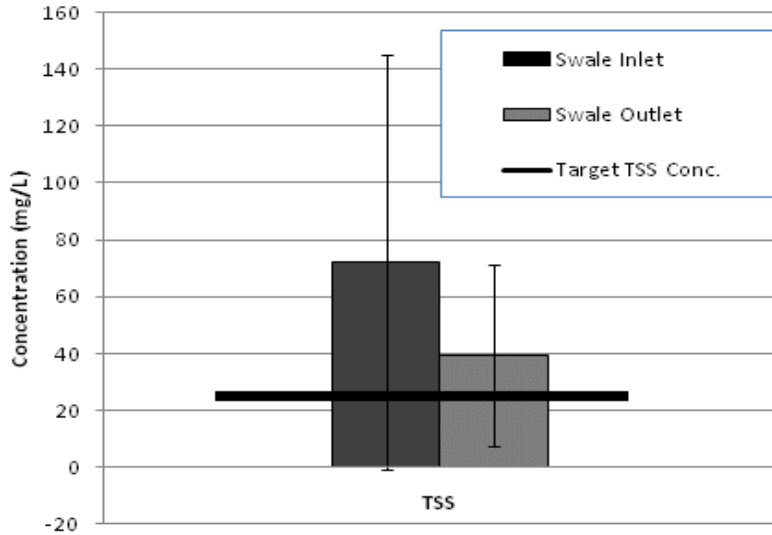


Figure 42. Average influent and effluent TSS concentrations in Mango Creek swale.

Cumulative probability plots (Figures 43-45) were created by ranking influent and effluent concentrations to illustrate the relative probability that a concentration would exceed the “good” water quality benchmarks of 0.99 mg/L, 0.11 mg/L, and 25 mg/L for TN, TP, and TSS, respectively. The influent TN and TP concentrations in the stormwater were relatively low, with 60% and 50% of the data points below the “good” water quality thresholds, respectively. Approximately 26% of the influent TSS data points were below the 25 mg/L threshold. Comparatively, 63%, 44%, and 42% of the effluent concentration of TN, TP, and TSS were at or below their target benchmarks, respectively.

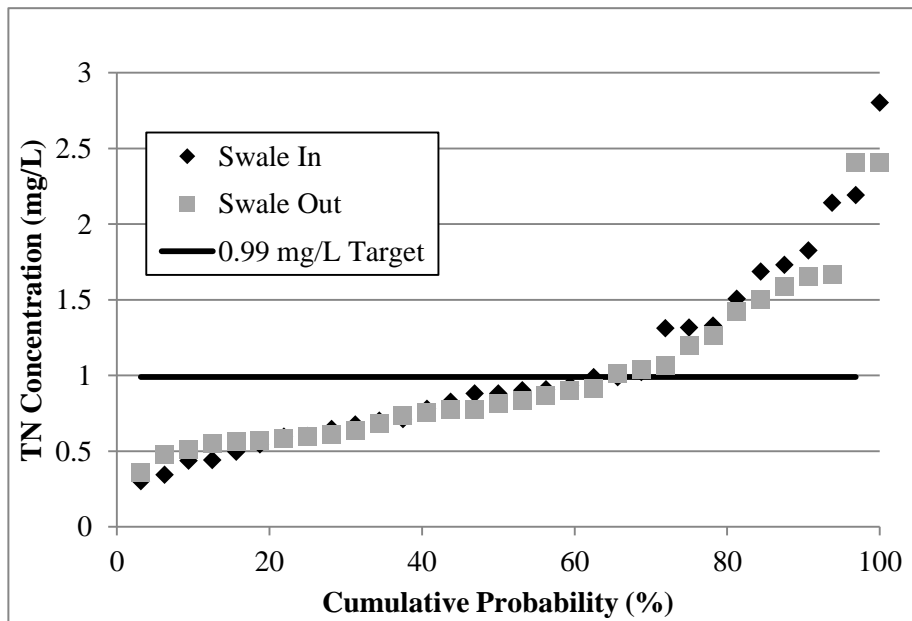


Figure 43. Swale cumulative probability plot for TN.

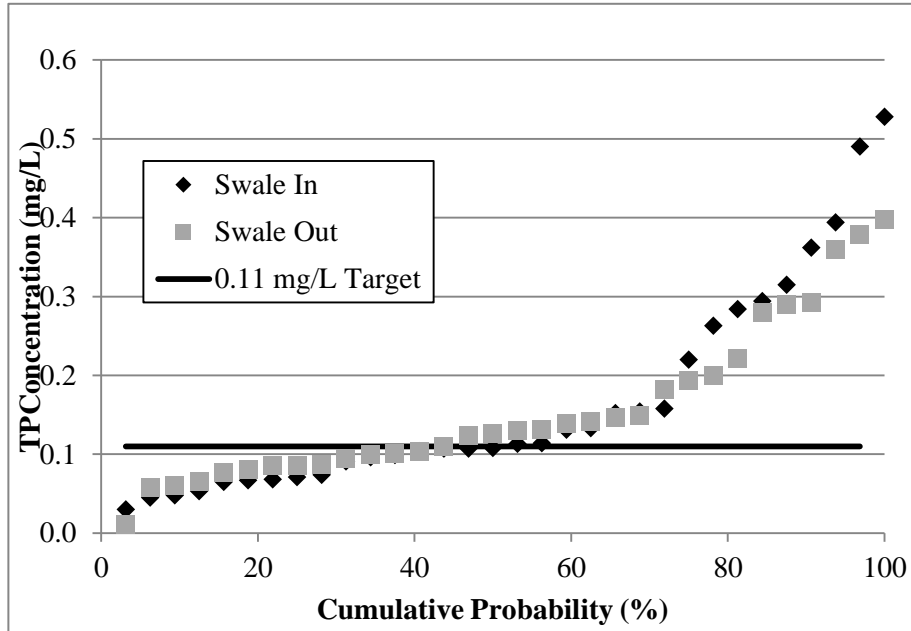


Figure 44. Swale cumulative probability plot for TP.

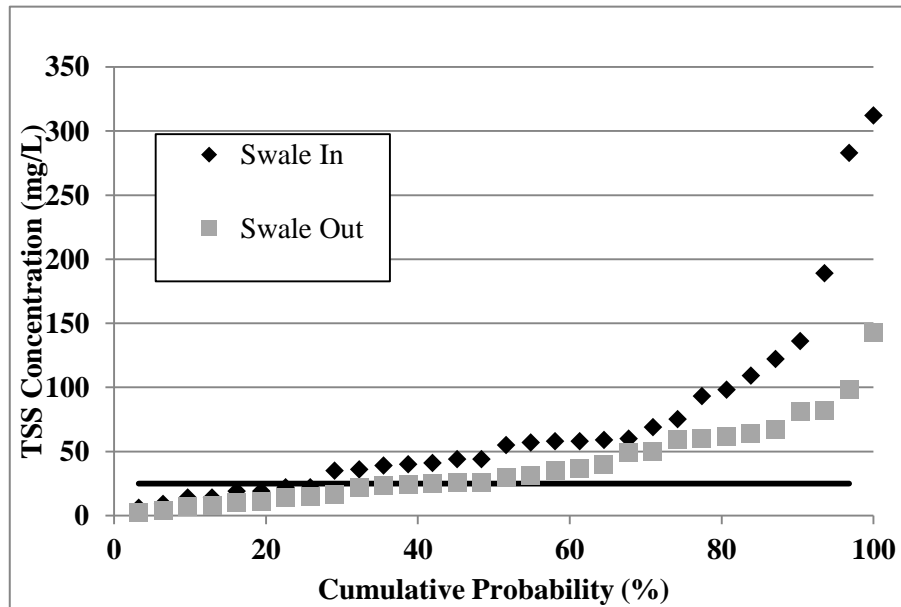


Figure 45. Swale cumulative probability plot for TSS.

Heavy Metals

Median heavy metals concentrations are presented in Table 31 for the ten storm events sampled for metals at the swale. Possible sources of these metals include brake emissions, tire wear, and the bridge deck structure itself (Davis et al., 2001; Zanders, 2005). Median total copper, zinc,

and lead concentrations were significantly reduced through the swale, possibly due to those metals' association with TSS (Opher and Friedler, 2010; Zanders, 2005; Sparks, 2003). Interestingly, the swale significantly reduced lead concentrations, while the bioretention cells did not. Perhaps this was due to the higher (non-significant) influent concentrations for the swale when compared to the influent concentrations for the bioretention cells. Dissolved copper and zinc concentrations were reduced (non-significant), which was likely a result of adsorption to the swale soil (Yousef et al., 1985; Bäckström, 2003). No conclusions could be drawn from the median dissolved lead concentrations reported for the swale, as most of the inlet data were below the laboratory detection limit (Appendix J).

Table 31. Median total and dissolved heavy metal concentrations for the Mango Creek swale.

Sampling Location	Median Concentrations					
	Total Metals (µg/L) ^[1]			Dissolved Metals (µg/L)		
	Cu	Zn	Pb	Cu	Zn	Pb
Swale Inlet	15.5	65.0	5.6	7.1	27.0	BDL ^[2]
Swale Outlet	11.0*	39.0*	2.0*	5.2	18.0	BDL

[1] Detection limit (DL) for Cu and Pb was 2 µg/L and 10 µg/L for Zn.

[2] BDL = Below the Detection Limit

* Statistically significant reduction in metal concentration when compared to inlet concentration

Mango Creek bridge deck metals concentrations were compared to metals concentrations in other bridge deck studies. The 15.5 µg/L influent copper concentration was essentially the same as the 15 µg/L median concentration for another bridge deck located in North Carolina (Wu et al., 1998) with similar surrounding land use and traffic loading. A bridge deck study conducted in central Florida with a similar average daily traffic volume had markedly higher average concentrations of 292 µg/L, 617 µg/L, and 48 µg/L for total Zn, Pb, and Cu, respectively (Yousef et al., 1984). Dissolved concentrations of Zn, Pb, and Cu at the central Florida site were 50 µg/L, 39 µg/L, and 22 µg/L, respectively; again, substantially higher than those of this study.

Pollutant Loads

Inflow volumes into the swale entrance from the bridge deck catchment were calculated using the Initial Abstraction method for the extent of the monitoring period (Pandit and Heck, 2009). This method likely over-predicted the amount of runoff coming from the contributing catchment because of the pipe leak but was still more representative than the volumes reported by the ISCO portable sampler. No direct rainfall was included in the inflow calculations because the swale was largely located underneath the southbound bridge deck. The reported hydrology data at the swale outlet were also considered unreliable and therefore were not used in load reduction calculations. The reported outflow volumes for the smaller events were not used in any load or volume reduction calculations. To be conservative, outflow volumes were set equal to inflow volumes for load calculations.

Average pollutant load reductions, based on calculated inflow and outflow volumes, are presented in Table 32. These load reductions accounted for runoff from 70.1 cm (27.6 in) of total rainfall. This technique allowed the largest events, and their associated loads, to proportionally influence the result. Since total nitrogen loads were calculated as the sum of TKN and NO_{2,3}-N

loads, with TKN being the largest contributor, TN was reduced even though NO_{2,3}-N increased through the swale.

Table 32. Pollutant load reductions for the swale at Mango Creek, calculated using the summation of loads technique.

Constituent	Sum of Influent Pollutant Loads (kg)	Sum of Effluent Pollutant Loads (kg)	Summation of Loads (%)
TKN	1.52	1.40	8.0
NO _{2,3} -N	0.74	0.74	-0.4
TN	2.26	2.14	5.3
NH ₄ -N	0.23	0.16	32.3
TP	0.36	0.33	7.5
TSS	177	91	49

A second load reduction method was also used (mean load reduction, Equation 4.3) which calculated the load reductions per storm event and then averaged these reductions over the entire number of sampled storms. This method equally weighted each storm, giving larger storms less influence.

Mean load reduction results are summarized in Table 33. This method generally showed a more negative performance by the swale, possibly because large storms had less effect on the reduction percentage but may have been more consistently associated with higher pollutant removals.

Table 33. Percent pollutant load reductions for the swale at Mango Creek as calculated using average mass reduction.

Constituent	Mean Load Reduction (%)
TKN	3.1
NO _{2,3} -N	-6.5
TN	4.3
NH ₄ -N	7.4
TP	-5.3
TSS	37.7

Normalized annual pollutant loads are shown in Table 34. Since there was no volume reduction, the slight differences in untreated load (load from the bridge deck catchment area) and treated load (load from the swale outlet) reflects the minimal reduction in pollutant concentration in the swale, particularly nutrient concentrations. All of the untreated annual loads were substantially less than those observed in previous studies (Barrett et al., 1998 a, b). The loads accounted for approximately 71 cm (28 in) of rainfall recorded on-site for the sampled events and 118 cm (46 in) of average annual rainfall recorded approximately 2.7 km (1.7 mi) from the research site (State Climate Office, 2011). During the 14-month monitoring period, the Mango Creek site received 142 cm (56 in) of rainfall (132 cm/yr (52 in/yr)), which was higher than average.

Table 34. Annual untreated and treated loads at the Mango Creek swale.

Constituent	Untreated Load (kg/yr)	Treated Load (kg/yr)	Untreated Load (kg/ha/yr)	Treated Load (kg/ha/yr)
TKN	2.52	2.32	5.51	5.07
NO _{2,3} -N	1.22	1.23	2.68	2.69
TN	3.74	3.55	8.18	7.75
NH ₄ -N	0.37	0.26	0.82	0.56
TP	0.59	0.55	1.29	1.19
TSS	293	151	640	330

Particle Size Distribution Analysis

The fate of particles in a swale system affects heavy metals and nutrient removal because of their association with fine soil fractions. The longitudinal slope and length of a swale have an effect on the fate of suspended particles. The ability of particles to settle is also dependent on the flow velocity and the swale’s soil infiltration rate (Bäckström, 2003). Bäckström (2002) showed that sedimentation accounted for a higher degree of trapping efficiency than did filtration, making the swale length an important design parameter. Yu et al. (2001) and Deletic (1999) both suggested that the removal efficiency of suspended particles and nutrients does not improve beyond a certain swale length regardless of channel slope and dependent upon velocity, flow depth, and particle size/density. Due to the compact soils of the Mango Creek swale, sedimentation and filtration through the swale’s vegetation were determined to be the key factors in solids removal, more so than infiltration.

Figures 46-48 show the particle size distributions (PSDs) of three storms, along with other particle size information, at the swale inlet and outlet. The influent mean particle size associated with the storm on 12 December, 2010, was less than half that of the other two sampled events. The smaller influent mean particle size may explain why the swale did not reduce the mean particle size for this rainfall event and may also explain why the percent TSS removal was less than for the other two storms, despite having a similar influent TSS concentration to the storm on 5 November, 2010 (Table 35).

Table 35. Hydrology and TSS data for storm events sampled for particle size distribution analysis.

Event No.	Date	Influent [TSS] (mg/L)	Effluent [TSS] (mg/L)	TSS Removal (%)	Rainfall (mm)	Inflow Volume (L)	Peak Discharge (L/s)
71	10/14/10	283	81	71.4	10.9	35,000	22
74	11/5/10	58	25	56.9	13.0	44,400	8
79	12/12/10	59	30	49.2	7.1	30,200	4

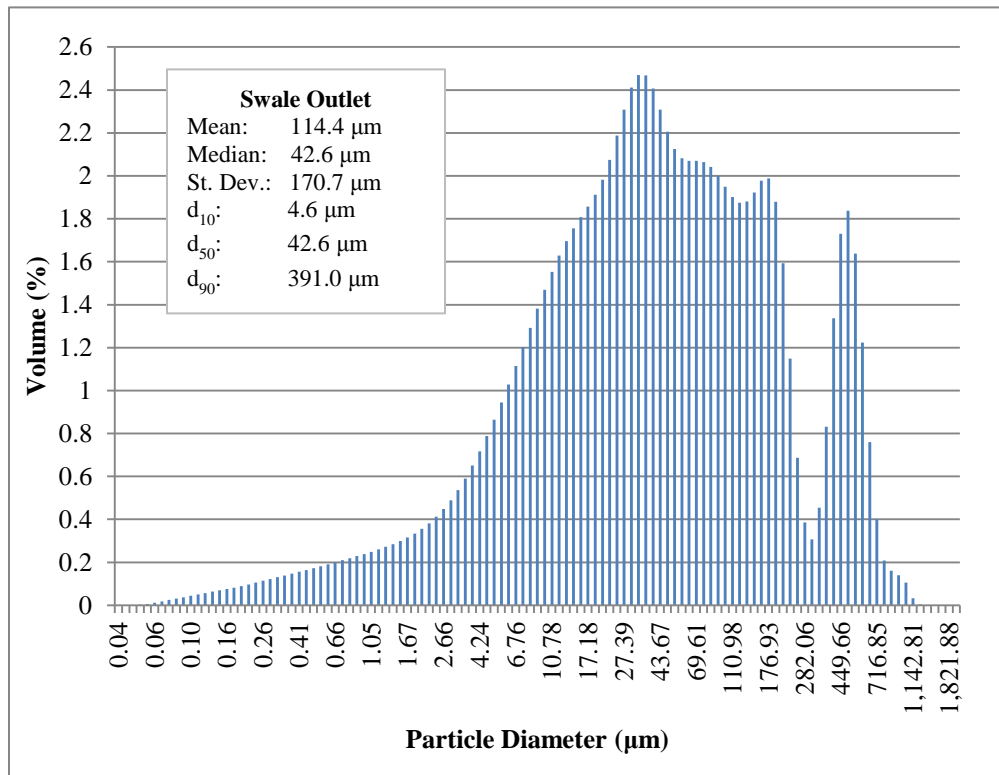
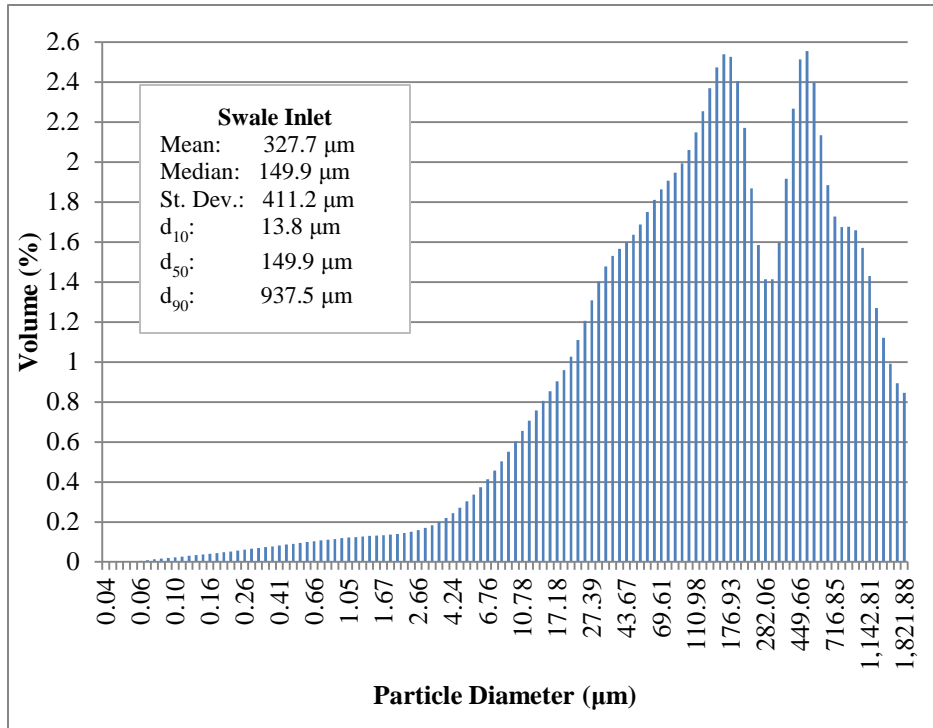
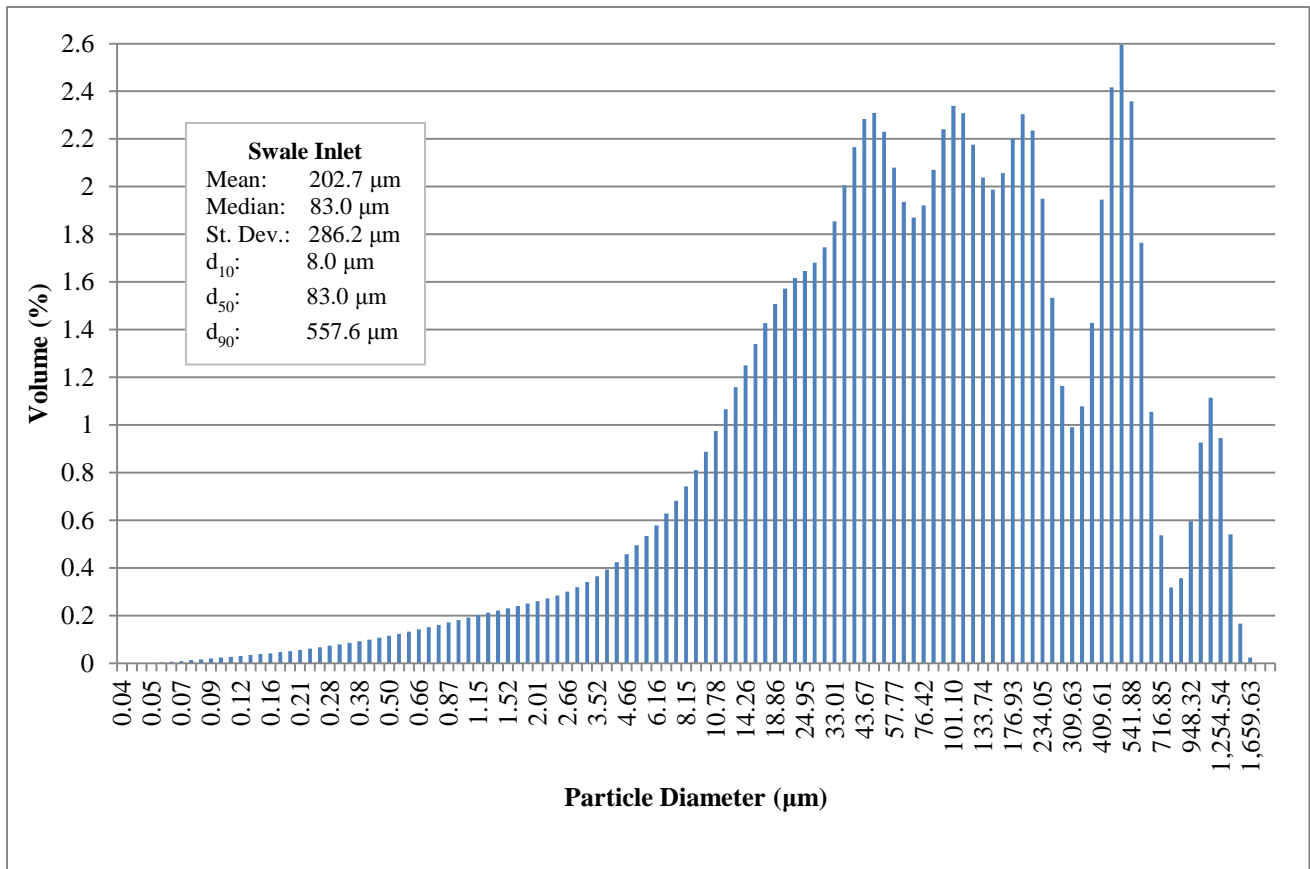


Figure 46. Swale influent and effluent particle size distribution (October 14, 2010).



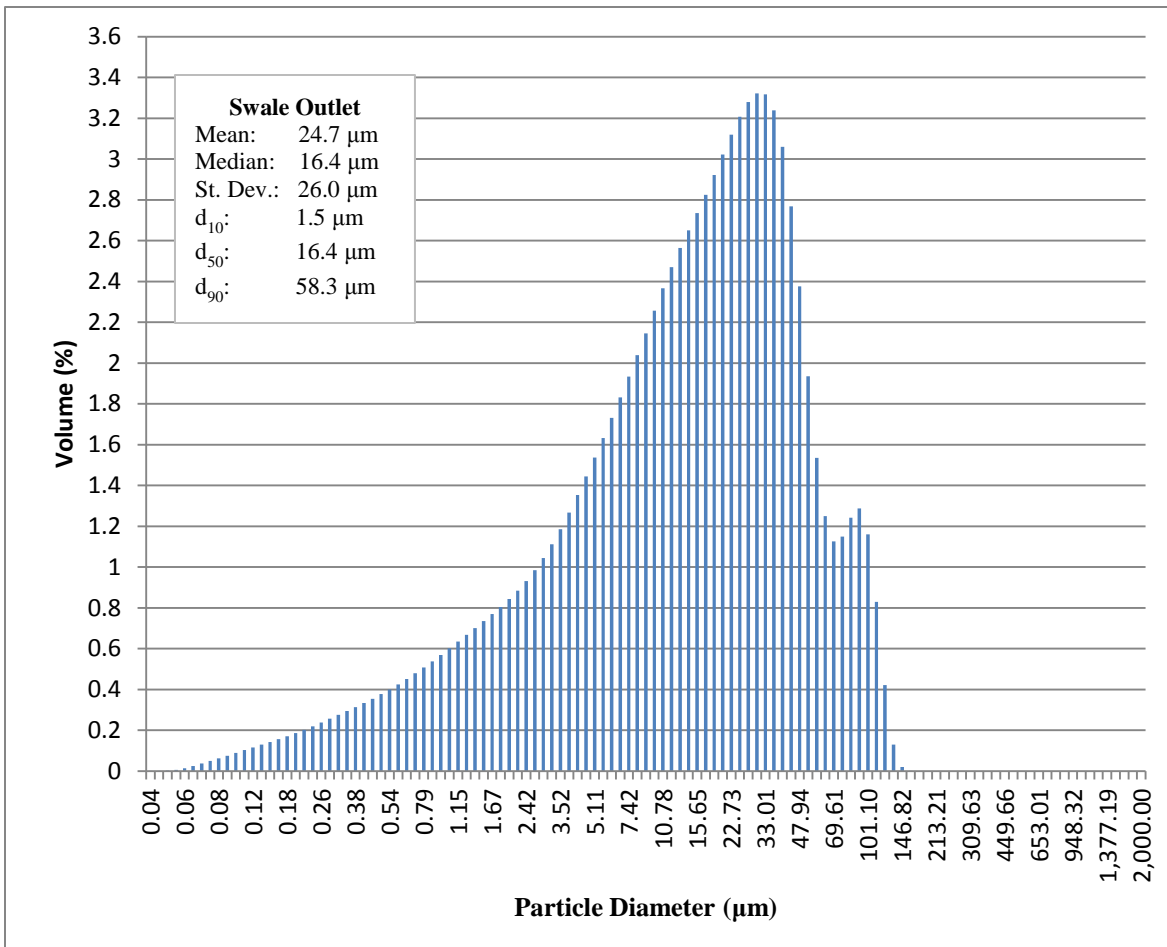


Figure 47. Swale influent and effluent particle size distribution (November 5, 2010).

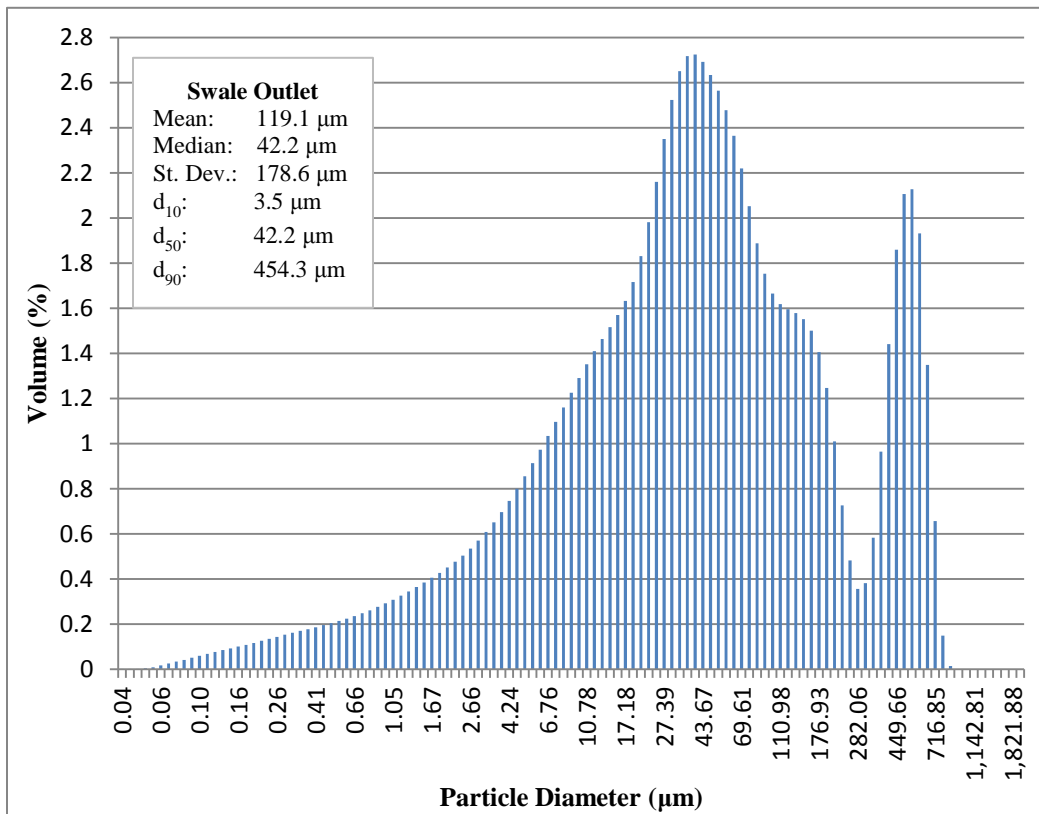
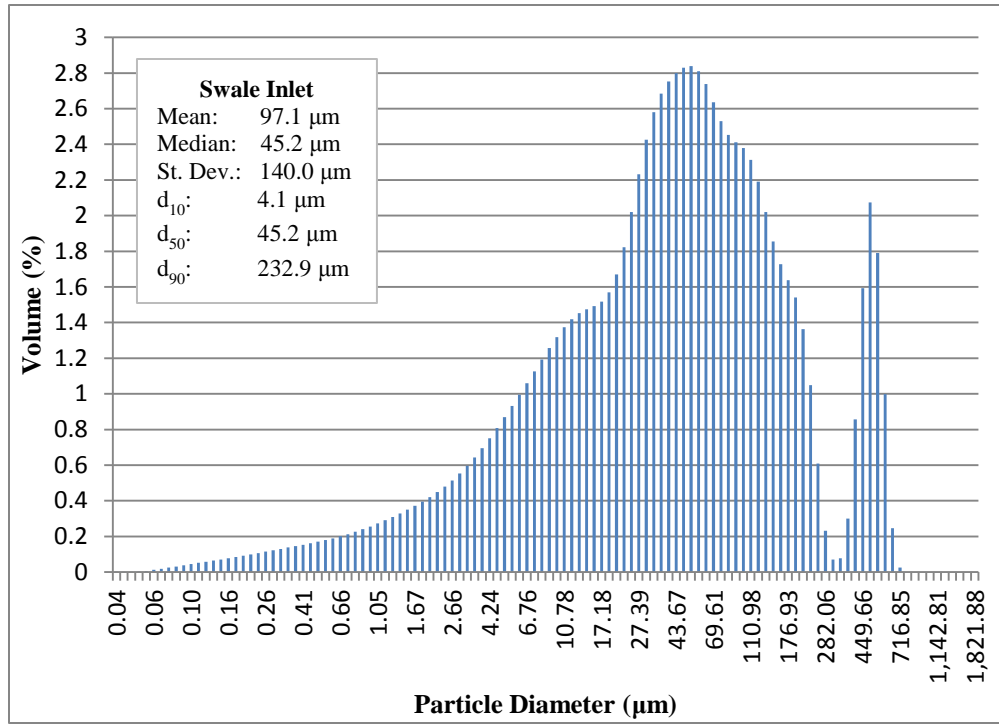


Figure 48. Swale influent and effluent particle size distribution (December 12, 2010).

Coarser sediment is often associated with high traffic volumes and heavy vehicles, which are typically linked to commercial and industrial land-uses (Skeen et al. 2009). Zanders (2005) studied road sediment samples from an asphalt road intersection in Hamilton, New Zealand, with a traffic loading of 25,000 vehicles/day and reported that 52% of the sediment was less than 250 μm . A study conducted in Auckland, New Zealand, on eight stormwater network sites had either d_{50} values ranging from 45 μm to 70 μm , depending on factors such as land use, catchment slope, traffic loads, and vehicle type (Skeen et al. 2009). Sediment was vacuumed directly from the roadside gutter in Zanders' (2005) study, while the samples in the Skeen et al. (2009) study were derived from the stormwater, which may account for the difference in sediment size between these two studies. The d_{50} values reported by Skeen et al. (2009) more closely related to the influent d_{50} values seen at the Mango Creek site (Figures 46-48).

Differential volume percentages (Appendix N) were summed and partitioned into the particle diameter ranges shown in Figure 49 to show whether the Mango Creek swale caused an increase or decrease in the fraction of particles in each of the ranges. This was done for each storm event sampled for PSD ($n=3$), and then the results were averaged. A negative percentage meant that the percent of particles in that range increased from the swale inlet to the swale outlet. It appeared that particles in the range of 0.04-40 microns were most easily transported from the swale, while the particles that were best detained within the swale-forebay system ranged from 100-2000 microns. Highway stormwater runoff has relatively coarse PSDs (Skeen et al., 2009; Sansalone et al., 1998); therefore, swales are an effective means of removing these coarser soils. Bäckström et al. (2006) observed that particles in the range of 9 to 15 microns were most easily transported from the studied roadside grassed swale at Sodra Hamnleden in Sweden, while the swale most effectively trapped particles larger than 25 μm during most rain events. The sediment d_{50} value was 6 μm for Bäckström et al.'s (2006) study, which may explain the smaller reported diameter of easily trapped sediment. Deletic (1999) performed a lab-scale grass filter strip study using a sediment/water mixture with a 50 μm median diameter and found that most particles above 60 μm were usually trapped. The flowrates in Deletic's (1999) study were similar to those observed during the Mango Creek swale PSD analysis.

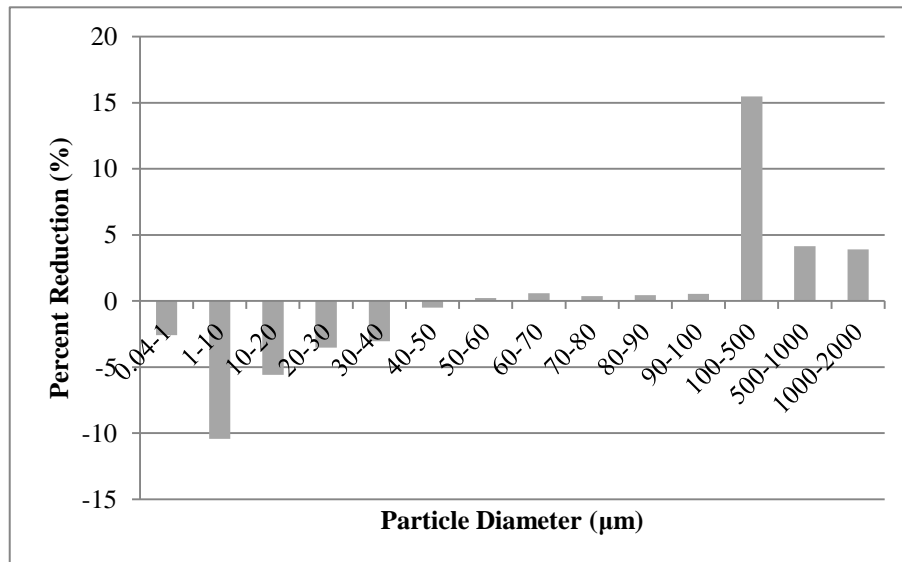


Figure 49. Particle removals at the Mango Creek swale.

Particle trapping efficiency in swales is improved with increased grass length (Bäckström, 2002; Deletic, 1999) since the grass acts as a sediment filter and slows water velocity to allow for settling to occur. Therefore, for water quality improvement purposes, the depth of flow through a swale should not exceed the height of the grass (US EPA, 1999). The average length of tall fescue during the year-long monitoring period in the swale at Mango Creek was 0.24 m (0.78 ft) (Appendix M). Flow depth during peak rainfall intensity was calculated using Manning's Equation for 27 storms with associated TSS removal data. Peak flowrates were found using the rainfall intensities provided by the ISCO 674™ rain gauge and calculated using the Rational Method (Haan et al., 1994) based on a 13 minute time of concentration. Of the 27 observed rainfall events, only 5 events exceeded the average height of the grass (Appendix N), indicating that the swale was acting as a water quality swale as opposed to a water conveyance swale on most occasions. No clear connection could be made between the effects that the water depth above the grass height had on the TSS trapping efficiency, given the limited data that were available.

Monitoring Challenges

There were several issues associated with the hydrologic monitoring that took place at the inlet and outlet of the swale. Visual evidence suggested that backwater conditions, instances of weir overtopping, and full pipe flow occurred on a fairly regular basis at the inlet pipe. There was approximately 9 m (30 ft) of elevation difference from the bridge deck to the inlet pipe, causing significant pressure behind the weir and consequently causing high velocity runoff to enter the swale. The configuration of the water conveyance pipes and the location of the swale were therefore not conducive for accurate monitoring with laminar, steady flow conditions at the weir. Also, the invert of the swale entrance (end of the forebay) was at roughly the same elevation as the invert of the weir located in the inlet pipe, causing frequent backwater conditions across the forebay (Figure 50).

Backwater conditions were also prevalent at the swale outlet (Figure 50). The weir box that was fitted to the outlet pipe did sometimes still the flows of smaller storms but the weir was often overwhelmed and the entire box overtopped.



Figure 50. Swale inlet pipe (left) and outlet weir box (right) during 3.0 cm (1.2 in) storm (June 2, 2010).

Another monitoring dilemma was inaccurate stage/discharge measurements caused by sediment that consistently entered the swale inlet pipe from the bridge deck and covered the bubbler tubing opening (Figure 51). The sand began to fill the swale forebay which decreased the storage volume in the forebay (Figure 52). The sediment was cleared from the forebay once during the monitoring period on 13 July, 2010.



Figure 51. Sediment in swale inlet pipe directly behind weir.



Figure 52. Swale inlet forebay prior to (left) and following (right) sand cleanout (July 13, 2010).

Substantial soil compaction occurred during construction of the swale itself, which was constructed with on-site soils, comprised of a compacted mix of native soils and construction fill soil (Figure 53, Appendix M). Due to these conditions, little to no infiltration was expected in the swale.



Figure 53. Soil compaction in Mango Creek swale during construction.

A leak in the stormwater runoff collection pipe which routed the southbound bridge deck runoff to the swale was observed on February 9, 2010. The NCDOT fixed the leaking pipe circa March 27, 2010. Event mean concentrations (EMCs) collected for the storms which occurred during the time that the collection pipe was leaking *were used* for water quality analysis and were also used in mass load reduction calculations. Water quality was not altered by the leak; therefore, the water quality samples were still considered representative.

Conclusions

Two bioretention cells, one of which being appropriately sized and the other being intentionally undersized per NCDENR (2007) design standards, were monitored to determine their effectiveness in treating bridge deck runoff. The following conclusions were drawn based on the study:

- Cumulative volume reductions were significant in both cells and were comparable to reductions achieved by previously studied bioretention cells with similarly shallow media depths (Passeport et al., 2009; Li et al., 2009). The large and small cell both achieved much greater volume reductions for storms less than 2.5 cm (1 in) (65.2% and 36.2% reductions, respectively) versus storms greater than 5 cm (2 in) (24.0% and 14.1% reductions, respectively). Differences in paired outflow volumes between the cells were not significant. These data promote the use of undersized bioretention cells to achieve volume reductions comparable to full-scale systems. However, the decision is left to the designer to determine if the marginal lost benefit associated with an undersized bioretention retrofit justifies its cheaper cost.
- Surface storage is an important factor in peak lag time (Li et al., 2009; Davis, 2008; Hunt et al., 2008). The small cell was even further undersized than intended, with a bowl volume of only 67% its design volume. The median peak flow lag time was eight times longer in the large cell than the small cell, indicating the importance of bowl storage volume.
- For future designs, it may be beneficial to build deeper cells to allow for more water storage space when underlying soils result in exceptionally slow exfiltration rates; this is

particularly true for cells with ISZ layers. The as-built media depths in the large and small cells were, on average, 20% and 50% greater than the design media depths, respectively. Deeper media detracted from the bowl volumes but, considering the tight *in situ* soils and inclusion of ISZ layers in the Mango Creek cells, may have provided some extra benefit by increasing storage volume within the media.

- Slow drawdown time encouraged overflow and therefore was an impediment to volume reduction. The slow drawdown is probably the result of a small driving head (due to the extension of the IWS to within 30 cm (12 in.) of the surface) and highly restrictive underlying soils. Additionally, care must be taken to keep bioretention cell surfaces unclogged by sediment during construction.
- Bridge deck runoff concentrations for TN, TP, and TSS at the Mango Creek site were well below those for other bridge deck runoff studies in the literature (Barrett et al., 1998a, Wu et al., 1998; Gan et al., 2007). Low influent concentrations had an impact on the pollutant reductions achieved by the cells, making the efficiency ratios low with respect to the cells' treatment effectiveness. While not realized at the time of experimentation, these concentrations did prove to be the lowest of all bridge decks examined by NCDOT.
- Neither cell significantly reduced total phosphorous. However, when comparing effluent concentrations to target North Carolina water quality standards as determined by benthic macroinvertebrate health, both cells released TP concentrations near the "good" water quality threshold. This suggests that TP may have been entering the cells at or near irreducible concentrations and that other metrics should be part of the evaluation of SCM performance.
- The large bioretention cell released lower median nutrient and TSS effluent concentrations than the small bioretention cell for every examined constituent. However, effluent concentrations of NH₄-N and TSS, and effluent loads of all examined constituents, were statistically similar between the cells. When employing the percent load reduction metric, the small bioretention cell achieved 60-90% of the load reductions that were achieved by the large cell for all pollutants except TP, despite the fact that the small cell only captured 30% of the design storm.
- Currently, in the Piedmont of North Carolina, bioretention cells with ISZs receive 85%, 40%, and 45% regulatory credit for TSS, TN, and TP, respectively (NCDENR, 2007). It may be reasonable for an undersized bioretention cell to be awarded a credit equal to its *proportion* of the full size cell. Undersized cells do provide a benefit and their use should be encouraged in locations with limited available space for retrofits. In short, undersized bioretention cells "punch more than their weight."
- Highway runoff is recognized as a major source of non-point source pollution (Opher and Friedler, 2010; Crabtree et al., 2006). However, before SCMs are retrofit in the bridge deck landscape, some initial water quality testing might be appropriate. This study shows that not all highway runoff may justify the expense of retrofits.

The Mango Creek grassed swale was monitored to determine its effectiveness in treating highway bridge deck runoff water quality and hydrology. The following conclusions were drawn:

- The swale did not significantly reduce nutrient concentrations or loads, but did significantly reduce TSS concentrations by 45%. The suspended solids were presumably removed due to slowed flow velocities and entrapment by the thick stand of tall fescue within the swale. Further pollutant load reduction would have likely occurred if the swale soil was less compacted and more permeable.
- Swales remove coarse sediment better than fine sediment due to the larger particles' higher settling velocities. The PSD data from the Mango Creek swale showed that particles ranging from 100-2000 microns were best detained within the swale-forebay system. Also, a higher TSS percent reduction was associated with the storm carrying coarser sediment. Since highway stormwater runoff is expected to have relatively coarse sediment (Sansalone et al., 1998), swales are a viable means of TSS reduction from highway runoff.
- Sedimentation and filtration are means of removal for TP, total Cu, and total Zn as a result of their tendency to adsorb to fine soil fractions. The Mango Creek swale better detained coarser soil fractions and released finer fractions, which may explain why only minor reductions were seen for the aforementioned pollutants. Swales should be used in combination with other stormwater treatment practices, or would need a different design and construction procedure, to achieve desirable nutrient, metal, and hydrologic attenuation.
- The I-540 southbound bridge deck runoff pollutant concentrations were relatively low for pollutants examined. Nutrient and TSS concentrations were typically less than those of other bridge deck runoff studies (Wu et al., 1998; Gan et al., 2007). These low influent concentrations may have had an impact on the pollutant reductions achieved by the swale. The untreated annual pollutant loads were also much less than those observed in other studies (Barrett et al., 1998 a, b).
- When comparing TN and TP swale effluent concentrations to target North Carolina water quality standards based on benthic macroinvertebrate health (McNett et al., 2010), the swale released “good” median TN concentrations and “good/fair” median TP concentrations. The swale did not meet the target effluent TSS level of 25 mg/L (Barrett et al., 2004).

Acknowledgements

The authors would like to thank the NCDOT for funding this research. We are also grateful to URS Corporation, who designed the SCMs, and NCDOT for SCM installation and upkeep. The authors thank Shawn Kennedy, who helped immensely with monitoring equipment installation and troubleshooting. Finally, the authors acknowledge the North Carolina State University Center for Applied Aquatic Ecology (CAAE) laboratory and the North Carolina Division of Water Quality laboratory for sample analysis.

References

- American Public Health Association (APHA), American Water Works Association (AWWA) and Water Environment Federation. (1998). *Standard methods for the examination of water and wastewater*, 20th Edition, APHA, Alexandria, VA.
- Bäckström, M. (2002). Sediment transport in grassed swales during simulated runoff events. *Water Science and Technology*, 45(7), 41-49.
- Bäckström, M. (2003). Grassed swales for stormwater pollution control during rain and snowmelt. *Water Science and Technology*, 48(9), 123-132.
- Bäckström, M., Viklander, M., and Malmqvist, P. A. (2006). Transport of stormwater pollutants through a roadside grassed swale, *Urban Water Journal*. 3(2), 55-67.
- Barrett, M.E., Irish, L., Malina, J.F., and Charbeneau, R.J. (1998a). Characterization of highway runoff in Austin, Texas, area. *Journal of Environmental Engineering*, 124(2), 131-137.
- Barrett, M. E., Walsh, P. M., Malina, J. F., and Charbeneau, R. J. (1998b). Performance of vegetative controls for treating highway runoff. *Journal of Environmental Engineering*, 124(11), 1121-1128.
- Barrett, M.E, Lantin, A., and Austrheim-Smith, S. (2004). Stormwater pollutant removal in roadside vegetated buffer strips. *Transportation Research Record*, 1890, 129-140.
- Beckman Coulter (2011) Beckman Coulter, Inc. Available at www.beckmancoulter.com. Accessed 11 February 2011.
- Bratieres, K., Fletcher, T. D., Deletic, A., and Zinger, Y. (2008). Nutrient and sediment removal by stormwater biofilters: A large-scale design optimisation study. *Water Research*, 42(14), 3930-3940.
- Blecken, G., Zinger, Y., Deletic, A., Fletcher, T., Viklander, M. (2009). Impact of a submerged zone and a carbon source on heavy metal removal in stormwater biofilters. *Ecological Engineering*, 35 (5), 769-777.
- Brown, R.A. and Hunt, W.F. (2011). Impacts of media depth on effluent water quality and hydrologic performance of under-sized bioretention cells. *Journal of Irrigation and Drainage Engineering*, 137(3), 132-143.
- Computer Hydraulics International (CHI). (2009). *PC Storm Water Management Model (PCSWMM) for Windows*. Ver. 2009. Ontario, Canada.
- Constantz, J. and Murphy, F. (1991). The temperature-dependence of ponded infiltration under isothermal conditions. *Journal of Hydrology*, 122(1-4), 119-128.

- Crabtree, B., Moy, F., Whitehead, M., and Roe, A. (2006). Monitoring pollutants in highway runoff. *Water and Environment Journal*, 20(4), 287-294.
- Davis, A. P. (2008). Field performance of bioretention: Hydrology impacts. *Journal of Hydrologic Engineering*, 13(2), 90-95.
- Davis, A. P., M. Shokouhian and Ni, S. (2001). Loading estimates of lead, copper, cadmium, and zinc in urban runoff from specific sources. *Chemosphere*, 44(5), 997-1009.
- Davis, A. P., Shokouhian, M., Sharma, H., and Minami, C. (2001). Laboratory study of biological retention for urban stormwater management. *Water Environment Research*, 73(1), 5-14.
- Davis, A. P., Shokouhian, M., Sharma, H., Minami, C., and Winogradoff, D. (2003). Water quality improvement through bioretention: lead, copper, and zinc removal, *Water Environment Research*, 75 (1), 73-75.
- Davis, A. P., Shokouhian, M., Sharma, H., and Minami, C. (2006). Water quality improvement through bioretention media: Nitrogen and phosphorus removal. *Water Environment Research*, 78(3), 284-293.
- Davis, A. P., Hunt, W. H., Traver, R. G., and Clar, M. (2009). Bioretention Technology: Overview of Current Practice and Future Needs. *Journal of Environmental Engineering*, 135(3), 109-117.
- Deletic, A. (1999). Sediment behaviour in grass filter strips. *Water Science and Technology*, 39(9), 129-136.
- Dietz, M. E. (2007). Low impact development practices: A review of current research and recommendations for future directions. *Water, Air, and Soil Pollution*, 186(1-4), 351-363.
- Dietz, M. E. and Clausen, J. C. (2005). A field evaluation of rain garden flow and pollutant treatment. *Water, Air, and Soil Pollution*, 167(1-4), 123-138.
- Dietz, M. E. and Clausen, J. C. (2006). Saturation to improve pollutant retention in a rain garden. *Environmental Science and Technology*, 40(4), 1335-1340.
- Emerson, C. and Traver, R. (2008). Multiyear and seasonal variation of infiltration from stormwater best management practices. *Journal of Irrigation and Drainage Engineering*, 134(5), 598-605.
- Gan, H., Zhuo, M., Li, D., and Zhou, Y. (2007). Quality characterization and impact assessment of highway runoff in urban and rural area of Guangzhou, China. *Environmental Monitoring Assessment*, 140, 147-159.

Haan, C.T, Barfield, B.J., and Hayes, J.C. (1994). Chapter 3: Rainfall-Runoff Estimation in Storm Water Computations. In *Design Hydrology and Sedimentology for Small Catchments, 37-103*. Academic Press, Inc. San Diego, CA.

Hardy, D. H., Tucker, M. R., and Stokes, C.E. (2003). Crop fertilization based on North Carolina soil tests. *Circular No. 1*, North Carolina Department of Agricultural and Consumer Services, Agronomic Division, Raleigh, NC.

Hatt, B. E., T.D. Fletcher, and A. Deletic. (2008). Hydraulic and pollutant removal performance of fine media stormwater filtration systems. *Environmental Science & Technology*, 42 (7), 2535-2541.

Hunt, W. F., Jarrett, A. R., Smith, J. T., and Sharkey, L. J. (2006). Evaluating bioretention hydrology and nutrient removal at three field sites in North Carolina. *Journal of Irrigation and Drainage Engineering*, 132(6), 600–608.

Hunt, W. F., Smith, J. T., Jadlocki, S. J., Hathaway, J. M., and Eubanks, P. R. (2008). Pollutant removal and peak flow mitigation by a bioretention basin in urban Charlotte, NC. *Journal of Environmental Engineering*, 134(5), 403–408.

Hunt, W.F., Kannan, N., Jeong, J., and Gassman, P.W. (2009). Stormwater best management practices: review of current practices and potential incorporation in SWAT. *International Agricultural Engineering Journal*, 18(1-2), 73-89.

ISCO Flowlink Software V 5.10.206. (2005). Teledyne ISCO, Inc. Lincoln, NE.

ISCO Open Channel Flow Measurement Handbook: Sixth Edition. (1978). Teledyne ISCO, Inc. Lincoln, NE.

Jones, M.P. and Hunt, W.F. (2009). Bioretention impact on runoff temperature in trout sensitive waters. *Journal of Environmental Engineering*, 135(8), 577-585.

Kercher, W.C., Landon, J.C., and Massarelli, R. (1983). Grassy swales prove cost-effective for water pollution control. *Public Works*, 114(4), 53–54.

Kim, H., Seagren, E. A., and Davis, A. P. (2003). Engineered bioretention for removal of nitrate from stormwater runoff. *Water Environment Research*, 75(4), 355–367.

Klute, A. (1986). Water retention: Laboratory methods. Methods of soil analysis. Part 1: Physical and mineralogical methods, A. Klute,ed., *Soil Science Society of America*, Madison, Wis., 635–662.

Lenhart, H.A. and Hunt W.F. (2011). Evaluating Four Stormwater Performance Metrics with a North Carolina Coastal Plain Stormwater Wetland. *Journal of Environmental Engineering*, 137(2), 155-62.

- Li, H. and Davis A. P. (2009). Water quality improvement through reductions of pollutant loads using bioretention. *Journal of Environmental Engineering*, 135(8), 567-576.
- Li, H., Sharkey, L. J., Hunt, W. F., and Davis, A. P. (2009). Mitigation of impervious surface hydrology using bioretention in North Carolina and Maryland. *Journal of Hydrologic Engineering*, 14(4), 407-415.
- Line, D.E. and Hunt, W.F. (2009). Performance of a bioretention area and a level spreader-grass filter strip at two highway sites in North Carolina. *Journal of Irrigation and Drainage Engineering*, 135(2), 217-224.
- Mazer, G., Booth, D., and Ewing, K. (2001). Limitations to vegetation establishment and growth in biofiltration swales. *Ecological Engineering*, 17(4), 429-443.
- McNett, J.K., Hunt, W.F., and Osborne, J.A. (2010). Establishing stormwater BMP evaluation metrics based upon ambient water quality associated with benthic macro-invertebrate populations. *Journal of Environmental Engineering*, 136(5), 535-541.
- Muench, S. (2003). WSDOT Gradation Specifications. Available: <http://training.ce.washington.edu/wsdot/state_information/03_materials/wsdot_gradations.htm#cc_plot> (1 March 2011).
- Muthanna, T., Viklander, M., and Thorolfsson, S. (2008). Seasonal climatic effects on the hydrology of a rain garden. *Hydrological Processes*, 22(11), 1640-1649.
- North Carolina Department of Environment and Natural Resources (NCDENR), Division of Water Quality. (2007). Stormwater Best Management Practices Manual. Raleigh, N.C. Available at: http://h2o.enr.state.nc.us/su/documents/BMPManual_WholeDocument_CoverRevisedDec2007.pdf. Accessed 13 November 2009.
- North Carolina Department of Transportation (NCDOT), State Road Maintenance Unit. (2009). *2008 highway and road mileage*. Available: <<http://www.ncdot.org/travel/statemapping/default.html>> (14 Jan 2010).
- NCDOT. (2010). Station 14: Quarterly Traffic Data for Bridge 911102 over Mango Creek. Unpublished data.
- NCDOT. (2011). Materials and Tests Unit, Soils Laboratory: Report on Samples of Soils for Quality. Unpublished data.
- North Carolina General Assembly (NCGA). 2008. The Current Operations and Capitol Improvements Appropriations Act of 2008. Session Law 2008-107. House Bill 2436. Session 2007. (July 16, 2008).

- Opher, T. and E. Friedler. (2010). Factors affecting highway runoff quality. *Urban Water Journal*. 7(3), 155-172.
- Ott, R.L. and Longnecker, M. (2001). An Introduction to Statistical Methods and Data Analysis: Fifth Edition. Thomson Learning, Inc. Pacific Grove, CA.
- Pandit, A., and Heck, H. H. (2009). Estimations of soil conservation service curve numbers for concrete and asphalt. *Journal of Hydrologic Engineering*, 14(4), 335–345.
- Passeport, E. and W. F. Hunt. (2009). Asphalt parking lot runoff nutrient characterization for eight sites in North Carolina, USA. *Journal of Hydrologic Engineering*, 14(4), 352-361.
- Passeport, E., Hunt, W.F., Line, D.E., Smith, R.A., and Brown, R.A. (2009). Field study of the ability of two grassed bioretention basins to reduce storm-water runoff pollution. *Journal of Irrigation and Drainage Engineering*, 135(4), 505-510.
- Pitt, R., Chen, S., Clark, S. E., Swenson, J., and Ong, C. K. (2008). Compaction's impacts on urban storm-water infiltration. *Journal of Irrigation and Drainage Engineering*, 134(5), 652-658.
- Prince George's County. (1999). Low-Impact Development Design Strategies: An Integrated Design Approach. Prince George's County, MD Department of Environmental Resources.
- R (version 2.11.1) [Software]. (2010). R Foundation for Statistical Computing.
- Richardson, J.L. and M.J. Vepraskas. Wetland Soils: Genesis, Hydrology, Landscapes, and Classification. (2001). CRC Press LLC. Boca Raton, FL.
- Sansalone, J.J., Koran, J.M., Smithson, J.A, and Buchberger, S.G. (1998). Physical characteristics of urban roadway solids transported during rain events. *Journal of Environmental Engineering*, 124(5), 427-440.
- Sansalone, J.J., Hird, J.P., Cartledge, F.K., and Tittlebaum, M.E. (2005). Event-based stormwater quality and quantity loadings from elevated urban infrastructure affected by transportation. *Water Environment Research*, 77(4), 348-365.
- SAS Institute Inc (version 9.2) [Software]. (2008). The SAS system for Windows.
- Skeen, M., Timperley, M., Ockleston, G., Lindgreen, M., and Mayhew, I. (2009) Analysis of particle size distributions from Auckland data. In proceedings of the 6th South Pacific Stormwater Conference. Auckland, New Zealand: NZWWA.
- Sparks, D.L. (2003). Environmental Soil Chemistry. 2nd Ed. San Diego, California: Elsevier.
- Spectrum Technologies. (2011). Plainfield, IL.: Spectrum Technologies, Inc. Available at: www.specmeters.com. Accessed 6 January 2011.

State Climate Office of North Carolina. (2011). *1971-2000 Climate Normals*. Available: < <http://www.nc-climate.ncsu.edu/cronos/normals.php>>. Accessed 11 April 2011.

Strecker, E. W., Quigley, M. M., Urbonas, B. R., Jones, E. J., and Clary, J. K. (2001). “Determining urban storm water BMP effectiveness.” *Journal of Water Resources Planning and Management*, 127(3),144–149.

Teledyne ISCO. (1995). *730 Bubbler Module Installation and Operation Guide*. Lincoln, NE. Teledyne Isco, Inc.

US Department of Agriculture – Natural Resources Conservation Service (USDA NRCS). (2004a). Chapter 9: Hydrologic soil-cover complexes. Part 630 –Hydrology: National Engineering Handbook, Washington D.C.

US Department of Agriculture – Natural Resources Conservation Service (USDA NRCS). (2004b). Chapter 10: Estimation of direct runoff from storm rainfall. Part 630 – Hydrology: National Engineering Handbook, Washington D.C.

US Department of Transportation: Federal Highway Administration. (USDOT). (2009). Washington, DC.: Available at: <www.fhwa.dot.gov>. Accessed 24 January 2011.

US Department of Transportation (USDOT): Planning. (2011). *The national highway system*. Available: < <http://www.fhwa.dot.gov/planning/nhs/> >. Accessed 5 Apr 2011.

United States Environmental Protection Agency (US EPA). (1993). Methods for Determination of Inorganic Substances in Environmental Samples. Document EPA/600/R-93/100. Office of Research and Development, U.S. EPA, Washington, DC.

US EPA. (1999). Storm Water Technology Fact Sheet: Vegetated Swales. EPA reference No. 832-F-99-006. Washington, D.C.: United States Environmental Protection Agency.

US EPA. (2000). Stormwater Phase II Final Rule: An Overview. EPA 833-F-00-001. Washington, D.C.: U.S. Environmental Protection Agency. Available at: <http://www.epa.gov/npdes/pubs/fact1-0.pdf>. Accessed 13 November 2009.

US EPA. (2009a). History of the Clean Water Act. Laws, Regulations, Guidance, and Dockets. United States Environmental Protection Agency. Available at: <http://www.epa.gov/lawsregs/laws.cwahistory/html>. Accessed 28 September 2009.

US EPA. (2009b). *Storm Water Management Model (SWMM) User’s Manual*. Ver. 5.0. Cincinnati, Ohio.

Walkowiak, D.K. (2008). ISCO Open Channel Flow Measurement Handbook, 6th Ed. Teledyne Isco, Inc. Lincoln, NE.

Wu, J.S., Allan, C.J., Saunders, W.L., and Evett, J.B. (1998). Characterization and pollutant loading estimation for highway runoff. *Journal of Environmental Engineering*, 124(7), 584-592.

Yousef, Y.A., Wanielista, M.P., Hvitved-Jacobsen, T., and Harper, H.H. (1984). Fate of heavy metals in stormwater runoff from highway bridges. *The Science of the Total Environment*, 33, 233-244.

Yousef, Y. A., Wanielista, M. P., and Harper, H. H. (1985). Removal of highway contaminants by roadside swales. *Transportation Research Record 1017*, Transportation Research Board, Washington, D.C., 62-68.

Yousef, Y. A., Hvitved-Jacobsen, T., Wanielista, M. P., and Harper, H. H. (1987). Removal of contaminants in highway runoff flowing through swales. *Science of the Total Environment*, 59 (1987), 391-399.

Yu, S. L., Kuo, J., Fassman, E.A., and Pan, H. (2001). Field test of grassed-swale performance in removing runoff pollution. *Journal of Water Resources Planning and Management*, 127(3), 168-171.

Zanders, J.M. (2005). Road sediment: Characterization and implications for the performance of vegetated strips for treating road run-off. *The Science of the Total Environment*, 339(1), 41-47.

Appendix A: Bioretention

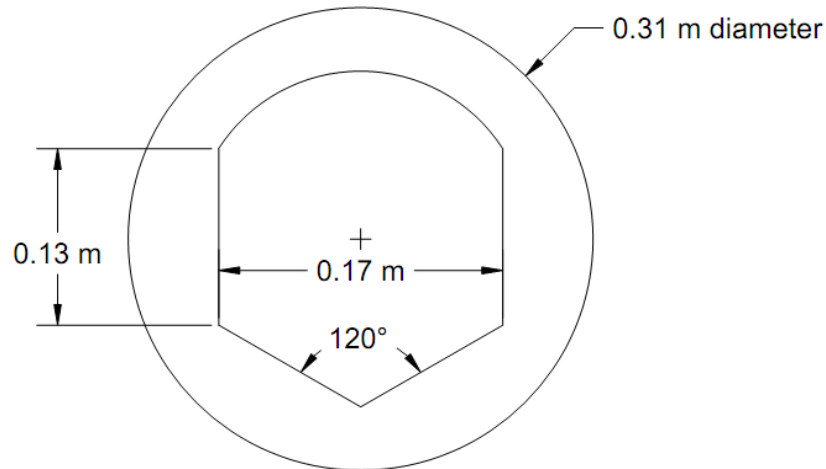


Figure 54. Bioretention cell inlet and outlet weir schematic.

Time of Concentration Calculation

Figure 55. Example time of concentration calculation for northbound bridge deck drainage system.

SWMM calculation of t_c through bridge deck pipes—northbound bridge deck.

Modeled storm events by selecting representative flow rates and solving for intensities using the Rational Method (Haan et al., 1994).

$A=0.98$ ac

$c=0.95$

		I	
Q (cfs)	Q(L/s)	(mm/hr)	t_c
1	28.3	20.73	7.50
1.5	42.48	31.09	4.88
2	56.63	41.45	3.50
3	84.95	62.18	2.50

$t_c = 4.60$ min

***Average 4.6 minute t_c through pipes. Found with SWMM.**

Intensities held constant for five hours.

Ignored pipe entrance/exit losses.

Average slope diagonal across upper portion of bridge deck = 0.67%

t_c on portion of bridge deck before pipe attachments begin:

bridge deck length	163.37 m = 535.85 ft	bridge deck width	14.6 m = 47.89 ft
bridge deck slope (length)	0.005	bridge deck slope (width)	0.02

$t_c = 0.0078 * L^{0.77} * (L/H)^{0.385}$

L= max length of flow in feet

H=diff in elev (ft) between the watershed outlet and the most hydraulically remote point in the watershed

drop along bridge	0.815 m = 2.67 ft
drop across bridge	0.292 m = 0.96 ft
H (total)	1.107 m = 3.63 ft
L	174.77 m = 573.39 ft

tc= 7.29 min *Average 7.29 minute tc over bridge deck.

total tc= 4.60 + 7.29 = 11.9 min *Total tc from most hydraulically remote point on the bridge deck to the bioretention splitter box. This time of concentration was also observed/ field verified.

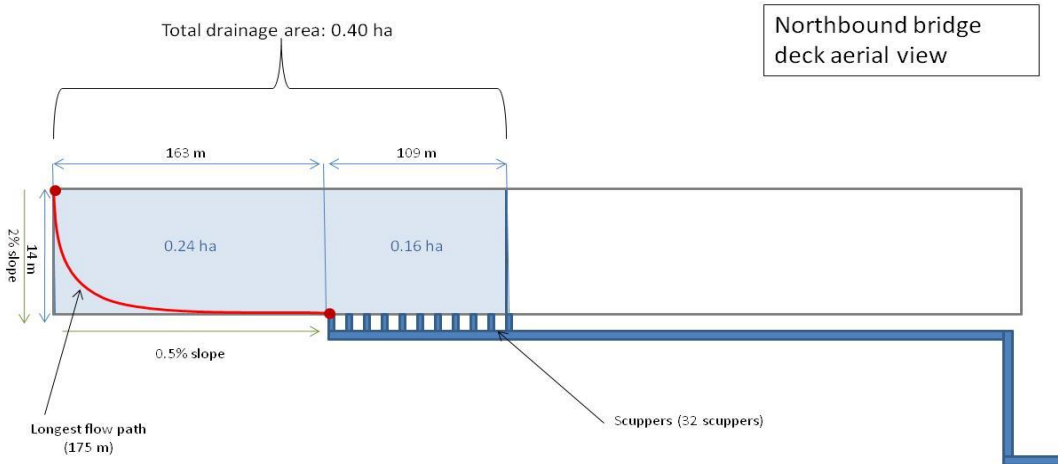


Figure 56. Aerial view of northbound bridge deck and longest flow path for t_c calculations.

Bioretention Hydrologic Data

Table 36. Calculated inflow volumes and ISCO reported outflow volumes.

Storm Event #	Corrected Tipping Bucket RG (cm)	Large Cell Inflow Vol ^[1] (L)	Small Cell Inflow Vol (L)	Large Cell Outflow Vol ^[2] (L)	Small Cell Outflow Vol (L)
0	-	-	-	1413.0	-
2	12.3	227170.3	7859.3	166356.7	201489.6
3	0.2	1755.7	58.5	-	-
4	0.3	3916.2	134.0	0.0	0.0
5	0.7	16282.3	567.7	0.0	15486.6
6	1.4	26003.5	898.3	0.0	21934.3
7	0.6	3245.1	98.1	0.0	0.0
8	4.0	76555.0	2652.0	72279.1	86162.4
9	1.2	22177.9	765.8	2452.3	16916.6
10	4.3	84495.1	2931.5	77056.2	77792.5
11	0.8	12402.8	424.5	0.0	7288.8
12	1.8	33742.5	1168.7	4210.7	18080.4
13	1.5	27784.6	960.7	17284.7	20444.9
14	0.8	11536.3	393.5	0.0	3398.0
15	0.3	4414.6	152.6	0.0	4230.6
16	4.0	71174.8	2457.2	63754.9	45273.2
17	2.8	51454.8	1778.2	26567.0	41280.5
18	2.3	42464.2	1469.6	26168.7	43888.5
19	0.4	804.2	15.3	-	-
20	0.6	7645.6	257.1	-	-
21	0.4	4762.9	159.3	1667.9	6173.1
22	4.8	95824.7	3327.7	104523.7	69618.8
23	0.8	12451.0	425.4	2959.1	4185.3
24	0.4	3582.1	119.1	-	3483.0
25	0.2	2922.3	98.4	-	0.0
26	0.7	6365.7	209.1	-	0.0
27	1.4	22044.8	756.9	-	8806.6
28	0.4	648.5	12.4	-	0.0
29	0.4	5734.2	194.9	-	0.0
30	1.4	25502.3	880.7	-	11437.2
31	0.3	4519.4	154.6	-	764.6
32	1.6	23514.4	802.1	-	2466.4
33	5.2	98135.4	3400.2	117583.2	33966.2
34	3.8	70840.6	2450.8	82212.7	16633.4
35	0.9	12238.6	415.5	-	0.0
36	1.3	15758.4	531.4	-	-
37	1.9	32029.4	1101.7	144.4	3355.6

38	7.3	119429.8	4104.2	193776.1	76897.6
39	1.7	29370.4	1014.5	30707.0	33901.1
40	1.4	25397.5	878.2	7413.4	18604.3
41	1.5	29713.0	1029.6	31548.0	37766.7
42	0.5	7940.1	271.3	5844.6	14877.8
43	5.1	92959.0	3213.0	134418.0	103073.9
44	1.8	31109.1	1072.8	25281.4	37236.9
45	3.1	59358.1	2058.2	91483.7	55317.3
46	0.9	16692.9	423.1	4021.0	17012.9
47	1.1	17307.4	436.1	1076.0	6606.4
48	0.9	17834.0	453.3	10987.0	19258.4
49	0.5	7220.8	182.1	3726.5	24720.7
50	1.0	20456.2	519.2	6334.5	9817.5
51	1.1	16115.2	405.3	4638.3	91667.8
52	0.9	12300.9	308.3	-	6048.5
53 ^[3]	-	-	-	44842.8	66887.6
54	-	-	-	2537.2	22152.4
55	1.6	26904.0	679.8	5218.8	20713.9
56	0.9	16112.4	408.0	1010.9	7945.8
57	2.3	49503.8	1259.2	26176.2	33867.7
58	0.9	18437.2	468.8	5419.5	19467.6
59	2.6	55829.8	1420.3	37409.9	61683.2
60	2.7	59508.2	1515.0	28578.6	66255.6
61	0.5	5773.8	143.4	-	7069.4
62	0.2	277.5	5.3	-	-
63	1.4	29965.0	761.4	-	17120.3
64	1.0	19156.5	486.3	9126.1	9141.0
65	1.1	28781.4	734.8	-	18838.3
66	6.3	164807.8	4210.8	185336.2	238198.9
67	0.5	10684.0	272.4	-	12431.6
68	0.3	617.3	11.8	-	-
69	8.4	187954.1	4786.6	60971.9	197142.7
70	9.7	225063.5	5736.0	153023.7	292016.2
71	1.1	17250.7	435.1	7783.1	2119.1
72	1.3	20495.8	517.2	6029.8	14811.3
73	0.2	1432.8	35.3	-	214.3
74	-	24593.3	623.6	19471.1	9652.9
75	-	2636.3	63.3	0.0	0.0
76	-	96.3	1.8	0.0	0.0

77	-	7671.1	194.5	0.0	3327.2
78	-	3265.0	79.3	0.0	-
79	-	16392.7	417.7	7444.8	-

[1] Inflow volume (calculated by initial abstraction method) plus direct rainfall.

[2] ISCO-reported outflow volumes.

[3] Events 19-21 and 24-25 were snow events. Rain gauge was clogged for events 53-54. Data were discarded.

Table 37. Edited flow data used in load reduction and flow volume calculations for large bioretention cell.

Event Number ^[1]	Large Cell In (L)	Large Cell Out (L)	Percent Reduction
2	227170.3	166356.7	26.77
4	3916.2	0.0	100.00
5	16282.3	0.0	100.00
6	26003.5	0.0	100.00
7	3245.1	0.0	100.00
8 ^[2]	76555.0	72279.1	5.59
9	22177.9	2452.3	88.94
10	84495.1	77056.2	8.80
11	12402.8	0.0	100.00
12	33742.5	4210.7	87.52
13	27784.6	17284.7	37.79
14	11536.3	0.0	100.00
15	4414.6	0.0	100.00
16	71174.8	63754.9	10.42
17	51454.8	26567.0	48.37
18	42464.2	26168.7	38.38
22	95824.7	95824.7 ^[3]	0.00
23	12451.0	2959.1	76.23
33	98135.4	98135.4	0.00
34	70840.6	70840.6	0.00
37,38,39 ^[4]	180829.5	180829.5	0.00
40,41,42	63047.8	44806.0	28.93
43	92959.0	92959.0	0.00
44	31109.1	25281.4	18.73
45	59358.1	59358.1	0.00
46	16692.9	4021.0	75.91
47,48,49	42365.1	15789.6	62.73
50	20456.2	6334.5	69.03
51	16115.2	4638.3	71.22
55	26904.0	5218.8	80.60
56	16112.4	1010.9	93.73
57	49503.8	26176.2	47.12

58	18437.2	5419.5	70.61
59	55829.8	37409.9	32.99
60	59508.2	28578.6	51.98
64	19156.5	9126.1	52.36
66	164807.8	164807.8	0.00
69	187954.1	60971.9	67.56
70	225063.5	153023.7	32.01
71	17250.7	7783.1	54.88
72	20495.8	6029.8	70.58
74	24593.3	19471.1	20.83
75	2636.3	0.0	100.00
76	96.3	0.0	100.00
77	7671.1	0.0	100.00
78	3265.0	0.0	100.00
79	16392.7	7444.8	54.59
SUM	2430677.5	1690380.5	30.5

[1] Events with unreliable or complete lack of data were omitted.

[2] Red indicates overflow occurred.

[3] Yellow indicates outflow was set equal to inflow.

[4] Indistinguishable, continuous outflow were combined.

Table 38. Edited flow data used in load reduction and flow volume calculations for small bioretention cell.

Event Number ^[1]	Small Cell In (L)	Small Cell Out (L)	Percent Reduction
2 ^[2]	222551.8	201489.6	9.46
4	3794.5	0.0	100.00
5	16075.6	15486.6	3.66
6	25437.2	21934.3	13.77
7	2777.9	0.0	100.00
8	75096.7	75096.7 ^[3]	0.00
9	21685.2	16916.6	21.99
10	83011.3	77792.5	6.29
11	12020.6	7288.8	39.37
12	33094.1	18080.4	45.37
13	27204.1	20444.9	24.85
14	11142.7	3398.0	69.51
15	4321.2	4230.6	2.10
16	69580.5	45273.2	34.93
17	50353.3	41280.5	18.02
18	41614.7	41614.7	0.00
22	94230.5	69620.2	26.12
23	12046.1	4185.3	65.26

26	5921.1	0.0	100.00
27	21433.1	8806.6	58.91
28	351.1	0.0	100.00
29	5519.0	0.0	100.00
30	24938.8	11437.2	54.14
31	4377.8	764.6	82.54
32	22713.1	2466.4	89.14
33	96283.5	33966.2	64.72
34	69399.3	16633.4	76.03
35	11765.7	0.0	100.00
37,38,39 ^[4]	176143.1	114154.3	35.19
40,41,42	61705.6	61705.6	0.00
43	90982.5	90982.5	0.00
44	30378.5	30378.5	0.00
45	58282.0	55317.3	5.08
50	14702.2	9817.5	33.22
52	8730.1	6048.5	30.72
55	19249.9	19249.9	0.00
56	11553.3	7945.8	31.23
57,58	48934.6	48934.6	0.00
59	40218.6	40218.6	0.00
60	42900.3	42900.3	0.00
63	21560.6	17120.3	20.60
64	13770.6	9141.0	33.62
65,66,67	147760.9	147760.9	0.00
69, 70	297968.5	297968.5	0.00
71	12320.7	2119.1	82.80
72	14645.6	14645.6	0.00
73	999.6	214.3	78.59
74	17658.5	9652.9	45.34
75	1792.5	0.0	100.00
76	51.0	0.0	100.00
77	5507.7	3327.2	39.59
SUM	2206559.7	1767804.8	19.9

[1] Events with unreliable or complete lack of data were omitted.

[2] Red indicates overflow occurred.

[3] Yellow indicates outflow was set equal to inflow.

[4] Indistinguishable, continuous outflow were combined.

Table 39. Peak inflow and outflow flowrates.

Storm Event No.	Rainfall				Rational Method		ISCO Reported	
	Start Date	Stop Date	Corrected Rnfl (cm)	Peak Intensity (cm/hr)	Large Cell Inflow Qp (L/s)	Small Cell Inflow Qp (L/s)	Large Cell Outflow Qp (L/s)	Small Cell Outflow Qp (L/s)
2 ^[1]	11/10/09	11/13/09	12.29	1.36	14.16	14.16	2.41	6.00
3	11/16/09	11/16/09	0.15	0.82	8.50	8.50	- [2]	-
4	11/18/09	11/18/09	0.25	0.70	7.36	7.36	0.00	-
5	11/19/09	11/19/09	0.74	1.87	19.26	19.26	0.00	0.91
6	11/22/09	11/23/09	1.45	0.85	8.78	8.78	0.00	0.59
7	11/30/09	11/30/09	0.61	1.61	16.71	16.71	0.00	0.00
8	12/2/09	12/3/09	4.04	2.01	20.95	20.95	8.75	12.23
9	12/4/09	12/5/09	1.24	0.60	6.23	6.23	0.14	0.34
10	12/8/09	12/9/09	4.32	3.14	32.56	32.56	12.66	17.73
11	12/13/09	12/13/09	0.81	0.32	3.40	3.40	0.00	0.28
12	12/18/09	12/19/09	1.78	0.48	5.10	5.10	0.25	1.05
13	12/25/09	12/25/09	1.52	0.61	6.23	6.23	0.59	2.89
14	12/31/09	12/31/09	0.79	0.72	7.65	7.65	0.00	0.25
15	12/31/09	12/31/09	0.25	0.48	5.10	5.10	0.00	0.14
16	1/17/10	1/18/10	4.01	1.55	16.14	16.14	13.76	5.27
17	1/21/10	1/22/10	2.84	0.88	9.06	9.06	0.51	4.39
18	1/24/10	1/25/10	2.29	2.40	24.92	24.92	0.54	16.37
19	1/31/10	1/31/10	0.43	0.85	8.78	8.78	0.00	0.00
20	2/2/10	2/2/10	0.64	0.22	2.27	2.27	0.00	0.00
21	2/2/10	2/3/10	0.43	1.07	11.04	11.04	12.43	0.11
22	2/5/10	2/5/10	4.80	1.21	12.46	12.46	8.35	6.88
23	2/9/10	2/9/10	0.84	0.80	8.21	8.21	0.25	0.20
24	2/13/10	2/13/10	0.36	0.52	5.38	5.38	-	0.17
25	2/14/10	2/14/10	0.23	0.34	3.68	3.68	-	0.00
26	2/22/10	2/22/10	0.69	0.44	4.53	4.53	-	0.00
27	3/2/10	3/3/10	1.37	0.39	3.96	3.96	-	0.45
28	3/10/10	3/11/10	0.36	0.34	3.68	3.68	-	0.00
29	3/11/10	3/11/10	0.41	0.52	5.38	5.38	-	0.00
30	3/13/10	3/13/10	1.42	2.08	21.52	21.52	-	0.54
31	3/14/10	3/14/10	0.30	0.29	3.11	3.11	-	0.08
32	3/22/10	3/22/10	1.63	7.53	78.15	78.15	-	0.17
33	3/28/10	3/29/10	5.16	3.51	36.25	36.25	35.57	7.90
34	4/8/10	4/9/10	3.84	3.53	36.53	36.53	56.32	7.16
35	4/21/10	4/21/10	0.91	1.71	17.84	17.84	-	0.00
36	4/24/10	4/25/10	1.27	0.39	3.96	3.96	-	-

37	5/16/10	5/17/10	1.93	3.18	32.85	32.85	0.00	0.17
38	5/17/10	5/18/10	7.32	4.93	51.25	51.25	46.69	12.32
39	5/19/10	5/19/10	1.65	1.49	15.29	15.29	0.68	9.12
40	5/22/10	5/23/10	1.40	2.64	27.47	27.47	0.28	2.83
41	5/23/10	5/23/10	1.55	3.34	34.55	34.55	0.62	14.89
42	5/24/10	5/24/10	0.53	1.00	10.48	10.48	0.20	0.42
43	5/28/10	5/29/10	5.13	8.32	86.37	86.37	71.47	31.80
44	6/1/10	6/1/10	1.78	1.64	16.99	16.99	4.02	8.38
45	6/2/10	6/2/10	3.07	6.43	66.83	66.83	50.29	19.17
46	6/6/10	6/7/10	0.89	1.49	15.29	15.29	0.28	0.54
47	6/12/10	6/12/10	1.12	5.17	53.52	53.52	0.11	-
48	6/13/10	6/13/10	0.86	2.16	22.37	22.37	0.31	-
49	6/13/10	6/13/10	0.46	1.75	18.12	18.12	0.20	-
50	6/16/10	6/16/10	1.04	3.19	33.13	33.13	0.20	1.13
51	6/23/10	6/23/10	1.09	0.89	9.34	9.34	0.20	5.04
52	6/29/10	6/29/10	0.91	1.04	10.76	10.76	-	0.20
53	7/9/10	7/10/10	-	-	-	-	4.02	57.20
54	7/16/10	7/18/10	-	-	-	-	0.23	1.98
55	7/23/10	7/23/10	1.60	5.63	58.33	58.33	0.25	7.90
56	7/27/10	7/27/10	0.89	0.91	9.63	9.63	0.11	0.40
57	7/29/10	7/29/10	2.31	5.78	60.03	60.03	0.57	24.44
58	7/31/10	8/1/10	0.86	0.99	10.19	10.19	0.28	0.54
59	8/5/10	8/5/10	2.59	7.92	82.12	82.12	19.99	83.51
60	8/5/10	8/5/10	2.69	6.73	69.94	69.94	3.00	77.08
61	8/11/10	8/12/10	0.53	1.65	17.27	17.27	-	0.17
62	8/18/10	8/19/10	0.15	0.29	3.11	3.11	-	-
63	8/19/10	8/20/10	1.45	2.82	29.17	29.17	-	10.85
64	8/22/10	8/22/10	0.97	3.12	32.56	32.56	0.28	1.87
65	8/23/10	8/23/10	1.14	2.83	29.45	29.45	-	8.92
66	8/24/10	8/24/10	6.27	5.32	55.22	55.22	55.95	75.55
67	8/24/10	8/25/10	0.46	0.60	6.23	6.23	-	0.48
68	9/11/10	9/12/10	0.33	0.60	6.23	6.23	-	-
69	9/26/10	9/28/10	8.36	4.58	47.57	47.57	5.01	17.22
70	9/29/10	10/1/10	9.68	4.42	45.87	45.87	32.42	37.86
71	10/14/10	10/14/10	1.09	0.70	7.36	7.36	-	0.08
72	10/25/10	10/26/10	1.27	1.88	19.54	19.54	-	0.28
73	10/28/10	10/28/10	0.15	0.38	3.96	3.96	-	-

[1] No data available for event 1.

[2] Blank cells mean no data were available.

Table 40. Large bioretention cell lag times per storm event.

Storm Event No. ^[1]	Date of peak Inflow	Date of Peak Outflow	Time of Peak Inflow	Time of Peak Outflow	Lag Time Days (Dates)	Lag Time Days (Times)	Lag Time (hr)
2	11/11/09	11/11/09	9:46	12:16	0.00	0.10	2.50
8	12/3/09	12/03/09	0:12	0:18	0.00	0.00	0.10
9	12/5/09	12/05/09	4:08	10:04	0.00	0.25	5.93
10	12/9/09	12/09/09	3:04	8:46	0.00	0.24	5.70
12	12/19/09	12/19/09	8:32	12:42	0.00	0.17	4.17
13	12/25/09	12/25/09	17:10	20:28	0.00	0.14	3.30
16	1/17/10	01/17/10	18:04	9:34	0.00	-0.35	-8.50
17	1/21/10	01/22/10	19:58	1:14	1.00	-0.78	5.27
18	1/25/10	01/25/10	5:02	5:42	0.00	0.03	0.67
21	2/3/10	02/03/10	0:30	16:14	0.00	0.66	15.73
22	2/5/10	02/05/10	20:12	20:16	0.00	0.00	0.07
23	2/9/10	02/09/10	16:42	22:28	0.00	0.24	5.77
33	3/29/10	03/29/10	2:28	3:36	0.00	0.05	1.13
34	4/9/10	04/09/10	1:04	1:06	0.00	0.00	0.03
38	5/17/10	05/17/10	20:30	20:36	0.00	0.00	0.10
39	5/19/10	05/19/10	4:20	6:44	0.00	0.10	2.40
40	5/22/10	05/23/10	21:42	10:22	1.00	-0.47	12.67
41	5/23/10	05/23/10	9:42	10:14	0.00	0.02	0.53
43	5/28/10	05/28/10	23:02	23:10	0.00	0.01	0.13
44	6/1/10	06/01/10	9:08	9:12	0.00	0.00	0.07
45	6/2/10	06/02/10	14:22	14:26	0.00	0.00	0.07
46	6/6/10	06/07/10	21:26	3:26	1.00	-0.75	6.00
47	6/12/10	06/13/10	17:54	0:42	1.00	-0.72	6.80
48	6/13/10	06/13/10	2:56	6:28	0.00	0.15	3.53
49	6/13/10	06/13/10	17:38	19:14	0.00	0.07	1.60
50	6/16/10	06/16/10	19:02	23:28	0.00	0.18	4.43
51	6/23/10	06/23/10	17:52	23:14	0.00	0.22	5.37
55	7/23/10	07/24/10	18:58	1:24	1.00	-0.73	6.43
56	7/27/10	07/27/10	14:06	20:42	0.00	0.28	6.60
57	7/29/10	07/30/10	22:48	19:40	1.00	-0.13	20.87
58	8/1/10	08/01/10	0:58	9:54	0.00	0.37	8.93
59	8/5/10	08/05/10	1:06	1:22	0.00	0.01	0.27
60	8/5/10	08/05/10	20:00	20:36	0.00	0.03	0.60
64	8/22/10	08/22/10	15:06	19:30	0.00	0.18	4.40
69	9/26/10	09/26/10	16:44	23:56	0.00	0.30	7.20
70	9/30/10	09/30/10	6:50	6:52	0.00	0.00	0.03

[1] Events with unreliable or lack of data were omitted.

Table 41. Small bioretention cell lag times per storm event.

Storm Event No. ^[1]	Peak Inflow Date	Peak Outflow Date	Time of Peak Inflow	Time of Peak Outflow	Lag Time Days (Dates)	Lag Time Days (Times)	Lag Time (hr)
2	11/11/09	11/11/09	9:46	11:38	0.00	0.08	1.87
5	11/19/09	11/19/09	7:52	8:48	0.00	0.04	0.93
6	11/23/09	11/23/09	10:42	11:26	0.00	0.03	0.73
8	12/3/09	12/3/09	0:12	0:16	0.00	0.00	0.07
9	12/5/09	12/5/09	4:08	12:18	0.00	0.34	8.17
10	12/9/09	12/9/09	3:04	3:02	0.00	0.00	-0.03
12	12/19/09	12/19/09	8:32	8:50	0.00	0.01	0.30
13	12/25/09	12/25/09	17:10	18:52	0.00	0.07	1.70
16	1/17/10	1/17/10	18:04	18:30	0.00	0.02	0.43
17	1/21/10	1/21/10	19:58	23:12	0.00	0.13	3.23
18	1/25/10	1/25/10	5:02	5:08	0.00	0.00	0.10
21	2/3/10	2/3/10	0:30	19:10	0.00	0.78	18.67
22	2/5/10	2/5/10	20:12	20:16	0.00	0.00	0.07
23	2/9/10	2/9/10	16:42	20:00	0.00	0.14	3.30
33	3/29/10	3/29/10	2:28	3:32	0.00	0.04	1.07
34	4/9/10	4/9/10	1:04	1:04	0.00	0.00	0.00
38	5/17/10	5/17/10	20:30	20:36	0.00	0.00	0.10
39	5/19/10	5/19/10	4:20	4:26	0.00	0.00	0.10
40	5/22/10	5/22/10	21:42	22:38	0.00	0.04	0.93
41	5/23/10	5/23/10	9:42	9:50	0.00	0.01	0.13
43	5/28/10	5/28/10	23:02	23:08	0.00	0.00	0.10
44	6/1/10	6/1/10	9:08	9:16	0.00	0.01	0.13
45	6/2/10	6/2/10	14:22	14:22	0.00	0.00	0.00
46	6/6/10	6/7/10	21:26	1:44	1.00	-0.82	4.30
50	6/16/10	6/16/10	19:02	19:30	0.00	0.02	0.47
51	6/23/10	6/23/10	17:52	17:24	0.00	-0.02	-0.47
55	7/23/10	7/23/10	18:58	19:06	0.00	0.01	0.13
56	7/27/10	7/27/10	14:06	20:58	0.00	0.29	6.87
57	7/29/10	7/29/10	22:48	23:00	0.00	0.01	0.20
58	8/1/10	8/1/10	0:58	7:40	0.00	0.28	6.70
59	8/5/10	8/5/10	1:06	1:10	0.00	0.00	0.07
60	8/5/10	8/5/10	20:00	20:00	0.00	0.00	0.00
64	8/22/10	8/22/10	15:06	15:34	0.00	0.02	0.47
67	8/24/10	8/25/10	21:30	1:12	1.00	-0.85	3.70
69	9/26/10	9/27/10	16:44	7:58	1.00	-0.37	15.23
70	9/30/10	9/30/10	6:50	6:50	0.00	0.00	0.00
71	10/14/10	10/14/10	9:42	16:14	0.00	0.27	6.53

72	10/25/10	10/25/10	12:56	23:56	0.00	0.46	11.00
----	----------	----------	-------	-------	------	------	-------

[1] Events with unreliable or lack of data were omitted.

Bioretention Inflow vs. Outflow Hydrographs

Figures 57 and 58 show inflow and outflow hydrograph examples for the large and small bioretention cells, respectively (ISCO, 2005). Figure 57 shows the hydrographs associated with a 1.07 cm (0.42 in) storm and Figure 58 shows the result of a 0.66 cm (0.26 in) storm. It should be noted that all inflow volumes were calculated using the Initial Abstraction method (Pandit and Heck, 2009) and the peak flow rates were calculated using the Rational Method (Haan et al., 1994) for each storm because the flow data at the bioretention inlets were generally considered unreliable. Therefore, neither flow volumes nor peak flow rates were obtained from the inflow hydrographs shown below. However, the hydrographs below are being shown as examples because the ISCO reported inflows were very similar to the inflows calculated by the Initial Abstraction method (Pandit and Heck, 2009) for these two events. Figures 57 and 58 are visual representations of the volume reductions and peak flow rate attenuations achieved by the bioretention cells. Overflow did not occur during either of these events.

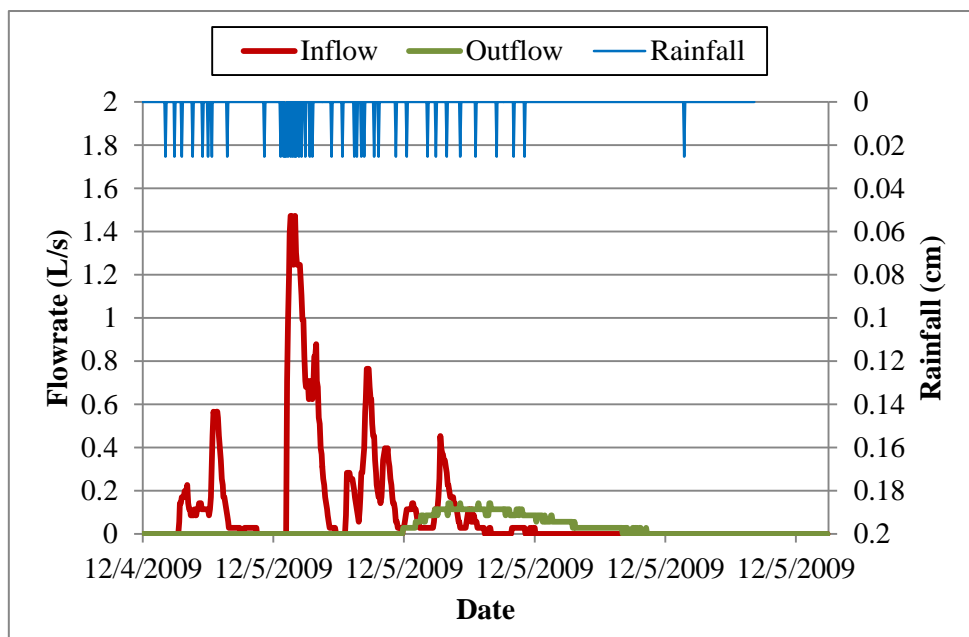


Figure 57. Large bioretention cell inflow and outflow hydrographs (1.07 cm storm).

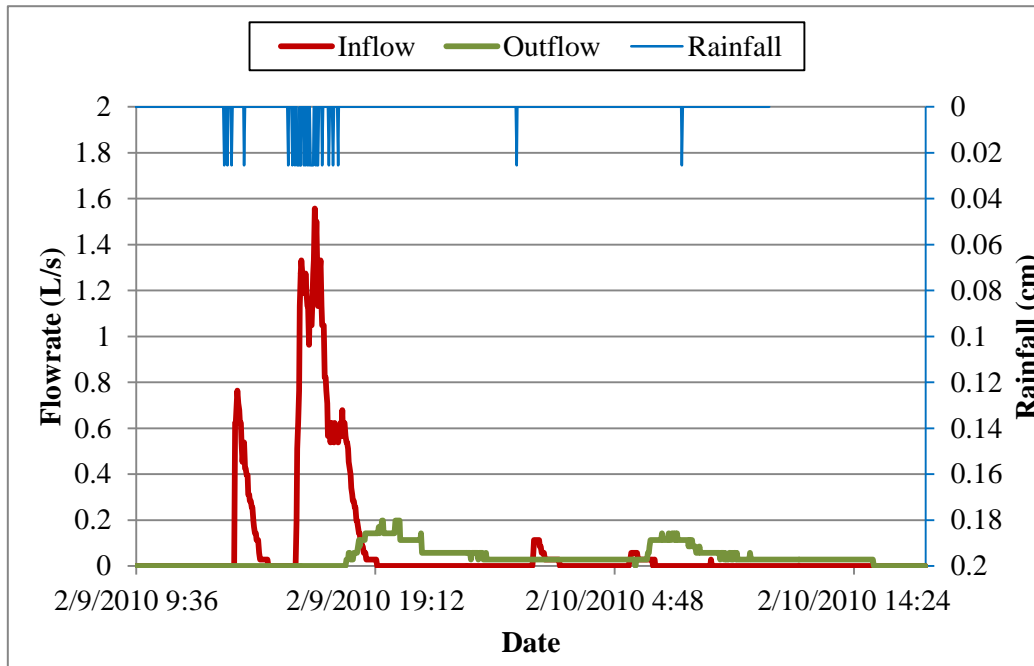


Figure 58. Small bioretention cell inflow and outflow hydrographs (0.66 cm storm).

Bioretention Rain Depth Adjustment Multiplier

The ISCO 674TM rain gauge's reported rain depths were corrected on a storm-by-storm basis using the measurements taken by the manual rain gauge. Multipliers were used to scale the ISCO 674TM rainfall data (reported in two-minute interval rainfall intensities) according to the manually recorded rain depth. The multiplier was applied to each two-minute rainfall interval. New storms were tabulated for an antecedent dry period of six hours. In the event that the manual rain gauge was not recorded, an average multiplier of 1.17 was used. The average multiplier was determined by averaging the multipliers calculated for the first 23 storm events with manually recorded rainfall data. For storms 74 through 79, rainfall depths were not recorded by the ISCOTM rain gauge due to equipment error. Instead, rain data were used from USGS Station 02087359, Walnut Creek at Sunnybrook Drive near Raleigh, NC, which was approximately 6.4 km (4 mi) southwest of the Mango Creek research site.

Table 42. Mango Creek study site rain data and corrected rain depths.

Storm Event #	Start Date	Stop Date	Start Time	Stop Time	Tipping Bucket RG (cm)	Manual Rain Gauge (cm)	Corrected Tipping Bucket RG (cm)
0	10/19/2009	10/21/2009	14:14	10:34	- ^[1]	1.42	-
1	-	-	-	-	-		-
2	11/10/2009	11/13/2009	17:28	7:04	10.77	11.51	12.29
3	11/16/2009	11/16/2009	11:30	11:38	0.18	1.17	0.15
4	11/18/2009	11/18/2009	18:06	19:48	0.28		0.25
5	11/19/2009	11/19/2009	4:02	8:38	0.81		0.74
6	11/22/2009	11/23/2009	22:20	12:42	1.30	1.45	1.45

7	11/30/2009	11/30/2009	19:10	21:44	0.43	0.61	0.61
8	12/2/2009	12/3/2009	7:56	1:52	3.58	4.04	4.04
9	12/4/2009	12/5/2009	23:36	18:44	1.07	1.24	1.24
10	12/8/2009	12/9/2009	19:30	10:04	4.01	4.32	4.32
11	12/13/2009	12/13/2009	3:18	16:30	0.66	0.81	0.81
12	12/18/2009	12/19/2009	19:32	11:22	1.88	4.34	1.78
13	12/25/2009	12/25/2009	10:46	18:54	1.60		1.52
14	12/31/2009	12/31/2009	0:00	5:58	0.84		0.79
15	12/31/2009	12/31/2009	20:20	23:08	0.25		0.25
16	1/17/2010	1/18/2010	0:20	18:28	3.58	4.01	4.01
17	1/21/2010	1/22/2010	14:12	0:02	2.46	2.84	2.84
18	1/24/2010	1/25/2010	19:24	9:32	2.06	2.29	2.29
19 ^[2]	1/31/2010	1/31/2010	13:04	14:36	0.25	1.50	0.43
20	2/2/2010	2/2/2010	10:24	15:42	0.38		0.64
21	2/2/2010	2/3/2010	23:12	1:14	0.25		0.43
22	2/5/2010	2/5/2010	8:08	23:26	4.55	4.80	4.80
23	2/9/2010	2/9/2010	13:06	17:44	0.66	0.84	0.84
24	2/13/2010	2/13/2010	16:28	19:14	0.25	0.58	0.36
25	2/14/2010	2/14/2010	11:00	12:40	0.18		0.23
26	2/22/2010	2/22/2010	12:10	15:50	0.58	0.69	0.69
27	3/2/2010	3/3/2010	15:18	9:10	1.32	1.37	1.37
28	3/10/2010	3/11/2010	21:34	1:16	0.25	0.76	0.36
29	3/11/2010	3/11/2010	17:00	21:56	0.30		0.41
30	3/13/2010	3/13/2010	1:44	3:42	1.22	1.73	1.42
31	3/14/2010	3/14/2010	5:40	11:02	0.25		0.30
32	3/22/2010	3/22/2010	4:42	6:22	1.37	1.63	1.63
33	3/28/2010	3/29/2010	22:48	8:32	4.85	5.16	5.16
34	4/8/2010	4/9/2010	22:04	2:48	3.58	3.84	3.84
35	4/21/2010	4/21/2010	2:22	20:16	0.86	2.18	0.91
36	4/24/2010	4/25/2010	22:04	5:58	0.79		1.27
37	5/16/2010	5/17/2010	17:54	8:58	1.78	1.93	1.93
38	5/17/2010	5/18/2010	16:22	5:40	5.46	7.32	7.32
39	5/19/2010	5/19/2010	1:24	5:02	1.40	not recorded	1.65
40	5/22/2010	5/23/2010	18:50	1:22	1.27	2.95	1.40
41	5/23/2010	5/23/2010	9:06	23:54	1.42		1.55
42	5/24/2010	5/24/2010	12:22	20:24	0.41	0.53	0.53
43	5/28/2010	5/29/2010	22:40	3:12	4.37	not recorded	5.13
44	6/1/2010	6/1/2010	4:58	16:42	1.52	not recorded	1.78
45	6/2/2010	6/2/2010	13:44	18:02	2.79	3.07	3.07
46	6/6/2010	6/7/2010	21:14	0:28	0.76	0.89	0.89

47	6/12/2010	6/12/2010	17:42	18:16	0.99	1.98	1.12
48	6/13/2010	6/13/2010	2:42	5:28	0.76		0.86
49	6/13/2010	6/13/2010	17:26	19:10	0.33	0.46	0.46
50	6/16/2010	6/16/2010	18:46	19:30	0.91	1.04	1.04
51	6/23/2010	6/23/2010	16:56	18:48	0.94	not recorded	1.09
52	6/29/2010	6/29/2010	17:30	19:36	0.79	not recorded	0.91
53	7/9/2010	-	-	-	-	not recorded	-
54	7/16/2010	-	-	-	-	2.18	-
55	7/23/2010	7/23/2010	18:16	19:10	1.37	1.60	1.60
56	7/27/2010	7/27/2010	11:36	14:46	0.74	0.89	0.89
57	7/29/2010	7/29/2010	22:34	23:16	2.08	2.31	2.31
58	7/31/2010	8/1/2010	21:20	7:48	0.79	3.48	0.86
59	8/5/2010	8/5/2010	0:50	7:14	2.34		2.59
60	8/5/2010	8/5/2010	19:40	21:40	2.44	2.69	2.69
61	8/11/2010	8/12/2010	23:52	2:20	0.53	0.53	0.53
62	8/18/2010	8/19/2010	19:30	0:16	0.13	1.60	0.15
63	8/19/2010	8/20/2010	22:58	2:22	1.24		1.45
64	8/22/2010	8/22/2010	14:52	15:18	0.86	0.97	0.97
65	8/23/2010	8/23/2010	16:44	17:34	1.22		1.14
66	8/24/2010	8/24/2010	5:12	10:10	6.76	7.87	6.27
67	8/24/2010	8/25/2010	21:10	5:46	0.48		0.46
68	9/11/2010	9/12/2010	20:02	4:06	0.28	0.33	0.33
69	9/26/2010	9/28/2010	16:06	3:00	7.87	8.36	8.36
70	9/29/2010	10/1/2010	3:02	6:54	9.12	9.63	9.68
71	10/14/2010	10/14/2010	9:30	11:02	0.99	1.09	1.09
72	10/25/2010	10/26/2010	12:48	7:42	1.12	1.27	1.27
73	10/28/2010	10/28/2010	0:40	9:24	0.10	0.15	0.15
74	11/4/2010	11/5/2010	8:45	7:30	1.30	1.65	-
75	11/17/2010	11/17/2010	0:15	4:00	0.41	0.43	-
76	11/26/2010	11/26/2010	8:30	10:45	0.05	0.30	-
77	12/1/2010	12/1/2010	1:15	6:00	0.41	0.66	-
78	12/11/2010	12/12/2010	12:30	2:30	0.43	1.47	-
79	12/12/2010	12/12/2010	10:15	17:30	0.71		-

[1] Dash implies rain gauge error.

[2] Blue shading implies snow event.

Antecedent Dry Period

Table 43. Antecedent dry period.

Storm Event #	Rainfall					Days	Days	Antec. Dry Pd.	Antec. Dry Pd.
	Start Date	Stop Date	Start Time	Stop Time	Rainfall (cm)	(Start Date - Stop Date)	(Start Time - Stop Time)	(days)	(hr)
2 ^[1]	11/10/2009	11/13/2009	17:28	7:04	10.77	20	0.29	20.29	486.90
3	11/16/2009	11/16/2009	11:30	11:38	0.18	3	0.18	3.18	76.43
4	11/18/2009	11/18/2009	18:06	19:48	0.28	2	0.27	2.27	54.47
5	11/19/2009	11/19/2009	4:02	8:38	0.81	1	-0.66	0.34	8.23
6	11/22/2009	11/23/2009	22:20	12:42	1.30	3	0.57	3.57	85.70
7	11/30/2009	11/30/2009	19:10	21:44	0.43	7	0.27	7.27	174.47
8	12/2/2009	12/3/2009	7:56	1:52	3.58	2	-0.58	1.43	34.20
9	12/4/2009	12/5/2009	23:36	18:44	1.07	1	0.91	1.91	45.73
10	12/8/2009	12/9/2009	19:30	10:04	4.01	3	0.03	3.03	72.77
11	12/13/2009	12/13/2009	3:18	16:30	0.66	4	-0.28	3.72	89.23
12	12/18/2009	12/19/2009	19:32	11:22	1.88	5	0.13	5.13	123.03
13	12/25/2009	12/25/2009	10:46	18:54	1.60	6	-0.03	5.98	143.40
14	12/31/2009	12/31/2009	0:00	5:58	0.84	6	-0.79	5.21	125.10
15	12/31/2009	12/31/2009	20:20	23:08	0.25	0	0.60	0.60	14.37
16	1/17/2010	1/18/2010	0:20	18:28	3.58	17	-0.95	16.05	385.20
17	1/21/2010	1/22/2010	14:12	0:02	2.46	3	-0.18	2.82	67.73
18	1/24/2010	1/25/2010	19:24	9:32	2.06	2	0.81	2.81	67.37
19 ^[1]	1/31/2010	1/31/2010	13:04	14:36	0.25	6	0.15	6.15	147.53
20	2/2/2010	2/2/2010	10:24	15:42	0.38	2	-0.18	1.83	43.80
21	2/2/2010	2/3/2010	23:12	1:14	0.25	0	0.31	0.31	7.50
22	2/5/2010	2/5/2010	8:08	23:26	4.55	2	0.29	2.29	54.90
23	2/9/2010	2/9/2010	13:06	17:44	0.66	4	-0.43	3.57	85.67
24	2/13/2010	2/13/2010	16:28	19:14	0.25	4	-0.05	3.95	94.73
25	2/14/2010	2/14/2010	11:00	12:40	0.18	1	-0.34	0.66	15.77
26	2/22/2010	2/22/2010	12:10	15:50	0.58	8	-0.02	7.98	191.50
27	3/2/2010	3/3/2010	15:18	9:10	1.32	8	-0.02	7.98	191.47
28	3/10/2010	3/11/2010	21:34	1:16	0.25	7	0.52	7.52	180.40
29	3/11/2010	3/11/2010	17:00	21:56	0.30	0	0.66	0.66	15.73
30	3/13/2010	3/13/2010	1:44	3:42	1.22	2	-0.84	1.16	27.80
31	3/14/2010	3/14/2010	5:40	11:02	0.25	1	0.08	1.08	25.97
32	3/22/2010	3/22/2010	4:42	6:22	1.37	8	-0.26	7.74	185.67

33	3/28/2010	3/29/2010	22:48	8:32	4.85	6	0.68	6.68	160.43
34	4/8/2010	4/9/2010	22:04	2:48	3.58	10	0.56	10.56	253.53
35	4/21/2010	4/21/2010	2:22	20:16	0.86	12	-0.02	11.98	287.57
36	4/24/2010	4/25/2010	22:04	5:58	0.79	3	0.08	3.08	73.80
37	5/16/2010	5/17/2010	17:54	8:58	1.78	21	0.50	21.50	515.93
38	5/17/2010	5/18/2010	16:22	5:40	5.46	0	0.31	0.31	7.40
39	5/19/2010	5/19/2010	1:24	5:02	1.40	1	-0.18	0.82	19.73
40	5/22/2010	5/23/2010	18:50	1:22	1.27	3	0.58	3.58	85.80
41	5/23/2010	5/23/2010	9:06	23:54	1.42	0	0.32	0.32	7.73
42	5/24/2010	5/24/2010	12:22	20:24	0.41	1	-0.48	0.52	12.47
43	5/28/2010	5/29/2010	22:40	3:12	4.37	4	0.09	4.09	98.27
44	6/1/2010	6/1/2010	4:58	16:42	1.52	3	0.07	3.07	73.77
45	6/2/2010	6/2/2010	13:44	18:02	2.79	1	-0.12	0.88	21.03
46	6/6/2010	6/7/2010	21:14	0:28	0.76	4	0.13	4.13	99.20
47	6/12/2010	6/12/2010	17:42	18:16	0.99	5	0.72	5.72	137.23
48	6/13/2010	6/13/2010	2:42	5:28	0.76	1	-0.65	0.35	8.43
49	6/13/2010	6/13/2010	17:26	19:10	0.33	0	0.50	0.50	11.97
50	6/16/2010	6/16/2010	18:46	19:30	0.91	3	-0.02	2.98	71.60
51	6/23/2010	6/23/2010	16:56	18:48	0.94	7	-0.11	6.89	165.43
52	6/29/2010	6/29/2010	17:30	19:36	0.79	6	-0.05	5.95	142.70
53	7/9/2010	7/10/2010	23:38	23:56	1.80	10	0.17	10.17	244.03
54	7/16/2010	7/18/2010	20:40	16:58	1.12	6	-0.14	5.86	140.73
55	7/23/2010	7/23/2010	18:16	19:10	1.37	5	0.05	5.05	121.30
56	7/27/2010	7/27/2010	11:36	14:46	0.74	4	-0.32	3.68	88.43
57	7/29/2010	7/29/2010	22:34	23:16	2.08	2	0.33	2.33	55.80
58	7/31/2010	8/1/2010	21:20	7:48	0.79	2	-0.08	1.92	46.07
59	8/5/2010	8/5/2010	0:50	7:14	2.34	4	-0.29	3.71	89.03
60	8/5/2010	8/5/2010	19:40	21:40	2.44	0	0.52	0.52	12.43
61	8/11/2010	8/12/2010	23:52	2:20	0.53	6	0.09	6.09	146.20
62	8/18/2010	8/19/2010	19:30	0:16	0.13	6	0.72	6.72	161.17
63	8/19/2010	8/20/2010	22:58	2:22	1.24	0	0.95	0.95	22.70
64	8/22/2010	8/22/2010	14:52	15:18	0.86	2	0.52	2.52	60.50
65	8/23/2010	8/23/2010	16:44	17:34	1.22	1	0.06	1.06	25.43
66	8/24/2010	8/24/2010	5:12	10:10	6.76	1	-0.52	0.48	11.63
67	8/24/2010	8/25/2010	21:10	5:46	0.48	0	0.46	0.46	11.00
68	9/11/2010	9/12/2010	20:02	4:06	0.28	17	0.59	17.59	422.27
69	9/26/2010	9/28/2010	16:06	3:00	7.87	14	0.50	14.50	348.00
70	9/29/2010	10/1/2010	3:02	6:54	9.12	1	0.00	1.00	24.03
71	10/14/2010	10/14/2010	9:30	11:02	0.99	13	0.11	13.11	314.60
72	10/25/2010	10/26/2010	12:48	7:42	1.12	11	0.07	11.07	265.77

73	10/28/2010	10/28/2010	0:40	9:24	0.10	2	-0.29	1.71	40.97
----	------------	------------	------	------	------	---	-------	------	-------

1 = dry, >120 hr antec dry pd. 2=avg, 48-120 hr. 3=wet, 6-48 hr (Brown and Hunt, 2011)

[1] No data available for event 1.

[2] Blue shading indicates snow event.

Bioretention Water Quality Data

Sampled Events

Table 44 shows the sampling schedule during the monitoring period. In some cases, it was necessary to combine individual hydrologic storms when sampling for water quality as indicated by the multiple storm events for one sampling event. This was unavoidable because of short antecedent dry periods between storms.

Table 44. Sampling date, rainfall depth, and samples taken at the bioretention cells for each sampled event.

Storm Event No.	Date Sampled	Rainfall Depth (cm)^[1]	Large Bioretention	Small Bioretention
1	11/2/2009	-	N,T ^[2]	
2	11/13/2009	12.29	N,T	N,T
4,5	11/20/2009	0.99		N,T
6	11/24/2009	1.45	N,T	N,T
8	12/4/2009	4.04	N,T	N,T
9	12/7/2009	1.24		N,T
10	12/10/2009	4.32	N,T	N,T
11	12/14/2009	0.81		N,T
16	1/18/2010	4.01	N,T	N,T
17	1/23/2010	2.84	N,T	N,T
18	1/26/2010	2.29	N,T	N,T
23	2/10/2010	0.84		N, T
27	3/3/2010	1.37	N, T	N, T
30,31	3/14/2010	1.73	N, T	N, T
33	3/30/2010	5.16	N, T	N, T
34	4/10/2010	3.84	N, T	N, T
37	5/17/2010	1.93		N,T
38	5/19/2010	7.32	N,T	N,T
40,41	5/24/2010	2.95	N,T	N,T
42	5/26/2010	0.53	N,T	N,T

47,48	6/13/2010	1.98	N,T	N,T
49	6/14/2010	0.46	N,T	N,T
50	6/17/2010	1.04	N,T	N,T
57	7/30/2010	2.31	N,T	N,T
60	8/6/2010	2.69	N,T	N,T
63	8/20/2010	1.45	N,T,M	N,T,M
64	8/23/2010	0.97	N,T,M	N,T,M
72	10/26/2010	1.27	N,T,M	N,T,M
74	11/5/2010 ^[3]	1.30	N,T,M	N,T,M
77	12/2/2010	0.41		N,T,M

[1] Corrected rainfall depths from ISCO™ tipping bucket rain gauge.

[2] N = nutrients, T = TSS, M = metals

[3] For events 74 and 77, rain data were not recorded by the ISCO™ rain gauge. Reported rainfall depths estimated from USGS station 02087359 Walnut Creek at Sunnybrook Drive near Raleigh, NC.

Raw Pollutant Data

Table 45. Nutrient and TSS concentration data as reported by the NC State University Center for Applied Aquatic Ecology.

Date Sampled	Sample Site	RL ^[1] =	RL =	TKN+NO ₂ 3N	RL =	RL =	RL =
		0.140mg/L	0.0056mg/L		0.007mg/L	0.010mg/L	1mg/L
		TKN (mg/L)	NO ₃ &NO ₂ (mg/L)	TN (mg/L)	NH ₃ N (mg/L)	TP (mg/L)	TSS (mg/L)
11/2/09	MCBRSIN	1.31	0.23	1.54	0.07	0.11	20
11/2/09	MCBRLOUT	0.33	0.15	0.48	0.03	0.05	7
11/13/09	MCBRSIN	0.12	0.11	0.23	0.02	0.02	3
11/13/09	MCBRSOUT	0.24	0.06	0.30	0.01	0.08	7 ^[2]
11/13/09	MCBRLOUT	0.31	0.08	0.40	0.02	0.10	14
11/20/09	MCBRSIN	0.50	0.30	0.79	0.05	0.08	29
11/20/09	MCBRSOUT	0.32	0.18	0.50	0.03	0.07	15
11/24/09	MCBRSIN	0.34	0.30	0.63	0.07	0.06	14
11/24/09	MCBRSOUT	0.25	0.20	0.45	0.01	0.08	10
11/24/09	MCBRLOUT	0.37	0.08	0.46	0.10	0.03	16
12/4/09	MCBRSIN	0.25	0.19	0.43	0.08	0.03	13
12/4/09	MCBRSOUT	0.31	0.19	0.50	0.04	0.08	12
12/4/09	MCBRLOUT	0.24	0.11	0.35	0.02	0.08	11

12/7/09	MCBRSIN	0.30	0.38	0.68	0.11	0.06	13
12/7/09	MCBRSOUT	0.31	0.19	0.50	0.02	0.07	9
12/10/09	MCBRSIN	0.27	0.17	0.44	0.11	0.05	27
12/10/09	MCBRSOUT	0.34	0.12	0.46	0.07	0.10	19
12/10/09	MCBRLOUT	0.21	0.08	0.29	0.03	0.07	7
12/14/09	MCBRSIN	0.44	0.24	0.68	0.26	0.04	5
12/14/09	MCBRSOUT	0.23	0.08	0.31	0.04	0.05	11
1/18/10	MCBRSIN	0.39	0.21	0.60	0.15	0.09	44
1/18/10	MCBRSOUT	0.23	0.13	0.37	0.08	0.11	13
1/18/10	MCBRLOUT	0.126 ^[3]	0.10	0.10	0.06	0.09	12
1/23/10	MCBRSIN	0.31	0.35	0.66	0.14	0.08	20
1/23/10	MCBRSOUT	0.29	0.23	0.52	0.12	0.10	14
1/23/10	MCBRLOUT	0.08	0.12	0.20	0.03	0.07	3
1/26/10	MCBRSIN	0.29	0.19	0.48	0.09	0.07	31
1/26/10	MCBRSOUT	0.21	0.11	0.32	0.09	0.09	22
1/26/10	MCBRLOUT	0.08	0.06	0.14	0.02	0.06	4
2/10/10	MCBRSIN	0.68	0.36	1.04	0.23	0.18	68
2/10/10	MCBRSOUT	0.23	0.13	0.36	0.09	0.07	10
3/3/10	MCBRSIN	0.51	0.54	1.06	0.24	0.18	18
3/3/10	MCBRSOUT	0.28	0.55	0.82	0.06	0.13	31
3/3/10	MCBRLOUT	0.14	0.29	0.43	0.07	0.05	4
3/14/10	MCBRSIN	1.14	0.13	1.28	0.05	0.45	325
3/14/10	MCBRSOUT	0.47	0.25	0.72	0.04	0.12	16
3/14/10	MCBRLOUT	0.21	0.09	0.30	0.04	0.08	24
3/30/10	MCBRSIN	0.34	0.22	0.56	0.02	0.10	48
3/30/10	MCBRSOUT	0.55	0.13	0.68	0.02	0.17	33
3/30/10	MCBRLOUT	0.29	0.11	0.40	0.03	0.10	35
4/10/10	MCBRSIN	0.633	0.20	0.83	0.03	0.15	41
4/10/10	MCBRSOUT	0.722	0.13	0.86	0.04	0.21	37
4/10/10	MCBRLOUT	0.46	0.15	0.61	0.03	0.09	18
5/17/10	MCBRSIN	1.23	0.84	2.07	0.04	0.17	81

5/17/10	MCBRSOUT	0.79	0.36	1.15	0.06	0.25	69
5/19/10	MCBRSIN	0.27	0.20	0.47	0.04	0.04	22
5/19/10	MCBRSOUT	0.41	0.11	0.53	0.03	0.15	36
5/19/10	MCBRLOUT	0.38	0.14	0.52	0.02	0.10	17
5/24/10	MCBRSIN	0.41	0.35	0.75	0.06	0.07	45
5/24/10	MCBRSOUT	0.56	0.12	0.67	0.04	0.22	36
5/24/10	MCBRLOUT	0.47	0.06	0.52	0.05	0.23	46
5/26/10	MCBRSIN	0.43	0.39	0.82	0.01	0.07	14
5/26/10	MCBRSOUT	0.41	0.03	0.44	0.05	0.28	22
5/26/10	MCBRLOUT	0.38	0.03	0.41	0.04	0.23	26
6/13/10	MCBRSIN	0.87	0.50	1.38	0.21	0.44	84
6/13/10	MCBRSOUT	0.71	0.06	0.76	0.02	0.20	33
6/13/10	MCBRLOUT	0.42	0.03	0.45	0.06	0.15	48
6/14/10	MCBRSIN	0.60	0.75	1.35	0.02	0.08	13
6/14/10	MCBRSOUT	0.55	0.01	0.56	0.03	0.17	43
6/14/10	MCBRLOUT	0.41	0.01	0.42	0.02	0.16	26
6/17/10	MCBRSIN	0.69	0.45	1.14	0.02	0.14	174
6/17/10	MCBRSOUT	0.81	0.04	0.85	0.03	0.23	51
6/17/10	MCBRLOUT	0.42	0.00	0.43	0.03	0.17	43
7/30/10	MCBRSIN	0.46	0.23	0.69	0.05	0.12	40
7/30/10	MCBRSOUT	0.50	0.19	0.69	0.02	0.07	39
7/30/10	MCBRLOUT	0.38	0.01	0.39	0.03	0.14	17
8/6/10	MCBRSIN	0.33	0.22	0.55	0.07	0.07	40
8/6/10	MCBRSOUT	0.52	0.13	0.65	0.03	0.21	84
8/6/10	MCBRLOUT	0.43	0.04	0.47	0.02	0.12	16
8/20/10	MCBRSIN	0.39	0.41	0.80	0.02	0.06	23
8/20/10	MCBRSOUT	0.64	0.17	0.81	0.02	0.07	13
8/20/10	MCBRLOUT	0.51	0.02	0.53	0.07	0.17	40
8/23/10	MCBRSIN	0.35	0.25	0.60	0.02	0.05	31
8/23/10	MCBRSOUT	0.43	0.01	0.44	0.02	0.09	21
8/23/10	MCBRLOUT	0.36	0.01	0.36	0.02	0.11	14

10/26/10	MCBRSIN	0.75	0.65	1.39	0.03	0.10	34
10/26/10	MCBRSOUT	0.28	0.03	0.31	0.04	0.06	6
10/26/10	MCBRLOUT	0.44	0.12	0.56	0.03	0.05	29
11/5/10	MCBRSIN	0.87	0.36	1.24	0.19	0.12	27
11/5/10	MCBRSOUT	0.24	0.05	0.29	0.03	0.06	9
11/5/10	MCBRLOUT	0.20	0.04	0.24	0.03	0.08	12
12/2/10	MCBRSIN	0.81	0.35	1.16	0.03	0.17	108
12/2/10	MCBRSOUT	0.46	0.11	0.57	0.10	0.09	23

MCBRLIN= large cell inlet MCBRLOUT= large cell outlet MCBRSOUT= small cell outlet

[1] (RL) = Reportable Limit

[2] yellow shading = QC Issue

[3] Green shading = value is less than reportable limit

Table 46. Metals concentration data reported by the North Carolina Division of Water Quality lab.

SAMPLE DATE	SITE	TOTAL			DISSOLVED		
		PQL= 2 ug/L Cu (ug/L)	PQL= 10 ug/L Pb (ug/L)	PQL= 10 ug/L Zn (ug/L)	PQL= 2 ug/L Cu (ug/L)	PQL= 10 ug/L Pb (ug/L)	PQL= 10 ug/L Zn (ug/L)
8/20/2010	MCBRSIN	6.2	10	43	2.9	10	14
	MCBRSOUT	5.2	10	10	2.3	10	10
	MCBRLOUT	8	10	11	2	10	10
8/23/2010	MCBRSIN	6.7	10	31	2.2	10	10
	MCBRSOUT	7	10	10	2.7	10	10
	MCBRLOUT	5.6	10	10	2	10	10
10/26/2010	MCBRSIN	13	10	49	5.9	10	11
	MCBRSOUT	10	10	10	4.1	10	10
	MCBRLOUT	8.8	10	12	2.4	10	10
11/5/2010	MCBRSIN	13	10	52	5.3	10	11
	MCBRSOUT	11	10	10	4.3	10	10
	MCBRLOUT	6.7	10	10	2.1	10	10
12/2/2010	MCBRSIN	19	10	100	4.1	10	10
	MCBRSOUT	13	10	18	3.4	10	10
4/29/2011	MCBRSIN	14	4.4	58	3	2	10
	MCBRSOUT	10	3.2	17	5.5	2	10

	MCBRLOUT	14	2.8	10		8.9	2	10
5/4/2011	MCBRSIN	7.3	2	30		4.2	2	10
	MCBRSOUT							
	MCBRLOUT	14	3.1	14		8.4	2	11
6/27/2011	MCBRSIN	13	4.2	64		3	2	14
	MCBRSOUT	6.5	2	24		4.4	2	13
	MCBRLOUT	14	2.9	20		8.8	2	13
7/6/2011	MCBRSIN	20	3.2	53		9.4	2	20
	MCBRSOUT	19	4.4	14		11	2	10
	MCBRLOUT	35	4.4	20		18	2	10
7/26/2011	MCBRSIN	18	4.9	69		5.5	2	10
	MCBRSOUT	13	2	10		10	2	10
	MCBRLOUT	9.2	2	10		5.9	2	10

Initial Abstraction Runoff Volume Calculations

Runoff volumes were calculated per storm for the bridge deck by subtracting the amount of rainfall abstracted at the road surface from the rain depth reported by the ISCO 674™ rain gauge. The surface storage, or initial abstraction, was determined using curve numbers for impervious areas which varied based on the antecedent moisture conditions (USDA, 2004a; USDA, 2004b). The curve numbers, initial abstraction values, and their corresponding antecedent moisture conditions are provided in Table 47.

Table 47. Initial abstractions and curve numbers for impervious surfaces under varying antecedent moisture conditions.

Antecedent Moisture Condition	Antecedent Dry Period (hr)	Curve Number	Initial Abstraction (cm)
I (dry)	>120	94	0.325
II (average)	48-120	98	0.104
III (wet)	<48	99	0.051

After accounting for initial abstraction, the remaining rainfall depth was multiplied by the drainage area to determine an approximate total runoff volume per storm event. Then direct rainfall volumes were added to the calculated runoff volumes to get a total volume entering each bioretention cell per storm event. The proportion of flow entering each bioretention cell from the drainage area was determined based on the inflow volumes reported by the ISCO 6712™ samplers located at each bioretention inlet. Storms between 0.5 and 2.5 cm (0.2 and 1 in) were used to determine the flow proportions to between the cells. Between the dates 19 October, 2009

and 4 June, 2010, the inflow volumes to the large and small cells were 49% and 51%, respectively. After observing an event in June that clearly exhibited disproportional flow entering the bioretention cells, the sluice gate at the entrance to the inlet pipe of the small bioretention cell was raised entirely. Despite this, the average flow ratio to the large and small cells became 58% and 42%, respectively. An example initial abstraction calculation is shown below (Pandit and Heck, 2009):

Storm Event 4—

CN for highway=98

S= $1000/CN-10=$ 0.2041 in
 IA = $0.2*S=$ 0.0408 (AMC 2)
 P= 0.11
 P-IA= 0.07 in
 Drainage area = 0.98 ac
 Drainage area = 42688.8 ft²
 Runoff total to both cells: 246.11 ft³
 Direct rainfall to large cell= 18.50 cf
 Direct rainfall to small cell= 9.97 cf
 Avg ratio of runoff to large cell= 0.49
 Avg ratio of runoff to small cell= 0.51

Predicted inflow to large cell=	139.77 cf	(3957.85 L)
Predicted inflow to small cell=	134.81 cf	(3817.39 L)

Load Data

Table 48. Large cell pollutant loads per storm event.

Storm Event No.	Large Cell Inlet (mg)						Large Cell Outlet (mg)					
	TKN	NO _{2,3} -N	TN	NH ₄ -N	TP	TSS	TKN	NO _{2,3} -N	TN	NH ₄ -N	TP	TSS
2	28171.99	23855.31	52027.30	3862.29	4998.26	681580.31	52241.54	13642.70	65884.24	3327.49	15971.94	2329240.70
4,5	10019.66	5979.47	15999.13	909.04	1575.67	585826.62	0.00	0.00	0.00	0.00	0.00	0.00
6	8711.92	7723.70	16435.62	1872.41	1534.34	364080.16	0.00	0.00	0.00	0.00	0.00	0.00
8	18987.96	14164.40	33152.36	6431.40	2526.62	995336.43	17276.55	8096.12	25372.67	1373.45	5421.51	795154.80
10	22731.56	14450.18	37181.74	8957.42	4056.19	2281606.70	15952.33	6242.22	22194.54	2543.12	5625.70	539450.69
11	5482.87	2915.10	8397.97	3212.81	471.38	62023.43	0.00	0.00	0.00	0.00	0.00	0.00
16	27618.77	14734.75	42353.52	10962.09	6406.42	3132025.12	8033.97	6312.40	14346.37	4016.98	5738.55	765139.56
17	15901.23	17805.27	33706.50	6998.60	4271.21	1029206.08	2072.45	3161.81	5234.26	717.39	1727.04	79709.47
18	12316.26	8239.15	20555.41	3822.29	2887.95	1316565.71	2146.06	1517.95	3664.01	628.12	1596.46	104686.01
33	33664.19	21101.46	54765.65	1962.93	9422.05	4711023.37	28462.43	10305.36	38767.80	3140.68	9814.63	3435121.21
34	44847.41	14028.10	14028.10	1983.77	10556.50	2904808.28	32590.53	10839.89	43430.43	1842.07	6376.41	1275281.68
37, 38,39	49009.71	36712.07	85721.79	7776.45	7595.60	3978648.43	68179.57	26042.06	94221.63	3255.26	17180.53	3074410.15

42	27176.98	24654.75	51831.73	882.78	4413.89	882778.94	17162.51	1254.70	18417.21	1747.62	10485.71	1165079.14
47, 48, 49	34915.31	23140.16	58055.47	7465.81	15915.00	3047590.12	6594.73	454.31	7049.05	821.93	2374.37	698919.93
50	14156.71	9185.50	23342.20	388.70	2761.79	3559635.12	2667.11	25.34	2692.45	158.38	1095.99	272412.91
57	22724.57	11337.53	34062.11	2524.95	5941.06	1980354.98	9948.02	314.15	10262.17	733.01	3534.17	445043.14
60	19580.44	12914.76	32495.20	3987.51	4285.08	2380600.90	12375.87	1000.36	13376.22	657.38	3344.06	457306.83
64	6724.84	4751.45	11476.29	383.18	881.32	593931.57	3276.63	45.64	3322.27	164.29	985.73	127779.56
72	15331.92	13241.20	28573.12	655.91	2131.71	696905.42	2659.42	699.53	3358.95	150.76	301.52	174882.54
74	21447.29	8952.77	30400.06	4574.77	3025.25	664079.00	3914.10	720.51	4634.61	662.09	1479.96	233677.72
77	6191.16	2715.82	8906.98	214.81	1327.22	828556.18	0.00	0.00	0.00	0.00	0.00	0.00

Table 49. Small cell pollutant loads per storm event.

Storm Event No.	Small Cell Inlet (mg)						Small Cell Outlet (mg)					
	TKN	NO _{2,3} -N	TN	NH ₄ -N	TP	TSS	TKN	NO _{2,3} -N	TN	NH ₄ -N	TP	TSS
2	27599.42	23370.48	50969.90	3783.79	4896.67	667727.92	47556.59	11889.15	59445.73	2821.15	16120.88	1410576.72
4,5	9856.29	5881.98	15738.27	894.22	1549.98	576275.03	0.00	0.00	0.00	0.00	0.00	0.00
6	8522.32	7555.61	16077.93	1831.66	1500.95	356156.73	5528.04	4321.52	9849.57	285.18	1667.19	219366.72
8	18625.83	13894.27	32520.10	6308.75	2478.44	976354.09	23282.29	13969.37	37251.66	2703.75	6083.44	901249.93
9	6549.96	8263.36	14813.31	2429.12	1214.56	281951.81	5227.78	3146.82	8374.59	304.53	1218.12	152265.31
10	22332.55	14196.53	36529.08	8800.19	3984.99	2241557.44	26063.24	9569.49	35632.72	5057.05	8013.47	1478213.38
11	5313.84	2825.23	8139.07	3113.76	456.85	60111.29	1654.73	568.59	2223.32	306.16	379.06	80185.25
16	26999.74	14404.50	41404.24	10716.39	6262.83	3061826.00	10595.06	5931.42	16526.48	3531.69	4844.75	588614.21
17	15560.90	17424.18	32985.08	6848.81	4179.79	1007177.88	11972.62	9495.53	21468.15	4789.05	4004.63	577988.54
18	12069.15	8073.84	20142.99	3745.60	2830.01	1290150.18	8531.64	4744.42	13276.06	3703.98	3703.98	915590.45
23	8216.68	4313.15	12529.83	2783.07	2156.58	819258.17	950.15	556.70	1506.85	368.34	276.26	41856.96
26	3044.31	3216.07	6260.37	1391.85	1054.25	106609.93	0.00	0.00	0.00	0.00	0.00	0.00
27	24522.52	2872.39	27394.92	1007.48	9581.79	6966625.64	4095.50	2237.11	6332.61	308.26	1056.90	140920.32
33	33028.74	20703.14	53731.88	1925.87	9244.19	4622097.08	18615.47	4551.96	23167.43	815.28	5605.02	1121004.72
34	43934.86	13742.66	13742.66	1943.41	10341.70	2845701.65	12010.59	2229.11	2229.11	665.41	3559.93	615501.22
37, 38,39	78021.53	56022.59	134044.12	7543.20	11584.32	5746358.79	54836.41	18111.36	72947.77	3708.13	18887.69	4788139.49
42	26597.69	24129.23	50726.92	863.96	4319.81	863962.12	25178.32	1974.77	27153.10	3085.58	16970.68	1357654.77
50	10174.76	6601.83	16776.58	279.36	1984.96	2558392.31	7972.66	363.29	8335.94	265.10	2248.45	500745.74
57	22462.75	11206.90	33669.65	2495.86	5872.61	1957537.74	24322.41	9249.37	33571.77	1027.71	3376.75	1908599.29
60	14115.58	9310.27	23425.85	2874.60	3089.12	1716179.51	22267.43	5448.87	27716.30	1201.33	8924.13	3603976.98
62,63	8431.58	8905.99	17337.58	474.41	1229.16	495975.42	10992.43	2927.89	13920.32	376.69	1215.67	222588.06
64	4834.35	3415.73	8250.08	275.46	633.56	426965.69	3912.77	109.70	4022.47	182.84	841.06	191981.56
72	10955.01	9461.14	20416.15	468.66	1523.16	497954.96	4042.22	439.37	4481.59	512.60	849.45	87874.41
74	15400.55	6428.67	21829.22	3284.98	2172.33	476851.97	2336.24	453.73	2789.97	299.27	540.62	86885.02
77	4444.95	1949.83	6394.78	154.22	952.88	594862.98	1530.66	369.35	1900.01	316.11	306.13	76532.85

Combined Water Quality/Hydrology Calculation

		Flow Volume (cf)	
Storm No.	Rain Depth (cm)	Small Cell In	Small Cell Out
37	1.93	1101.7	118.5
38	7.32	4104.2	2715.6
39	1.65	1014.5	1197.2
SUM	10.9	6220.36 cf	4031.30 cf
		176160.60 L	114166.42 L

		Concentration Data (mg/L)	
		Bioretention Inlet	Small Cell Outlet
Storm No.	Date	TKN	TKN
37	5/17/10	1.226	0.787
38,39	5/19/10	0.271	0.413

To determine the total volume fraction allotted to each storm event:

$$\begin{aligned} \text{(storm 37)/(total rainfall)} &= 1.93/10.9 = 0.18 \\ \text{(storm 38+39)/(total rainfall)} &= (7.32+1.65)/10.9 = 0.82 \end{aligned}$$

To calculate TKN influent loading (mg):

$$\begin{aligned} \text{TKN}_{\text{IN}} \text{ load} &= (C_{\text{TKN37-IN}})(V_{\text{SMALL-IN}})(0.18) + (C_{\text{TKN38,39-IN}})(V_{\text{SMALL-IN}})(0.82) \\ &= (1.226 \text{ mg/L})(176160.6 \text{ L})(0.18) + (0.271 \text{ mg/L})(176160.6 \text{ L})(0.82) = 78021.53 \text{ mg} \end{aligned}$$

Where,

$\text{TKN}_{\text{IN}} \text{ load}$ = influent TKN load (mg)

$C_{\text{TKN37-IN}}$ = TKN inflow concentration from storm no. 37 (mg/L)

$V_{\text{SMALL-IN}}$ = small cell inflow volume (L)

$C_{\text{TKN38,39-IN}}$ = TKN inflow concentration from storm no. 38 and 39 combined (mg/L)

The same process was done for effluent loading.

	TKN Pollutant Loads	
Storm Event No.	Small Cell Inlet (mg)	Small Cell Outlet (mg)
37,38,39	78021.53	54836.41

Fractionation of Load Reduction Attributed to Concentration and Volume Reduction

When the influent concentration was greater than the effluent concentration, the following equation was used to determine the load reduction associated with concentration reduction.

$$F_{\text{conc}} = [(V_{\text{out}} * C_{\text{in}}) - (V_{\text{out}} * C_{\text{out}})] \quad (\text{D.1})$$

Where,

F_{conc} = Load reduction due to concentration loss (mg)

V_{out} = Effluent volume (L)

C_{in} = Influent concentration (mg/L)

C_{out} = Effluent concentration (mg/L)

V_{in} = Influent volume (L)

The remaining fraction of the load reduction was therefore assumed to be associated with volume reduction.

$$F_{\text{vol}} = L - [(V_{\text{out}} * C_{\text{in}}) - (V_{\text{out}} * C_{\text{out}})] \quad (\text{D.2})$$

Where,

F_{vol} = Load reduction due to volume loss (mg)

L = Total load reduction (mg)

This calculation was performed per water quality storm event. When the effluent concentration was greater than the influent concentration, it was necessary to use a different approach because Equation F.1 would not accurately represent such a situation. Therefore, for events with increasing concentration, the following equations (Equations F.3 and F.4) were used to find the fraction of the load reduction associated with concentration reduction and volume reduction, respectively.

$$F_{\text{conc}} = V_{\text{in}} * (C_{\text{in}} - C_{\text{out}}) \quad (\text{F.3})$$

$$F_{\text{vol}} = (V_{\text{in}} - V_{\text{out}}) * C_{\text{out}} \quad (\text{F.4})$$

Equation F.3 holds volume constant to account for the change in concentration while equation F.4 holds concentration constant to account for volume loss.

The portion of the load reduction due to either concentration or volume loss was then divided by the total load reduction to determine the percentages displayed in Tables 26 and 27 (Equations F.5 and F.6).

$$F = \left(\frac{\sum F_{\text{conc}}}{\sum L} \right) * 100 \quad (\text{F.5})$$

$$F = \left(\frac{\sum F_{\text{vol}}}{\sum L} \right) * 100 \quad (\text{F.6})$$

Where,

F = Total fraction of a pollutant load contributed to either concentration loss or volume loss.

Appendix B: Swale

Swale Water Quality Sampled Events

Table 50. Sampling date, rainfall depth, and samples taken at the swale for each water quality sampled event.

Storm Event No.	Date Sampled	Rainfall Depth (cm) ^[1]	Swale Sample
1	11/2/2009	-	N,T ^[2]
4,5	11/20/2009	0.99	N,T
6	11/24/2009	1.45	N,T
8	12/4/2009	4.04	N,T
9	12/7/2009	1.24	N,T
10	12/10/2009	4.32	N,T
16	1/18/2010	4.01	N,T
17	1/23/2010	2.84	N,T
18	1/26/2010	2.29	N,T
23	2/10/2010	0.84	N, T, M
26	2/23/2010	0.69	N, M
27	3/3/2010	1.37	N, T, M
28,29	3/12/2010	0.56	N, T, M
30,31	3/14/2010	1.73	N, T, M
33	3/30/2010	5.16	N, T, M
34	4/10/2010	3.84	N, T, M
37	5/17/2010	1.93	N,T
38	5/19/2010	7.32	N,T
40,41	5/24/2010	2.95	N,T
42	5/26/2010	0.53	N,T
47,48	6/13/2010	1.98	N,T
50	6/17/2010	1.04	N,T
54	7/17/2010	.[3]	N,T
56	7/28/2010	0.89	N,T
60	8/6/2010	2.69	N,T

64	8/23/2010	0.97	N,T,M
70	10/1/2010	9.68	N,T,M
71	10/15/2010	1.09	N,T
72	10/26/2010	1.27	N,T,M
74	11/5/2010 ^[4]	1.30	N,T,M
77	12/2/2010	0.41	N,T,M
79	12/13/10	0.71	N,T

[1] Corrected rainfall depths from ISCO tipping bucket rain gauge.

[2] N = nutrients, T = TSS, M = metals

[3] ISCO rain gauge clogged. No accurate reading for this date.

[4] For events 74-79, rain data were not recorded by the ISCO rain gauge. The reported rainfall depths were estimated from USGS station 02087359 Walnut Creek at Sunnybrook Drive near Raleigh, NC.

Swale Pollutant Concentration Data

Table 51. Nutrient and TSS concentration data as reported by the NC State University Center for Applied Aquatic Ecology.

		RL ^[1] = 0.140mg/L	RL= 0.0056mg/L	TKN+ NO23N	RL= 0.007mg/L	RL= 0.010mg/L	RL= 1mg/L
Date Sampled	Sample Site	TKN (mg/L)	NO3&NO2 (mg/L)	TN (mg/L)	NH3N (mg/L)	TP (mg/L)	TSS (mg/L)
11/2/09	MCSWIN	0.48	0.22	0.70	0.03	0.07	22
11/2/09	MCSWOUT	0.45	0.15	0.60	0.02	0.10	22
11/20/09	MCSWIN	0.62	0.21	0.83	0.10	0.10	39
11/20/09	MCSWOUT	0.68	0.23	0.90	0.06	0.14	67
11/24/09	MCSWIN	0.36	0.29	0.65	0.07	0.07	14
11/24/09	MCSWOUT	0.45	0.31	0.76	0.07	0.08	10
12/4/09	MCSWIN	0.59	0.13	0.71	0.31	0.07	19
12/4/09	MCSWOUT	0.46	0.18	0.64	0.08	0.01	16
12/7/09	MCSWIN	0.24	0.30	0.55	0.10	0.03	6
12/7/09	MCSWOUT	0.34	0.24	0.57	0.05	0.07	7
12/10/09	MCSWIN	0.25	0.10	0.35	0.08	0.05	41
12/10/09	MCSWOUT	0.45	0.11	0.56	0.07	0.11	50
1/18/10	MCSWIN	0.36	0.14	0.50	0.15	0.11	36
1/18/10	MCSWOUT	0.36	0.22	0.58	0.14	0.15	11
1/23/10	MCSWIN	0.25 ^[2]	0.19	0.44	0.13	0.07	22

1/23/10	MCSWOUT	0.44	0.24	0.68	0.13	0.12	14
1/26/10	MCSWIN	0.33	0.11	0.44	0.11	0.10	57
1/26/10	MCSWOUT	0.35	0.16	0.51	0.11	0.10	23
2/10/10	MCSWIN	0.67	0.24	0.91	0.16	0.29	109
2/10/10	MCSWOUT	0.61	0.31	0.92	0.12	0.29	82
2/23/10	MCSWIN	1.03	0.48	1.51	0.26	0.49	NS ^[3]
2/23/10	MCSWOUT	0.91	0.51	1.43	0.20	0.40	NS
3/3/10	MCSWIN	0.85	0.84	1.69	0.18	0.32	75
3/3/10	MCSWOUT	0.76	0.91	1.67	0.16	0.28	40
3/12/10	MCSWIN	1.57	1.23	2.80	0.06	0.39	136
3/12/10	MCSWOUT	1.16	1.26	2.41	0.04	0.29	49
3/14/10	MCSWIN	1.26	0.08	1.33	0.03	0.53	312
3/14/10	MCSWOUT	0.81	0.23	1.04	0.03	0.38	143
3/30/10	MCSWIN	0.45	0.15	0.60	0.03	0.15	122
3/30/10	MCSWOUT	0.35	0.13	0.48	0.04	0.13	64
4/10/10	MCSWIN	0.88	0.14	1.02	0.02	0.15	98
4/10/10	MCSWOUT	0.67	0.20	0.87	0.02	0.13	31
5/17/10	MCSWIN	1.14	1.05	2.19	0.04	0.13	58
5/17/10	MCSWOUT	1.45	0.97	2.41	0.04	0.22	62
5/19/10	MCSWIN	0.40	0.28	0.68	0.03	0.10	60
5/19/10	MCSWOUT	0.38	0.23	0.61	0.02	0.09	26
5/24/10	MCSWIN	0.53	0.37	0.90	0.06	0.09	44
5/24/10	MCSWOUT	0.52	0.32	0.84	0.07	0.09	24
5/26/10	MCSWIN	0.52	0.36	0.88	0.02	0.11	14
5/26/10	MCSWOUT	0.53	0.28	0.81	0.02	0.06	2
6/13/10	MCSWIN	0.70	0.62	1.32	0.03	0.11	44
6/13/10	MCSWOUT	0.70	0.50	1.20	0.03	0.14	37
6/17/10	MCSWIN	0.74	0.58	1.31	0.02	0.11	69
6/17/10	MCSWOUT	0.70	0.57	1.27	0.02	0.13	59

7/17/10	MCSWIN	1.01	0.72	1.73	0.04	0.13	55
7/17/10	MCSWOUT	0.93	0.73	1.65	0.04	0.15	35
7/28/10	MCSWIN	0.47	0.52	0.99	0.02	0.36	35
7/28/10	MCSWOUT	0.56	0.45	1.02	0.02	0.10	8
8/6/10	MCSWIN	0.40	0.20	0.60	0.02	0.07	40
8/6/10	MCSWOUT	0.49	0.24	0.73	0.04	0.09	26
8/23/10	MCSWIN	0.49	0.29	0.78	0.02	0.05	19
8/23/10	MCSWOUT	0.49	0.29	0.78	0.02	0.08	15
10/1/10	MCSWIN	0.24	0.06	0.30	0.03	0.05	9
10/1/10	MCSWOUT	0.26	0.10	0.36	0.03	0.06	4
				0.00			
10/15/10	MCSWIN	1.49	0.65	2.14	0.13	0.28	283
10/15/10	MCSWOUT	0.96	0.63	1.59	0.09	0.20	81
10/26/10	MCSWIN	1.18	0.65	1.83	0.03	0.11	189
10/26/10	MCSWOUT	0.84	0.66	1.50	0.04	0.10	60
11/5/10	MCSWIN	0.61	0.32	0.93	0.08	0.26	58
11/5/10	MCSWOUT	0.35	0.20	0.55	0.07	0.18	25
12/2/10	MCSWIN	0.72	0.27	0.99	0.03	0.16	93
12/2/10	MCSWOUT	0.83	0.24	1.06	0.06	0.19	98
12/13/10	MCSWIN	0.64	0.24	0.88	0.18	0.22	59
12/13/10	MCSWOUT	0.55	0.23	0.78	0.26	0.36	30

[1] (RL) = Reportable Limit

[2] Shading means QC Issue

[3] NS=no sample

Table 52. Metals concentration data as reported by the North Carolina Division of Water Quality lab.

SAMPLE DATE	SITE	TOTAL			DISSOLVED		
		PQL= 2 ug/L	PQL= 10 ug/L	PQL= 10 ug/L	PQL= 2 ug/L	PQL= 10 ug/L	PQL= 10 ug/L
		Cu (ug/L)	Pb (ug/L)	Zn (ug/L)	Cu (ug/L)	Pb (ug/L)	Zn (ug/L)
8/20/2010	MCSWIN	10	10	47	7.8	10	31
	MCSWOUT	6.6	10	16	4.4	10	10

10/1/2010	MCSWIN	4.7	10	22		2.6	10	10
	MCSWOUT	3.2	10	10		2.6	10	10
10/1/2010	MCSWIN	4.7	10	22		2.6	10	10
	MCSWOUT	3.2	10	10		2.6	10	10
10/26/2010	MCSWIN	43	15	240		9.4	10	27
	MCSWOUT	20	10	120		8.6	10	36
11/5/2010	MCSWIN	13	10	65		4.4	10	17
	MCSWOUT	11	10	49		5.1	10	16
12/2/2010	MCSWIN	18	10	92		7.1	10	37
	MCSWOUT	22	10	110		4.4	10	10
4/23/2011	MCSWIN	29	7.1	180				
	MCSWOUT	13	2.3	75				
5/4/2011	MCSWIN	27	5.6	270		10	2	120
	MCSWOUT	7.7	2	26		6.4	2	19
6/27/2011	MCSWIN	12	2.6	58		4.9	2	30
	MCSWOUT	11	2	39		8.2	2	25
7/6/2011	MCSWIN	310	37	320		22	2	10
	MCSWOUT	26	10	150		12	2	23
7/26/2011	MCSWIN	12	3.2	47		5	2	17
	MCSWOUT	7.2	2	25		5.2	2	18

Swale Pollutant Load Data

Table 53. Pollutant loads per storm event.

Swale Inlet (mg)							
Event Number	Date	TKN	NO _{2,3} -N	TN	NH ₄ -N	TP	TSS
4,5	11/20/09	24097	8006	32104	3809	3731	1515788
6	11/24/09	22069	17704	39773	4119	3996	860623
8	12/4/09	107226	22795	130020	57078	12218	3464780
9	12/7/09	13316	16427	29743	5621	1637	327447
10	12/10/09	47414	19081	66495	15226	9252	7902357

16	1/18/10	61074	22776	83850	24632	18221	6073643
17	1/23/10	30714	24070	54784	16548	8901	2758013
18	1/26/10	32837	11378	44215	10580	10380	5689043
23	2/10/10	22440	8130	30570	5207	9876	3661665
26	2/23/10	17031	7887	24918	4233	8102	_[1]
27	3/3/10	40476	40380	80856	8622	15089	3592534
28,29	3/12/10	27820	21740	49559	972	6964	2403734
30,31	3/14/10	93243	5647	98890	2378	39229	23180826
33	3/30/10	99444	32264	131708	7514	33590	26960403
34	4/10/10	141793	22481	164274	2409	24729	15736908
37	5/17/10	84034	77129	161163	2718	9770	4260468
38	5/19/10	133217	91690	224907	10299	32889	19932645
40,41	5/24/10	67534	47746	115280	7660	11617	5617204
42	5/26/10	11420	8025	19446	507	2359	308660
47,48	6/13/10	51624	45162	96786	2350	8298	3231085
50	6/17/10	31607	24746	56353	944	4889	2959170
56	7/28/10	16701	18820	35521	790	13002	1257080
60	8/6/10	48130	24185	72315	2767	8904	4812972
64	8/23/10	19313	11532	30845	869	2093	750395
70	10/1/10	105531	27262	132793	12752	19787	3957395
71	10/15/10	52228	22754	74982	4691	9942	9906543
72	10/26/10	62948	34846	97794	1820	5727	10116661
74	11/5/10	27226	14257	41484	3464	11681	2576063
77	12/2/10	10024	3683	13707	429	2188	1287591
79	12/13/10	19345	7243	26588	5432	6640	1780599
Swale Outlet							
Event Number	Date	TKN	NO _{2,3} -N	TN	NH ₄ -N	TP	TSS
4,5	11/20/09	26274	8784	35057	2215	5480	2604047
6	11/24/09	27724	18995	46720	4057	4733	614730
8	12/4/09	84067	32095	116161	14953	1915	2917710
9	12/7/09	18501	12825	31326	2947	3547	382021
10	12/10/09	86035	20891	106926	13105	20702	9496121
16	1/18/10	33801	20392	54194	12571	13688	1024278
17	1/23/10	55035	30338	85373	16172	15545	1755099
18	1/26/10	6211	2813	9024	1876	1787	406970
23	2/10/10	20468	10217	30686	4020	9782	2746978
26	2/23/10	15080	8483	23563	3241	6581	-
27	3/3/10	36548	43446	79994	7520	13412	1916018

28,29	3/12/10	20432	22199	42631	689	5126	866051
30,31	3/14/10	60255	17014	77269	2229	28159	10624545
33	3/30/10	78229	27844	106074	9281	28728	14143162
34	4/10/10	107268	31956	139223	3372	20233	4978001
37	5/17/10	106218	70959	177177	3232	16234	4554293
38	5/19/10	125908	77073	202981	5980	28902	8637479
40,41	5/24/10	65874	41108	106982	8426	10979	3063929
42	5/26/10	11685	6261	17946	485	1323	44094
47,48	6/13/10	51550	36423	87974	2130	10207	2717049
50	6/17/10	29892	24360	54251	901	5661	2530305
56	7/28/10	20221	16234	36455	646	3735	287333
60	8/6/10	59079	29118	88198	5294	10348	3128432
64	8/23/10	19234	11493	30727	711	3199	592417
70	10/1/10	112566	44850	157416	12312	25503	1758842
71	10/15/10	33605	21948	55554	3010	6966	2835442
72	10/26/10	44963	35542	80505	2034	5353	3211638
74	11/5/10	15634	8883	24517	3198	8084	1110372
77	12/2/10	11436	3281	14717	803	2672	1356817
79	12/13/2010	16478	6941	23419	7967	10865	905389
[1] No data available.							

Swale Initial Abstraction Runoff Volume Calculations

Runoff volumes were calculated per storm for the bridge deck by subtracting the amount of rainfall abstracted at the road surface from the corrected rain depth. The surface storage, or initial abstraction, was determined using curve numbers for impervious areas which varied based on the antecedent moisture conditions (USDA, 2004a; USDA, 2004b). The curve numbers, initial abstraction values, and their corresponding antecedent moisture conditions are provided in Table 54.

Table 54. Initial abstractions and curve numbers for impervious surfaces under varying antecedent moisture conditions.

Antecedent Moisture Condition	Antecedent Dry Period (hr)	Curve Number	Initial Abstraction (cm)
I (dry)	>120	94	0.325
II (average)	48-120	98	0.104
III (wet)	<48	99	0.051

After accounting for initial abstraction, the remaining rainfall depth was multiplied by the drainage area to determine an approximate total runoff volume per storm event.

Swale Inflow Volume

Table 55. Calculated runoff volumes based on Initial Abstraction method (Pandit and Heck, 2009).

Storm Event #	AMC	CN	Initial Abstraction (cm)	Rainfall Amount (cm)	Corrected Tipping Bucket RG (cm)	IA Estimated Runoff Volume (L/s)
2 ^[1]	1	94	0.324	10.77	12.29	547394.4
3	2	98	0.104	0.18	0.15	2738.544
4	2	98	0.104	0.28	0.25	7014.864
5	3	99	0.051	0.81	0.74	31851.5
6	2	98	0.104	1.30	1.45	61474.22
7	1	94	0.324	0.43	0.61	13049.86
8	3	99	0.051	3.58	4.04	182358.1
9	3	99	0.051	1.07	1.24	54575.47
10	2	98	0.104	4.01	4.32	192740.3
11	2	98	0.104	0.66	0.81	32432.06
12	1	94	0.324	1.88	1.78	66835.2
13	1	94	0.324	1.60	1.52	54694.42
14	1	94	0.324	0.84	0.79	21588.34
15	3	99	0.051	0.25	0.25	8688.576
16	1	94	0.324	3.58	4.01	168713.6
17	2	98	0.104	2.46	2.84	125364.1
18	2	98	0.104	2.06	2.29	99808.18
19 ^[2]	1	94	0.324	0.25	0.43	4752.096
20	3	99	0.051	0.38	0.64	27025.78
21	3	99	0.051	0.25	0.43	17235.55
22	2	98	0.104	4.55	4.80	214812.9
23	2	98	0.104	0.66	0.84	33593.18
24	2	98	0.104	0.25	0.36	10974
25	3	99	0.051	0.18	0.23	8654.592
26	1	94	0.324	0.58	0.69	16536.05
27	1	94	0.324	1.32	1.37	47900.45
28	1	94	0.324	0.25	0.36	1011.024
29	3	99	0.051	0.30	0.41	16663.49
30	3	99	0.051	1.22	1.42	63026.16
31	3	99	0.051	0.25	0.30	11271.36
32	1	94	0.324	1.37	1.63	59517.31
33	1	94	0.324	4.85	5.16	220986.6
34	1	94	0.324	3.58	3.84	160580.1
35	1	94	0.324	0.86	0.91	26592.48
36	2	98	0.104	0.79	1.27	53737.2

37	1	94	0.324	1.78	1.93	73456.42
38	3	99	0.051	5.46	7.32	332210.6
39	3	99	0.051	1.40	1.65	72609.65
40	2	98	0.104	1.27	1.40	58820.64
41	3	99	0.051	1.42	1.55	68843.09
42	3	99	0.051	0.41	0.53	22047.12
43	2	98	0.104	4.37	5.13	229666.7
44	2	98	0.104	1.52	1.78	77027.57
45	3	99	0.051	2.79	3.07	138212.9
46	2	98	0.104	0.76	0.89	35915.42
47	1	94	0.324	0.99	1.12	36385.54
48	3	99	0.051	0.76	0.86	37048.22
49	3	99	0.051	0.33	0.46	18563.76
50	2	98	0.104	0.91	1.04	42887.81
51	1	94	0.324	0.94	1.09	35595.41
52	1	94	0.324	0.79	0.91	27419.42
53	1	94	0.324	1.80	-	-
54	1	94	0.324	1.12	-	-
55	1	94	0.324	1.37	1.60	58356.19
56	2	98	0.104	0.74	0.89	35915.42
57	2	98	0.104	2.08	2.31	100992
58	3	99	0.051	0.79	0.86	37625.95
59	2	98	0.104	2.34	2.59	113886
60	3	99	0.051	2.44	2.69	120323.2
61	1	94	0.324	0.53	0.53	9566.496
62	1	94	0.324	0.13	0.15	0
63	3	99	0.051	1.24	1.45	64252.42
64	2	98	0.104	0.86	0.97	39495.07
65	3	99	0.051	1.22	1.14	49509.02
66	3	99	0.051	6.76	6.27	285023.8
67	3	99	0.051	0.48	0.46	18178.61
68	1	94	0.324	0.28	0.33	249.22
69	1	94	0.324	7.87	8.36	366891.3
70	3	99	0.051	9.12	9.68	439710.5
71	1	94	0.324	0.99	1.09	35006.35
72	1	98	0.104	1.12	1.27	53527.63
73	3	99	0.051	0.10	0.15	4621.82
74	1	94	0.324	1.30	-	44414.26
75	1	94	0.324	0.41	-	3758.06
76	1	94	0.324	0.05	-	0

77	2	98	0.104	0.41	-	13845.65
78	1	94	0.324	0.43	-	4919.18
79	3	99	0.051	0.71	-	30180.62

[1] No data available for event 1.

[2] Crossed-through values indicate snow event.

Swale Concentration Calculations

SWMM calculation of tc through bridge deck pipes:					
(Modeled storm events by selecting representative flow rates and solving for intensities with $q=ciA$)					
A=1.13 ac (0.46 ha) c=0.95					
Q (cfs)	Q(L/s)	i (in/hr)	i (mm/hr)	tc (min) (Found with SWMM)	
1	28.3	0.82	20.73	7.50	
1.5	42.48	1.22	31.09	6.88	
2	56.63	1.63	41.45	4.50	
3	84.95	2.45	62.18	2.75	
average:				5.41	
Intensities held constant for five hours.					
Average slope diagonal across upper portion of bridge deck = 0.67%					
Ignored pipe entrance/exit losses					
tc through portion of bridge deck before pipe attachments begin:					
m					
Bridge deck length	172.87 =		567 ft		
slope (length)	0.005				
			Bridge deck width=	14.63 m	= 48 ft
tc=0.0078*L^0.77*(L/H)^.385			Slope (width)=	0.02	
L= max length of flow in feet					
H=diff in elev in ft between the outlet of the watershed and the hydraulically most remote point in the watershed					
drop along bridge	0.86 m	=	2.83	ft	
drop across bridge	0.29 m	=	0.96	ft	
H (total)	1.16 m	=	3.79	ft	
L	184.22 m	=	604.40	ft	
tc=		7.62 min			
total tc=		13.0 min			

Figure 59. Time of concentration calculations for southbound bridge deck.

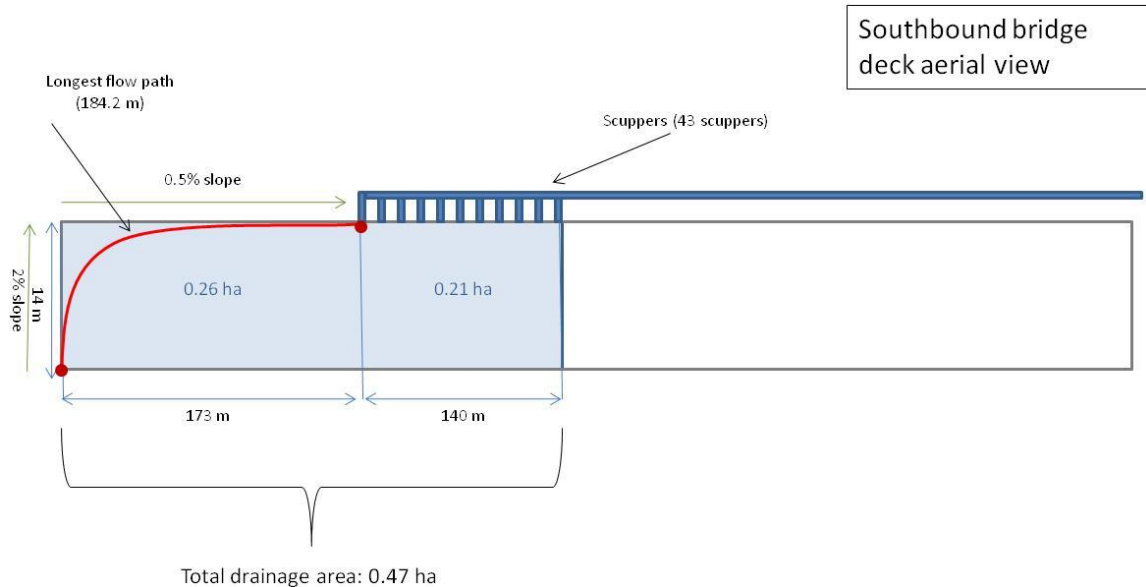


Figure 60. Aerial view of southbound bridge deck and longest flow path for t_c calculations.

Swale Soil Compaction

Table 56 shows the results from the soil compaction test performed at three distances ((9 m, 18 m, 27 m) (30 ft, 60 ft, 90 ft)) from the check dam at the end of the swale. Compaction was measured with a Spectrum SC900 Soil Compaction Meter (Spectrum Technologies, 2011). Soil is considered compacted when it has a reading of 300 psi (2070 kPa) at a depth of 7.5 cm (3 in) (Pitt et al., 2008). Table 56 shows psi readings obtained by the Spectrum SC900™ Soil Compaction Meter. Some duplicate measurements were taken, as shown. The table shows that the swale was indeed compact, which consequently affected the infiltration ability of the swale.

Table 56. Spectrum SC900 Soil Compaction Meter readings for soil compaction along the swale measured in psi. The shallowest readings at or above 300 psi (2070 kPa) are shaded red.

Dist. From Outlet (ft)	Position across swale	No.	Depth into soil (in)												
			0	1	2	3	4	5	6	7	8	9	10	11	12
30	center	N= 1	10	10	97	361	366	265	672	0	0	0	0	0	0
30	center	N= 2	10	10	92	127	280	606	0	0	0	0	0	0	
30	left	N= 3	10	163	199	407	280	0	0	0	0	0	0	0	
30	right	N= 4	5	10	127	117	356	402	0	0	0	0	0	0	
60	center	N= 5	15	15	15	468	677	366	0	0	0	0	0	0	
60	center	N= 6	5	5	209	514	550	738	702	738	733	0	0	0	
60	center	N= 7	5	5	5	219	326	453	443	611	672	667	422	550	
60	left	N= 8	10	10	453	484	667	0	0	0	0	0	0	0	
60	left	N= 9	5	132	321	473	667	0	0	0	0	0	0	0	
60	right	N= 10	10	143	331	417	417	0	0	0	0	0	0	0	
60	right	N= 12	10	148	132	122	117	321	412	0	0	0	0	0	

90	center	N= 13	10	112	224	295	453	473	366	433	611	0	0	0	0
90	center	N= 14	20	71	148	204	616	0	0	0	0	0	0	0	0
90	left	N= 15	5	56	137	127	158	224	494	494	0	0	0	0	0
90	left	N= 16	61	117	117	275	575	514	438	239	0	0	0	0	0
90	right	N= 17	10	51	81	71	102	341	0	0	0	0	0	0	0
90	right	N= 18	5	61	97	97	112	667	468	0	0	0	0	0	0

Swale Grass Length and Density Analysis

On February 21, 2010, a grass blade length and grass density analysis was performed in the swale (Tables 57 and 58). A 10.2 x 10.2 cm (4 x 4 in) square template was placed on the left bank, center, and right bank of the swale every 9 m (30 ft), starting at the check dam (Figure 61). All grass blades within the square were counted, and the average height of the grass blades within the square was also measured. There was some difficulty performing the blade count along the centerline because deposited sediment covered a large amount of blades.

The blade length increased during the growing season. The swale was mowed on June 29, 2010 by DOT's highway maintenance. Another grass length and density analysis was performed on September 10, 2010 to compare the stand among seasons (Tables 59 and 60).



Figure 61. Flag placement in swale (left) and grass counting template (right).

Table 57. Grass length and count 2/21/10 raw data.

	Count all the blades in the square			*Measure avg. ht. of 10 cm x10 cm section*		
Distance from Outlet Pipe (m)	Grass Blade Count			Grass Height (m)		
	Left side	centerline	right side	Left side	centerline	right side
9	69	151	205	0.20	0.20	0.28
18	263	115	272	0.24	0.23	0.28
27	323	19	300	0.24	0.09	0.20
37	183	107	93	0.27	0.23	0.20
Averages:	209.5	98	217.5	0.24	0.19	0.24

Table 58. Grass density 2/21/10.

Distance from Outlet Pipe (m)	Grass Density (blades/m ²)		
	Left side	centerline	right side
9	6677	14613	19839
18	25452	11129	26323
27	31258	1839	29032
37	17710	10355	9000
Averages:	20274	9484	21048

Table 59. Grass length and count 9/10/10 raw data.

	Count all the blades in the square			*Measure avg. ht. of 10 cm x10 cm section*		
Distance from Outlet Pipe (m)	Grass Blade Count			Grass Height (m)		
	Left side	centerline	right side	Left side	centerline	right side
9	196	52	87	0.21	0.30	0.15
18	140	84	171	0.25	0.22	0.23
27	156	69	196	0.27	0.27	0.33
37	198	92	162	0.27	0.24	0.24
Averages:	172.5	74.25	154	0.25	0.26	0.24

Table 60. Grass density 9/10/10.

Distance from Outlet Pipe (m)	Grass Density (blades/m ²)		
	Left side	centerline	right side
9	18968	5032	8419
18	13548	8129	16548
27	15097	6677	18968
37	19161	8903	15677
Averages:	16694	7185	14903

Swale Particle Size Distribution Analysis Results

Table 61. Particle size distribution analysis results reported by NC State University’s Marine, Earth and Atmospheric Science Department.

Inlet 10/15/2010		Outlet 10/15/2010		Inlet 11/5/2010		Outlet 11/5/2010		Inlet 12/13/2010		Outlet 12/13/2010	
From	0.04	From	0.04	From	0.04	From	0.04	From	0.04	From	0.04
To	2000	To	2000	To	2000	To	2000	To	2000	To	2000
Volume	100	Volume	100	Volume	100	Volume	100	Volume	100	Volume	100
Mean:	327.70	Mean:	114.42	Mean:	202.67	Mean:	24.71	Mean:	97.11	Mean:	119.14
Median:	149.92	Median:	42.57	Median:	82.96	Median:	16.37	Median:	45.19	Median:	42.16
Mode:	517.18	Mode:	34.58	Mode:	517.18	Mode:	31.50	Mode:	55.13	Mode:	41.68
S.D.:	411.17	S.D.:	170.68	S.D.:	286.23	S.D.:	26.05	S.D.:	140.04	S.D.:	178.64
Variance:	169057.00	Variance:	29133.00	Variance:	81929.90	Variance:	678.37	Variance:	19611.00	Variance:	31910.30
d10:	13.79	d10:	4.61	d10:	7.98	d10:	1.48	d10:	4.13	d10:	3.51
d50:	149.92	d50:	42.57	d50:	82.96	d50:	16.37	d50:	45.19	d50:	42.16
d90:	937.50	d90:	390.99	d90:	557.64	d90:	58.34	d90:	232.89	d90:	454.26
% < Size		% < Size		% < Size		% < Size		% < Size		% < Size	
10	13.79	10.00	4.61	10.00	7.98	10.00	1.48	10.00	4.13	10.00	3.51
25	45.19	25.00	14.23	25.00	25.68	25.00	5.58	25.00	14.49	25.00	13.66
50	149.92	50.00	42.57	50.00	82.96	50.00	16.37	50.00	45.19	50.00	42.16
75	473.29	75.00	131.39	75.00	243.48	75.00	34.81	75.00	109.21	75.00	121.98
90	937.50	90.00	390.99	90.00	557.64	90.00	58.34	90.00	232.89	90.00	454.26
Volume %	Swale Inlet	Volume %	Swale Outlet	Volume %	Swale Inlet	Volume %	Swale Outlet	Volume %	Swale Inlet	Volume %	Swale Outlet
	Particle Diameter		Particle Diameter		Particle Diameter		Particle Diameter		Particle Diameter		Particle Diameter
	um <		um <		um <		um <		um <		um <
10	13.79	10	4.61	10	7.98	10	1.48	10	4.13	10	3.51
25	45.19	25	14.23	25	25.68	25	5.58	25	14.49	25	13.66
50	149.92	50	42.57	50	82.96	50	16.37	50	45.19	50	42.16
75	473.29	75	131.39	75	243.48	75	34.81	75	109.21	75	121.98
90	937.50	90	390.99	90	557.64	90	58.34	90	232.89	90	454.26
Channel Diameter (Lower)	Diff. Volume % ^{III}	Channel Diameter (Lower)	Diff. Volume %								
	um		um		um		um		um		um
	0.04		0.04		0.04		0.04		0.04		0.04
	0.04		0.04		0.04		0.04		0.04		0.04
	0.05		0.05		0.05		0.05		0.05		0.05
	0.05		0.05		0.05		0.05		0.05		0.05
	0.06		0.06		0.06		0.06		0.06		0.06
	0.06		0.06		0.06		0.06		0.06		0.06
	0.07		0.07		0.07		0.07		0.07		0.07

0.08	0.01	0.08	0.02	0.08	0.01	0.08	0.05	0.08	0.03	0.08	0.03
0.08	0.02	0.08	0.03	0.08	0.02	0.08	0.06	0.08	0.03	0.08	0.04
0.09	0.02	0.09	0.04	0.09	0.02	0.09	0.08	0.09	0.04	0.09	0.05
0.10	0.02	0.10	0.04	0.10	0.02	0.10	0.09	0.10	0.05	0.10	0.06
0.11	0.03	0.11	0.05	0.11	0.03	0.11	0.10	0.11	0.05	0.11	0.07
0.12	0.03	0.12	0.06	0.12	0.03	0.12	0.12	0.12	0.06	0.12	0.08
0.13	0.03	0.13	0.06	0.13	0.03	0.13	0.13	0.13	0.06	0.13	0.08
0.15	0.04	0.15	0.07	0.15	0.04	0.15	0.14	0.15	0.07	0.15	0.09
0.16	0.04	0.16	0.08	0.16	0.04	0.16	0.16	0.16	0.08	0.16	0.10
0.18	0.04	0.18	0.08	0.18	0.05	0.18	0.17	0.18	0.08	0.18	0.11
0.20	0.05	0.20	0.09	0.20	0.05	0.20	0.19	0.20	0.09	0.20	0.12
0.21	0.05	0.21	0.10	0.21	0.06	0.21	0.20	0.21	0.10	0.21	0.13
0.24	0.06	0.24	0.11	0.24	0.06	0.24	0.22	0.24	0.11	0.24	0.14
0.26	0.06	0.26	0.11	0.26	0.07	0.26	0.24	0.26	0.11	0.26	0.14
0.28	0.07	0.28	0.12	0.28	0.07	0.28	0.26	0.28	0.12	0.28	0.15
0.31	0.07	0.31	0.13	0.31	0.08	0.31	0.28	0.31	0.13	0.31	0.16
0.34	0.07	0.34	0.14	0.34	0.09	0.34	0.29	0.34	0.14	0.34	0.17
0.38	0.08	0.38	0.15	0.38	0.09	0.38	0.31	0.38	0.15	0.38	0.18
0.41	0.08	0.41	0.16	0.41	0.10	0.41	0.33	0.41	0.15	0.41	0.19
0.45	0.09	0.45	0.16	0.45	0.11	0.45	0.35	0.45	0.16	0.45	0.20
0.50	0.09	0.50	0.17	0.50	0.12	0.50	0.38	0.50	0.17	0.50	0.20
0.54	0.10	0.54	0.18	0.54	0.12	0.54	0.40	0.54	0.18	0.54	0.21
0.60	0.10	0.60	0.19	0.60	0.13	0.60	0.42	0.60	0.19	0.60	0.22
0.66	0.10	0.66	0.20	0.66	0.14	0.66	0.45	0.66	0.20	0.66	0.24
0.72	0.11	0.72	0.21	0.72	0.15	0.72	0.48	0.72	0.21	0.72	0.25
0.79	0.11	0.79	0.22	0.79	0.16	0.79	0.51	0.79	0.23	0.79	0.26
0.87	0.12	0.87	0.23	0.87	0.17	0.87	0.54	0.87	0.24	0.87	0.28
0.95	0.12	0.95	0.24	0.95	0.18	0.95	0.57	0.95	0.26	0.95	0.29
1.05	0.12	1.05	0.25	1.05	0.19	1.05	0.60	1.05	0.27	1.05	0.31
1.15	0.12	1.15	0.26	1.15	0.20	1.15	0.63	1.15	0.29	1.15	0.33
1.26	0.13	1.26	0.27	1.26	0.21	1.26	0.67	1.26	0.31	1.26	0.35
1.38	0.13	1.38	0.28	1.38	0.22	1.38	0.70	1.38	0.33	1.38	0.36
1.52	0.13	1.52	0.30	1.52	0.23	1.52	0.73	1.52	0.35	1.52	0.38
1.67	0.13	1.67	0.32	1.67	0.24	1.67	0.77	1.67	0.37	1.67	0.41
1.83	0.14	1.83	0.33	1.83	0.25	1.83	0.80	1.83	0.40	1.83	0.43
2.01	0.14	2.01	0.36	2.01	0.26	2.01	0.84	2.01	0.42	2.01	0.45
2.21	0.14	2.21	0.38	2.21	0.27	2.21	0.88	2.21	0.45	2.21	0.48
2.42	0.15	2.42	0.41	2.42	0.29	2.42	0.93	2.42	0.48	2.42	0.50
2.66	0.16	2.66	0.45	2.66	0.30	2.66	0.98	2.66	0.51	2.66	0.54
2.92	0.17	2.92	0.49	2.92	0.32	2.92	1.04	2.92	0.55	2.92	0.57
3.21	0.18	3.21	0.54	3.21	0.34	3.21	1.11	3.21	0.60	3.21	0.61
3.52	0.20	3.52	0.59	3.52	0.36	3.52	1.19	3.52	0.64	3.52	0.65
3.86	0.22	3.86	0.65	3.86	0.39	3.86	1.27	3.86	0.70	3.86	0.70
4.24	0.24	4.24	0.72	4.24	0.42	4.24	1.35	4.24	0.75	4.24	0.75
4.66	0.27	4.66	0.79	4.66	0.46	4.66	1.44	4.66	0.81	4.66	0.80
5.11	0.30	5.11	0.86	5.11	0.49	5.11	1.54	5.11	0.87	5.11	0.86
5.61	0.34	5.61	0.94	5.61	0.53	5.61	1.63	5.61	0.93	5.61	0.91
6.16	0.37	6.16	1.03	6.16	0.58	6.16	1.73	6.16	1.00	6.16	0.97
6.76	0.41	6.76	1.11	6.76	0.63	6.76	1.83	6.76	1.06	6.76	1.03
7.42	0.46	7.42	1.20	7.42	0.68	7.42	1.93	7.42	1.13	7.42	1.10
8.15	0.50	8.15	1.29	8.15	0.74	8.15	2.04	8.15	1.19	8.15	1.16
8.94	0.55	8.94	1.38	8.94	0.81	8.94	2.15	8.94	1.26	8.94	1.23
9.82	0.60	9.82	1.47	9.82	0.89	9.82	2.26	9.82	1.32	9.82	1.29
10.78	0.66	10.78	1.55	10.78	0.97	10.78	2.37	10.78	1.37	10.78	1.35
11.83	0.71	11.83	1.63	11.83	1.07	11.83	2.47	11.83	1.42	11.83	1.41
12.99	0.76	12.99	1.70	12.99	1.16	12.99	2.56	12.99	1.45	12.99	1.46
14.26	0.81	14.26	1.76	14.26	1.25	14.26	2.65	14.26	1.47	14.26	1.52
15.65	0.85	15.65	1.81	15.65	1.34	15.65	2.73	15.65	1.49	15.65	1.57
17.18	0.90	17.18	1.86	17.18	1.43	17.18	2.82	17.18	1.52	17.18	1.63
18.86	0.96	18.86	1.91	18.86	1.51	18.86	2.92	18.86	1.57	18.86	1.72
20.71	1.03	20.71	1.98	20.71	1.57	20.71	3.02	20.71	1.67	20.71	1.83
22.73	1.11	22.73	2.07	22.73	1.62	22.73	3.12	22.73	1.82	22.73	1.98
24.95	1.21	24.95	2.19	24.95	1.65	24.95	3.21	24.95	2.02	24.95	2.16
27.39	1.31	27.39	2.31	27.39	1.68	27.39	3.28	27.39	2.23	27.39	2.35

30.07	1.40	30.07	2.41	30.07	1.75	30.07	3.32	30.07	2.43	30.07	2.52
33.01	1.48	33.01	2.47	33.01	1.85	33.01	3.32	33.01	2.58	33.01	2.65
36.24	1.53	36.24	2.47	36.24	2.01	36.24	3.24	36.24	2.68	36.24	2.72
39.78	1.57	39.78	2.41	39.78	2.17	39.78	3.06	39.78	2.75	39.78	2.72
43.67	1.60	43.67	2.31	43.67	2.28	43.67	2.77	43.67	2.80	43.67	2.69
47.94	1.64	47.94	2.21	47.94	2.31	47.94	2.38	47.94	2.83	47.94	2.63
52.62	1.69	52.62	2.13	52.62	2.23	52.62	1.94	52.62	2.84	52.62	2.56
57.77	1.75	57.77	2.08	57.77	2.08	57.77	1.54	57.77	2.81	57.77	2.48
63.41	1.81	63.41	2.07	63.41	1.94	63.41	1.25	63.41	2.74	63.41	2.36
69.61	1.86	69.61	2.07	69.61	1.87	69.61	1.13	69.61	2.64	69.61	2.22
76.42	1.91	76.42	2.06	76.42	1.92	76.42	1.15	76.42	2.53	76.42	2.05
83.89	1.95	83.89	2.04	83.89	2.07	83.89	1.24	83.89	2.45	83.89	1.89
92.09	1.99	92.09	2.00	92.09	2.24	92.09	1.29	92.09	2.41	92.09	1.75
101.10	2.06	101.10	1.95	101.10	2.34	101.10	1.16	101.10	2.38	101.10	1.66
110.98	2.15	110.98	1.90	110.98	2.31	110.98	0.83	110.98	2.31	110.98	1.62
121.83	2.26	121.83	1.87	121.83	2.18	121.83	0.42	121.83	2.19	121.83	1.60
133.74	2.37	133.74	1.88	133.74	2.04	133.74	0.13	133.74	2.02	133.74	1.58
146.82	2.47	146.82	1.92	146.82	1.99	146.82	0.02	146.82	1.85	146.82	1.55
161.17	2.54	161.17	1.98	161.17	2.06	161.17	0.00	161.17	1.73	161.17	1.50
176.93	2.53	176.93	1.99	176.93	2.20	176.93	0.00	176.93	1.64	176.93	1.41
194.22	2.41	194.22	1.88	194.22	2.30	194.22	0.00	194.22	1.54	194.22	1.25
213.21	2.17	213.21	1.59	213.21	2.24	213.21	0.00	213.21	1.36	213.21	1.01
234.05	1.87	234.05	1.15	234.05	1.95	234.05	0.00	234.05	1.05	234.05	0.73
256.94	1.59	256.94	0.69	256.94	1.53	256.94	0.00	256.94	0.61	256.94	0.48
282.06	1.41	282.06	0.39	282.06	1.16	282.06	0.00	282.06	0.23	282.06	0.36
309.63	1.41	309.63	0.31	309.63	0.99	309.63	0.00	309.63	0.07	309.63	0.38
339.90	1.60	339.90	0.45	339.90	1.08	339.90	0.00	339.90	0.08	339.90	0.58
373.13	1.92	373.13	0.83	373.13	1.43	373.13	0.00	373.13	0.30	373.13	0.97
409.61	2.27	409.61	1.34	409.61	1.95	409.61	0.00	409.61	0.86	409.61	1.44
449.66	2.51	449.66	1.73	449.66	2.42	449.66	0.00	449.66	1.59	449.66	1.86
493.62	2.56	493.62	1.84	493.62	2.60	493.62	0.00	493.62	2.07	493.62	2.11
541.88	2.40	541.88	1.64	541.88	2.36	541.88	0.00	541.88	1.79	541.88	2.13
594.85	2.13	594.85	1.22	594.85	1.76	594.85	0.00	594.85	1.00	594.85	1.93
653.01	1.88	653.01	0.76	653.01	1.06	653.01	0.00	653.01	0.25	653.01	1.35
716.85	1.73	716.85	0.40	716.85	0.54	716.85	0.00	716.85	0.03	716.85	0.66
786.93	1.68	786.93	0.21	786.93	0.32	786.93	0.00	786.93	0.00	786.93	0.15
863.87	1.68	863.87	0.16	863.87	0.36	863.87	0.00	863.87	0.00	863.87	0.01
948.32	1.66	948.32	0.14	948.32	0.60	948.32	0.00	948.32	0.00	948.32	0.00
1041.03	1.57	1041.03	0.11	1041.03	0.93	1041.03	0.00	1041.03	0.00	1041.03	0.00
1142.81	1.43	1142.81	0.03	1142.81	1.11	1142.81	0.00	1142.81	0.00	1142.81	0.00
1254.54	1.27	1254.54	0.00	1254.54	0.94	1254.54	0.00	1254.54	0.00	1254.54	0.00
1377.19	1.12	1377.19	0.00	1377.19	0.54	1377.19	0.00	1377.19	0.00	1377.19	0.00
1511.83	0.99	1511.83	0.00	1511.83	0.17	1511.83	0.00	1511.83	0.00	1511.83	0.00
1659.63	0.89	1659.63	0.00	1659.63	0.02	1659.63	0.00	1659.63	0.00	1659.63	0.00
1821.88	0.85	1821.88	0.00	1821.88	0.00	1821.88	0.00	1821.88	0.00	1821.88	0.00
2000.00		2000.00		2000.00		2000.00		2000.00		2000.00	

[1] Differential volume percentage = The percent of the total volume of particles within a given diameter range. Sums to 100% for the entire range of particle sizes.

Swale Flow Depth Calculations

Swale Dimensions

Table 62. Swale side slopes.

Side slopes: (measured in AutoCAD from site survey edited 8.4.10)										
right bank					left bank					
hypotenuse length (m)	y	θ (rad)	x	x/y (m/m)	hypotenuse length (m)	y	θ (rad)	x	x/y (m/m)	
3.9	0.70	0.18	3.84	5.47	3.2	0.54	0.17	3.11	5.79	
4.1	0.47	0.11	4.12	8.81	2.9	0.47	0.16	2.86	6.03	
3.0	0.46	0.15	2.98	6.48	3.4	0.34	0.1	3.37	9.86	
3.3	0.50	0.15	3.29	6.64	4.3	0.30	0.07	4.26	14.34	
3.6	0.34	0.09	3.59	10.67	2.5	0.26	0.1	2.52	9.53	
2.9	0.32	0.11	2.91	9.14	1.6	0.23	0.14	1.59	7.05	
2.5	0.53	0.21	2.46	4.64					avg: 8.77	
				avg: 7.41						
7.4 m in x direction for 1 m in y					8.78 m in x direction for 1 m in y					
Average for both sides: 8.03 m/m										

Table 63. Thalweg slope.

Thalweg slope (start to end point):		
Elevation Change (m)	Thalweg Length (m)	slope (decimal)
0.67	36.6	0.018

Manning's Equation and Rational Method

Manning's Equation for Triangular Swale (Haan et al., 1994):

$$Q = \left(\frac{1.49}{n} \right) R^{(2/3)} S^{(1/2)} A$$

$$Q = \left(\frac{1.49}{n} \right) \left(\frac{Zd}{2\sqrt{(Z^2 + 1)}} \right)^{\frac{2}{3}} (S^{\frac{1}{2}}) (Zd^2)$$

Where,

Q, cfs S, decimal %

R, ft A, ft²

Z = x/y n = 0.35 (Chosen for water quality purposes)

Peak Flow Equation (Haan et al., 1994):

$$Q_p = C_i A$$

Where,

A = 1.13Ac (0.46 ha)

C = 0.95

I = Peak rainfall intensity based on 13 minute t_c (in/hr)

Table 64. Depths of flow and flowrate associated with peak rainfall intensities for select storms at the Mango Creek swale.

Sample Date	Storm Event #	Rain Intensity (in/13 min)	Rain Intensity (i) (in/hr)	Peak Flow (cfs) ($Q_p = c_i A$)	Z	n	S	d (ft)	Manning's Eqn (cfs)	Manning's Eqn (L/s)
11/24/09	6	0.16	0.72	0.77	8.03	0.35	0.018	0.61	0.77	21.80
12/4/09	8	0.16	0.73	0.78	8.03	0.35	0.018	0.61	0.78	22.09
12/7/09	9	0.05	0.22	0.23	8.03	0.35	0.018	0.39	0.23	6.51
12/10/09	10	0.25	1.14	1.22	8.03	0.35	0.018	0.72	1.22	34.55
1/18/10	16	0.13	0.59	0.63	8.03	0.35	0.018	0.57	0.63	17.84
1/23/10	17	0.08	0.35	0.37	8.03	0.35	0.018	0.46	0.37	10.48
1/26/10	18	0.20	0.92	0.99	8.03	0.35	0.018	0.67	0.99	28.03
2/10/10	23	0.06	0.29	0.31	8.03	0.35	0.018	0.43	0.31	8.78
3/3/10	27	0.03	0.14	0.15	8.03	0.35	0.018	0.33	0.15	4.25
3/12/10	28,29	0.04	0.19	0.20	8.03	0.35	0.018	0.37	0.20	5.66
3/14/10	30,31	0.16	0.76	0.81	8.03	0.35	0.018	0.62	0.81	22.94
3/30/10	33	0.29	1.32	1.42	8.03	0.35	0.018	0.76	1.42	40.21
4/10/10	34	0.29	1.33	1.43	8.03	0.35	0.018	0.77	1.43	40.49
5/17/10	37	0.27	1.23	1.32	8.03	0.35	0.018	0.74	1.32	37.38
5/19/10	38	0.42	1.92	2.06	8.03	0.35	0.018	0.88 ^[1]	2.06	58.33
5/24/10	40,41	0.27	1.26	1.36	8.03	0.35	0.018	0.75	1.36	38.51
5/26/10	42	0.08	0.36	0.39	8.03	0.35	0.018	0.47	0.39	11.04
6/13/10	47,48	0.41	1.91	2.05	8.03	0.35	0.018	0.88	2.05	58.05
6/17/10	50	0.26	1.21	1.30	8.03	0.35	0.018	0.74	1.30	36.81
7/28/10	56	0.08	0.36	0.39	8.03	0.35	0.018	0.47	0.39	11.04
8/6/10	60	0.56	2.58	2.76	8.03	0.35	0.018	0.98	2.76	78.15
8/23/10	64	0.26	1.21	1.30	8.03	0.35	0.018	0.74	1.30	36.81
10/1/10	70	0.36	1.66	1.78	8.03	0.35	0.018	0.83	1.78	50.40
10/15/10	71	0.16	0.74	0.79	8.03	0.35	0.018	0.61	0.79	22.37
10/26/10	72	0.80	3.70	3.97	8.03	0.35	0.018	1.12	3.97	112.42
11/5/10	74	0.07	0.32	0.35	8.03	0.35	0.018	0.45	0.35	9.91

12/2/10	77	0.13	0.60	0.64	8.03	0.35	0.018	0.57	0.64	18.12
---------	----	------	------	------	------	------	-------	------	------	-------

[1] Red-shaded depths exceed average tall fescue grass length in swale.

Table 65. TSS data associated with depth of flow and peak flowrates through Mango Creek swale.

Sample Date	Storm Event #	Flow Depth (m)	Manning's Q (L/s)	Influent TSS Conc (mg/L)	Effluent TSS Conc (mg/L)	% Conc Reduction
11/24/2009	6	0.18	21.81	14	10	28.6
12/4/2009	8	0.18	22.09	19	16	15.8
12/7/2009	9	0.12	6.51	6	7	-16.7
12/10/2009	10	0.22	34.55	41	50	-22.0
1/18/2010	16	0.17	17.84	36	11	69.4
1/23/2010	17	0.14	10.48	22	14	36.4
1/26/2010	18	0.20	28.04	57	23	59.6
2/10/2010	23	0.13	8.78	109	82	24.8
3/3/2010	27	0.10	4.25	75	40	46.7
3/12/2010	28,29	0.11	5.66	136	49	64.0
3/14/2010	30,31	0.19	22.94	312	143	54.2
3/30/2010	33	0.23	40.21	122	64	47.5
4/10/2010	34	0.23	40.50	98	31	68.4
5/17/2010	37	0.22	37.38	58	62	-6.9
5/19/2010	38	0.26 ^[1]	58.34	60	26	56.7
5/24/2010	40,41	0.23	38.52	44	24	45.5
5/26/2010	42	0.14	11.04	14	2	85.7
6/13/2010	47,48	0.26	58.06	44	37	15.9
6/17/2010	50	0.22	36.82	69	59	14.5
7/28/2010	56	0.14	11.04	35	8	77.1
8/6/2010	60	0.29	78.16	40	26	35.0
8/23/2010	64	0.22	36.82	19	15	21.1
10/1/2010	70	0.25	50.41	9	4	55.6
10/15/2010	71	0.18	22.37	283	81	71.4
10/26/2010	72	0.34	112.43	189	60	68.3
11/5/2010	74	0.14	9.91	58	25	56.9
12/2/2010	77	0.17	18.12	93	98	-5.4

[1] Red-shaded depths exceed average tall fescue grass length in swale.

Appendix C: Bridge Deck Runoff Analyses

Bridge Deck First Flush Analysis

Fisher's least significant difference (Ott and Longnecker, 2011) was used to statistically determine if there was a difference in mean runoff concentrations for each rainfall depth range shown in Tables 66-68. This analysis was done as a surrogate first-flush analysis (Sansalone et al., 2005) based on the influent composite water quality samples collected at the site. The analysis was performed to compare the runoff concentrations for small storm events (less than 1.27 cm) to those of larger storm events for the northbound and southbound bridge decks to determine if smaller events carried higher nutrient and TSS concentrations. Since the first-flush event was represented by a rainfall depth of 1.27 cm or less, the results showed that there was no first-flush effect on either bridge deck for any of the constituents tested. However, for TKN, NO₂₃-N, and TN, storms ≤1.27 cm were statistically similar to storms between 1.27 and 2.54 cm, but were statistically different from storms ≥2.54 cm, indicating some amount of pollutant dilution for larger events.

Table 66. Northbound bridge deck mean nutrient and TSS runoff concentrations per rainfall depth range.

		Mean Concentration (mg/L)					
Rainfall Depth (cm)	n	TKN	NO ₂₃ -N	TN	NH ₄ -N	TP	TSS
≤1.27	10	0.5546	0.41100	0.9656	0.07810	0.09550	48.90
1.27-2.54	9	0.6780	0.39111	1.0691	0.10589	0.18478	71.44
≥ 2.54	10	0.3320	0.21950	0.4882	0.07120	0.07040	30.30

Table 67. Statistical results for difference in means of nutrient and TSS runoff concentrations per rainfall depth range for the northbound bridge deck.

Rainfall Depth (cm)	TKN	NO ₂₃ -N	TN	NH ₄ -N	TP	TSS
≤1.27	A ^[1]	A	A	A	A	A
1.27-2.54	A	A	A	A	B	A
≥ 2.54	B	B	B	A	A	A

[1] Rain depth ranges that share the same letter are not significantly different.

Table 68. Southbound bridge deck mean nutrient and TSS runoff concentrations per rainfall depth range.

		Mean Concentration (mg/L)					
Rainfall Depth (cm)	n	TKN	NO ₂₃ -N	TN	NH ₄ -N	TP	TSS
≤1.27	13	0.7982	0.4631	1.2613	0.08115	0.20838	85.58
1.27-2.54	8	0.7221	0.4601	1.1823	0.07400	0.20150	82.75
≥ 2.54	9	0.4239	0.1529	0.5768	0.08911	0.09089	49.67